

INFORMATION TO USERS

This manuscript has been reproduced from the microfilm master. UMI films the text directly from the original or copy submitted. Thus, some thesis and dissertation copies are in typewriter face, while others may be from any type of computer printer.

The quality of this reproduction is dependent upon the quality of the copy submitted. Broken or indistinct print, colored or poor quality illustrations and photographs, print bleedthrough, substandard margins, and improper alignment can adversely affect reproduction.

In the unlikely event that the author did not send UMI a complete manuscript and there are missing pages, these will be noted. Also, if unauthorized copyright material had to be removed, a note will indicate the deletion.

Oversize materials (e.g., maps, drawings, charts) are reproduced by sectioning the original, beginning at the upper left-hand corner and continuing from left to right in equal sections with small overlaps.

ProQuest Information and Learning
300 North Zeeb Road, Ann Arbor, MI 48106-1346 USA
800-521-0600

UMI[®]

**Free-Vibration and Buckling of Prismatic and Thin-Walled Composite
Beam-Columns with Stochastic Properties**

Vijay K. Kowda

A Thesis

in

The Department

of

Mechanical & Industrial Engineering

Presented in Partial Fulfillment of the Requirements

for the

Degree of Master of Applied Science

at

Concordia University

Montreal, Quebec, Canada

October, 2002

© Vijay K. Kowda, 2002



**National Library
of Canada**

**Acquisitions and
Bibliographic Services**

**395 Wellington Street
Ottawa ON K1A 0N4
Canada**

**Bibliothèque nationale
du Canada**

**Acquisitions et
services bibliographiques**

**395, rue Wellington
Ottawa ON K1A 0N4
Canada**

Your file Votre référence

Our file Notre référence

The author has granted a non-exclusive licence allowing the National Library of Canada to reproduce, loan, distribute or sell copies of this thesis in microform, paper or electronic formats.

The author retains ownership of the copyright in this thesis. Neither the thesis nor substantial extracts from it may be printed or otherwise reproduced without the author's permission.

L'auteur a accordé une licence non exclusive permettant à la Bibliothèque nationale du Canada de reproduire, prêter, distribuer ou vendre des copies de cette thèse sous la forme de microfiche/film, de reproduction sur papier ou sur format électronique.

L'auteur conserve la propriété du droit d'auteur qui protège cette thèse. Ni la thèse ni des extraits substantiels de celle-ci ne doivent être imprimés ou autrement reproduits sans son autorisation.

0-612-77700-6

Canada

Abstract

Free-Vibration and Buckling of Prismatic and Thin-Walled Composite Beam-Columns with Stochastic Properties

Vijay K. Kowda

The present thesis considers the beam-columns that have a stochastic distribution of material and geometric properties, boundary conditions and loadings, and made of polymer-matrix fiber-reinforced composite material. Both the prismatic and thin-walled beam-columns are analyzed for their free-vibration response and buckling. In the case of thin-walled beam-columns, the local buckling occurs before the global buckling and therefore, the local buckling is considered in the stability analysis. Both the undamped free-vibration and static stability analyses are conducted based on a probabilistic approach. In this regard, the perturbation method is employed in the context of stochastic analysis. The analysis of symmetric composite beam-columns can be conducted based on the (i) Cylindrical Bending Theory and (ii) One-Dimensional Laminated Beam Theory. However, the differences between the values of natural frequencies and buckling loads obtained using these two theories will be significant. In the present thesis, the above-mentioned differences between the values of natural frequencies and buckling loads are quantified for different laminate configurations. The differential equations and boundary conditions for the stochastic response of symmetric beam-columns are written based on the equilibrium conditions using both the theories. Using the stochastic perturbation analysis and the second-order moment method of probabilistic analysis, the mean values, mean square values and variances of the undamped natural frequencies and buckling loads are obtained. For the thin-walled beams, the bending rigidities are obtained based on the laminate analysis of flange and web sections. The local buckling analysis is conducted using the Ritz method in the context of stochastic plate analysis. A detailed parametric study is conducted to determine the influences of various boundary conditions, the aspect ratios of flange and web sections of thin-walled beam-columns, the material, structural and geometric properties, their variabilities, laminate configurations, and the proximity of the applied axial loads to the critical loads, on the natural frequencies and buckling loads.

Acknowledgements

I gratefully acknowledge my mentor Dr. Rajamohan Ganesan, for his invaluable supervision, financial support, patience, and advise throughout the course of my research.

I would like to thank my colleagues and also best friends Amit K. Nigam and Shashank M.Venugopal for their refreshing viewpoints, which often helped me to overcome obstacles in my thesis work. I would also like to thank all my other friends.

I would like to acknowledge Vijay M. Dharanipathi and Qi Zhao for their friendship and valuable technical discussions.

Shayamala Mantha and Ashwani K. Mantha deserve my warmest thanks for their care and love.

Finally, I would like to convey my love and devotion to my parents, for their cooperation, patience, love and support throughout my study period.

Table of Contents

Abstract.....	iii
Acknowledgement.....	iv
Table of contents.....	v
List of Tables.....	ix
List of Figures.....	xiii
Nomenclature.....	xvii
Chapter 1 INTRODUCTION.....	1
1.1 Stochastic mechanics of composites.....	1
1.2 Literature overview	2
1.3 Scope and objectives of the thesis.....	7
1.4 Organization of the thesis.....	9
Chapter 2 ONE-DIMENSIONAL DETERMINISTIC ANALYSIS.....	11
2.1 Introduction.....	11
2.2 Cylindrical bending theory.....	11
2.3 One-dimensional laminated beam theory.....	14
2.4 Buckling analysis using cylindrical bending theory.....	17
2.5 Buckling analysis using one-dimensional laminated beam theory.....	20
2.6 Free-vibration analysis using cylindrical bending theory.....	23
2.7 Free-vibration analysis using one-dimensional laminated beam theory..	24
2.8 Numerical examples.....	26

2.9	Conclusions and discussions.....	29
Chapter 3	FREE-VIBRATION RESPONSE OF COMPOSITE BEAM-COLUMNS WITH STOCHASTIC PROPERTIES.....	31
3.1	Introduction.....	31
3.2	Formulation for the free-vibration of composite beam-column.....	32
3.2.1	General solution to the stochastic equation.....	38
3.3	Parametric study.....	50
3.3.1	Random axial load.....	51
3.3.1.1	Numerical examples.....	56
3.3.2	Ratio of the coefficients of variation of input and output.....	62
3.3.3	Random material and geometric properties.....	67
3.3.3.1	Case 1: Uniform auto-correlation and cross-correlation functions.....	68
3.3.3.1.1	Numerical examples.....	70
3.3.3.2	Case 2: Exponential auto and cross-correlation functions.....	75
3.3.3.2.1	Numerical examples.....	78
3.4	Equivalent elastic constants.....	82
3.4.1	Equivalent elastic constants for symmetric laminates.....	82
3.4.2	Equivalent elastic constants for un-symmetric laminates.....	89
3.5	Calculation of flexural rigidity for symmetrical bending.....	95
3.6	Formulation for thin-walled beam-columns.....	97

3.7	Parametric study.....	101
3.7.1	Random axial force.....	101
3.7.1.1	Numerical examples.....	102
3.7.2	Random material and geometric properties.....	105
3.7.2.1	Case 1: Uniform auto-correlation and cross-correlation functions.....	106
3.7.2.1	Numerical examples.....	107
3.7.2.2	Case 2: Exponential auto and cross-correlation functions.....	109
3.7.2.2.1	Numerical examples.....	110
3.8	Conclusions and discussions.....	112
Chapter 4	BUCKLING OF COMPOSITE BEAM-COLUMNS WITH STOCHASTIC PROPERTIES.....	114
4.1	Introduction.....	114
4.2	Formulation for the buckling of composite beam-column.....	115
4.2.1	General solution to the stochastic equation.....	118
4.3	Parametric study.....	124
4.3.1	Random stiffness and geometric properties.....	125
4.3.1.1	Case 1: Uniform auto-correlation function.....	125
4.3.1.1.1	Numerical examples.....	129
4.3.1.2	Case 2: Exponential auto-correlation function.....	135
4.3.1.1.2	Numerical examples.....	138

4.4	Deterministic local buckling of thin-walled composite beam-columns.....	141
4.4.1	Flange buckling.....	143
4.4.1.1	SCSF flange support conditions.....	143
4.4.1.2	FCFF flange support conditions.....	147
4.4.2	Web buckling.....	149
4.4.2.1	SCSC web support conditions.....	149
4.4.2.2	FCFC web support conditions.....	150
4.5	Stochastic local buckling of thin-walled composite beam-columns....	151
4.5.1	Stochastic simulation of laminate bending stiffness matrix...	155
4.6	Parametric study.....	157
4.7	Conclusions and discussions.....	168
Chapter 5	CONCLUSIONS AND RECOMMENDATIONS.....	170
	References.....	173
	Appendix.....	182

List of Tables

Table 2.1	Buckling loads for symmetric cross-ply laminate $[0/90]_{9s}$	27
Table 2.2	Buckling loads for symmetric angle-ply laminate $[+45/-45]_{9s}$	27
Table 2.3	Buckling loads for quasi-isotropic laminate $[0/-60/60]_{6s}$	27
Table 2.4	Buckling loads for un-symmetric laminate $[0/45]_{18T}$	28
Table 2.5	The 1 st natural frequency of free-vibration for given $P_o / P_{cr} = 1/4$	28
Table 2.6	The 1 st natural frequency of free-vibration for given $P_o / P_{cr} = 1/2$	29
Table 3.1	Mean value and variance of 1 st natural frequency for the $[0/90]_{9s}$ laminate with $P_o / P_{cr} = 1/4$	57
Table 3.2	Mean value and variance of 1 st natural frequency for the $[0/90]_{9s}$ laminate with $P_o / P_{cr} = 1/2$	57
Table 3.3	Mean value and variance of 1 st natural frequency for the $[45/-45]_{9s}$ laminate with $P_o / P_{cr} = 1/4$	58
Table 3.4	Mean value and variance of 1 st natural frequency for the $[45/-45]_{9s}$ laminate with $P_o / P_{cr} = 1/2$	58
Table 3.5	Mean value and variance of 1 st natural frequency for the $[0/-60/60]_{6s}$ laminate with $P_o / P_{cr} = 1/4$	59
Table 3.6	Mean value and variance of 1 st natural frequency for the $[0/-60/60]_{6s}$ laminate with $P_o / P_{cr} = 1/2$	59
Table 3.7	Mean value and variance of 1 st natural frequency for $[0/45]_{18T}$ laminate using cylindrical bending analysis.....	60

Table 3.8	Ratio of the coefficients of variation of input and output when $n = 1$	65
Table 3.9	Ratio of the coefficients of variation of input and output when $n = 2$	65
Table 3.10	Mean value and variance of 1^{st} natural frequency for the $[0/90]_{9s}$ laminate with $P_o / P_{cr} = 1/4$	71
Table 3.11	Mean value and variance of 1^{st} natural frequency for the $[0/90]_{9s}$ laminate with $P_o / P_{cr} = 1/2$	71
Table 3.12	Mean value and variance of 1^{st} natural frequency for the $[45/-45]_{9s}$ laminate with $P_o / P_{cr} = 1/4$	72
Table 3.13	Mean value and variance of 1^{st} natural frequency for the $[45/-45]_{9s}$ laminate with $P_o / P_{cr} = 1/2$	72
Table 3.14	Mean value and variance of 1^{st} natural frequency for the $[0/-60/60]_{6s}$ laminate with $P_o / P_{cr} = 1/4$	73
Table 3.15	Mean value and variance of 1^{st} natural frequency for the $[0/-60/60]_{6s}$ laminate with $P_o / P_{cr} = 1/2$	73
Table 3.16	Mean value and variance of 1^{st} natural frequency for $[0/45]_{18T}$ laminate corresponding to cylindrical bending analysis.....	74
Table 3.17	Mean value and variance of 1^{st} natural frequency for given P_o / P_{cr}	104
Table 3.18	Mean value and variance of 1^{st} natural frequency when material and geometric properties have uniform correlation.....	107
Table 4.1	Mean value and variance of critical buckling load for the $[0/90]_{9s}$ laminate corresponding to cylindrical bending theory.....	130

Table 4.2	Mean value and variance of critical buckling load for the $[0/90]_{9s}$ laminate corresponding to one-dimensional laminated beam theory.....	130
Table 4.3	Mean value and variance of critical buckling load for the $[45/-45]_{9s}$ laminate corresponding to cylindrical bending theory.....	131
Table 4.4	Mean value and variance of critical buckling load for the $[45/-45]_{9s}$ laminate corresponding to one-dimensional laminated beam theory.....	131
Table 4.5	Mean value and variance of critical buckling load for the $[0/-60/60]_{6s}$ laminate corresponding to cylindrical bending theory.....	132
Table 4.6	Mean value and variance of critical buckling load for the $[0/-60/60]_{6s}$ laminate corresponding to one-dimensional laminated beam theory.....	132
Table 4.7	Mean value and variance of critical buckling load for the $[0/45]_{18T}$ laminate corresponding to cylindrical bending theory.....	133
Table 4.8	Mean values, standard deviations and coefficients of variation of various material properties of NCT 301 graphite-epoxy composite material.....	156
Table 4.9(a)	Deterministic, mean and variance values of critical buckling loads: $[0/90]_{9s}$ laminate with free boundary conditions on loading edges.....	160
Table 4.9(b)	Deterministic, mean and variance values of critical buckling loads: $[45/-45]_{9s}$ laminate with free boundary conditions on loading edges....	160
Table 4.9(c)	Deterministic, mean and variance values of critical buckling loads: $[0/-60/-60]_{6s}$ laminate with free boundary conditions on loading edges	161

Table 4.9(d)	Deterministic, mean and variance values of critical buckling loads: [0/90] _{9s} laminate with simply supported boundary conditions on loading edges.....	161
Table 4.9(e)	Deterministic, mean and variance values of critical buckling loads: [45/-45] _{9s} laminate with simply supported boundary conditions on loading edges.....	161
Table 4.9(f)	Deterministic, mean and variance values of critical buckling loads: [0/-60/60] _{6s} laminate with simply supported boundary conditions on loading edges.....	162

List of Figures

Figure 2.1	A plate with infinite length.....	12
Figure 2.2	Laminated beam.....	14
Figure 2.3	Composite laminate.....	26
Figure 3.1	Composite beam-column.....	33
Figure 3.2	Variance of 1 st natural frequency vs σ_v^2 for $P_o / P_{cr} = 1/4$	60
Figure 3.3	Variance of 1 st natural frequency vs σ_v^2 for $P_o / P_{cr} = 1/2$	61
Figure 3.4	Ratio of the coefficients of variation of P and ϖ_n for given P_o / P_{cr}	66
Figure 3.5	The variance of 1 st natural frequency vs σ^2	74
Figure 3.6	The variance of 1 st natural frequency vs σ^2 for $P_o/P_{cr} = 1/4$	79
Figure 3.7	The variance of 1 st natural frequency vs σ^2 for $P_o/P_{cr} = 1/2$	79
Figure 3.8	Variance of 1 st natural frequency corresponding to cylindrical bending analysis for $[0/90]_{9s}$ laminate when $P_o/P_{cr} = 1/2$	80
Figure 3.9	Variance of 1 st natural frequency corresponding to cylindrical bending analysis for $[+45/-45]_{9s}$ laminate when $P_o/P_{cr} = 1/2$	80
Figure 3.10	Variance of 1 st natural frequency corresponding to cylindrical bending analysis for $[0/-60/60]_{6s}$ laminate when $P_o/P_{cr} = 1/2$	81
Figure 3.11	Variance of 1 st natural frequency corresponding to cylindrical bending analysis for $[0/45]_{18T}$ laminate when $P_o/P_{cr} = 1/2$	81
Figure 3.12	Laminate subjected to N_x only.....	85
Figure 3.13	Laminate subjected to M_x only.....	87

Figure 3.14	Symmetrical bending of a composite section.....	96
Figure 3.15	Symmetric I-section.....	102
Figure 3.16	The variance of 1 st natural frequency vs σ_v^2	104
Figure 3.17	The variance of 1 st natural frequency vs σ^2	108
Figure 3.18	The variance of 1 st natural frequency vs σ^2 for given correlation length and P_o / P_{cr} when material and geometric properties have exponential correlation.....	111
Figure 3.19	The variance of 1 st natural frequency vs ε for given variance and $P_o / P_{cr} = 1/2$	111
Figure 4.1	Composite beam-column.....	116
Figure 4.2	The variance of critical buckling load vs σ^2 corresponding to simply supported boundary conditions for uniform correlation.....	133
Figure 4.3	The variance of critical buckling load vs σ^2 corresponding to simply supported boundary conditions for exponential correlation.....	138
Figure 4.4	The variance of critical buckling load vs σ^2 for [0/90] _{9s} laminate corresponding to cylindrical bending theory.....	139
Figure 4.5	The variance of critical buckling load vs σ^2 for [45/-45] _{9s} laminate corresponding to cylindrical bending theory.....	139
Figure 4.6	The variance of critical buckling load vs σ^2 for [0/-60/60] _{6s} laminate corresponding to cylindrical bending theory.....	140
Figure 4.7	The variance of critical buckling load vs σ^2 for [0/45] _{18T} laminate corresponding to cylindrical bending theory.....	140

Figure 4.8	I-section beam-column and coordinate system.....	142
Figure 4.9	Solutions for λ_n corresponding to $[+45/-45]_{9s}$ laminate.....	147
Figure 4.9	A set of sample realizations of the stochastic bending stiffness matrix at different Gauss points in regions 2 and 10.....	157
Figure 4.10	I-section beam-column with dimensions.....	158
Figure 4.11	Deterministic and mean values of critical buckling load for the $[0/90]_{9s}$ laminate with free boundary conditions on loading edges.....	162
Figure 4.12	Deterministic and mean values of critical buckling load for the $[45/-45]_{9s}$ laminate with free boundary conditions on loading edges.....	163
Figure 4.13	Deterministic and mean values of critical buckling load for the $[0/-60/60]_{6s}$ laminate with free boundary conditions on loading edges.....	163
Figure 4.14	Variance values of critical buckling load for different laminate configurations with free boundary conditions on loading edges.....	164
Figure 4.15	Deterministic and mean values of critical buckling load for the $[0/90]_{9s}$ laminate with simply supported boundary conditions on loading edges.....	164
Figure 4.16	Deterministic and mean values of critical buckling load for the $[45/-45]_{9s}$ laminate with simply supported boundary conditions on loading edges.....	165

Figure 4.17	Deterministic and mean values of critical buckling load for the [0/60/60] _{6s} laminate with simply supported boundary conditions on loading edges.....	165
Figure 4.18	Variance values of critical buckling load for different laminate configurations with simply supported boundary conditions on loading edges.....	166

Nomenclature

A_{ij}	Axial stiffness coefficient
B_{ij}	Axial-bending coupling stiffness coefficient
D_{ij}	Bending stiffness coefficient
D_{ij}^*	Bending compliance coefficient
u_o, v_o, w	Mid-plane displacements
$\varepsilon_x^o, \varepsilon_y^o, \gamma_{xy}^o$	Mid-plane strains
k_x, k_y, k_{xy}	Mid-plane curvatures
N_x	In-plane axial force intensity in the x-direction per unit width
N_y	In-plane axial force intensity in the y-direction per unit width
N_{xy}	In-plane shear force intensity in the xy-plane direction per unit width
M_x	Moment intensity about the y-axis per unit width
M_y	Moment intensity about the x-axis per unit width
M_{xy}	Twisting moment intensity in the xy-plane per unit width
E_x	Young's modulus in x-direction
E_y	Young's modulus in y-direction
G_{xy}	Shear modulus in x-y plane
ρ_s	A quantity which is a function of density $\rho(x)$
q	Transverse surface load
E_x^b	Effective bending modulus in x-direction
N_o	Critical buckling load per unit width

P_{cr}	Critical buckling load
ω_m	Free-vibration frequency
t	Time
l	Length of a beam-column
$w(x, t)$	Lateral displacement as a function of spatial co-ordinate x and time t
b(x)	Width of the laminate as a function of x
$D_{11}(x)$	Laminate bending stiffness coefficient as a function of x
P	Axial compressive force
$\rho(x)$	Density of the material as a function of x
A(x)	Cross-sectional area of the laminate as a function of x
α_1 and α_2	Coefficients of boundary rigidities
D_{11o}	Mean value of $D_{11}(x)$
b_o	Mean value of b(x)
ρ_o	Mean value of $\rho(x)$
A_o	Mean value of A(x)
α_{1o}	Mean value of α_1
α_{2o}	Mean value of α_2
P_o	Mean value of P
$a(x)$	Stationary random function of $D_{11}(x)$
$b_1(x)$	Stationary random function of b(x)
$c(x)$	Stationary random function of $\rho(x)$

$d(x)$	Stationary random function of $A(x)$
s	Random variable corresponding to α_1
u	Random variable corresponding to α_2
v	Random variable corresponding to P
ξ	Non-dimensional co-ordinate
λ_n	Non-dimensional function of the natural frequency ω_n
α, β	Expansion parameters
$E[]$	Expected value
$\sigma []$	Standard deviation
$\text{var}[]$	Variance
$E[\lambda_n]$	Expected value of λ_n
$E[\lambda_n^2]$	Mean square value of λ_n
$E[\omega_n]$	Expected value of ω_n
$\sigma[\lambda_n]$	Standard deviation of λ_n
$\text{var}[\lambda_n]$	Variance of λ_n
$\text{var}[\omega_n]$	Variance of ω_n
V_p	Coefficient of variation of P
V_{ω_n}	Coefficient of variation of ω_n
$R_a(\xi_1 - \xi_2)$	Auto-correlation function of $a(\xi)$
$R_{b_1}(\xi_1 - \xi_2)$	Auto-correlation function of $b_1(\xi)$
$R_c(\xi_1 - \xi_2)$	Auto-correlation function of $c(\xi)$

$R_d(\xi_1 - \xi_2)$	Auto-correlation function of $d(\xi)$
$R_{ac}(\xi_1 - \xi_2)$	Cross-correlation function corresponding to $a(\xi)$ and $c(\xi)$
$R_{b,d}(\xi_1 - \xi_2)$	Cross-correlation function corresponding to $b_1(\xi)$ and $d(\xi)$
$R_{ad}(\xi_1 - \xi_2)$	Cross-correlation function corresponding to $a(\xi)$ and $d(\xi)$
C_{ac}	Covariance of a and c
ε	Correlation length
h	Thickness of a laminate
b	Width of a laminate
$X_n(\xi)$	Normal mode of beam-column
μ	Non-dimensional function of the static buckling load P
b_f	Width of the flange
t_f	Thickness of the flange
h_w	Height of the web
$W(x, z)$	Flange out-of-plane displacement
$U(y, z)$	Web out-of-plane displacement
C_{aa}	Covariance matrix
[T]	Transformation matrix
[L]	Lower triangular matrix
R	Aspect ratio
S	Simple supports
C	Clamped supports
F	Free supports

Chapter 1

INTRODUCTION

1.1 Stochastic mechanics of composites

Composite materials and structures are becoming more and more popular among engineers, researchers and practitioners all over the world. In recent years, laminated composite materials have become more important engineering materials in the development of automobile, structural, mechanical, aerospace, biomedical and marine structures. The great advantages of using such composite materials outweigh the significantly increased costs involved. Beam-columns made of polymer-matrix fiber-reinforced composite materials are increasingly being used in many engineering industries. Such structures operate in a static and dynamic loading environment and hence, their vibration and buckling response is of paramount importance in the design and development of high-performance composite mechanical components.

The composite laminates display significant variability in their material, geometric and structural properties. This variability is attributed to the variations in the properties of the fibers, matrices and interfaces, in the fiber orientations, in the void content and in the ply thickness. These variations are unavoidable and are induced during manufacturing and service. Therefore, in the design and failure prediction these variations have to be taken into account.

Considering the randomness in the properties of composite materials and structures, the stochastic approach to the analysis and design of composite structures is appropriate.

1.2 Literature overview

Deterministic one-dimensional free vibration and buckling analysis of laminated plates are very well established and are covered in the texts by Whitney [1] and Bertholet [2]. In those texts, the authors describe the one-dimensional analyses corresponding to the cylindrical bending and one-dimensional laminated beam theories derived from two-dimensional laminate analysis.

The analysis of structures, involving deterministic or random material properties, geometric properties, loads and boundary conditions has been developed mainly under the assumption that the structure's parameters are deterministic quantities. For a significant number of circumstances, this assumption is not valid, and the probabilistic aspects of the structure need to be taken into account. The necessity to account for property randomness in determining the response of any system is due, in general, to random material and geometric properties, random boundary conditions and random loadings. One of the origins of the treatment of differential equations with stochastic or probabilistic coefficients can be found in random eigen problems. Keller [3] presented the problem of wave propagation in random media in which he first solved for the eigen values in terms of the coefficients of the governing differential equation and then introduced the probabilistic treatment to the results. Boyce and Goodwin [4] reported the

theoretical results of random transverse vibrations of elastic beams. Determination of random eigen values for simple cases is summarized by Bharucha-Ried [5]. Hoshiya and Shah [6] presented the free vibration of stochastic beam-column for metals using the perturbation method. In their study, the general stochastic equations of the n -th natural frequency of a metallic beam-column are determined when the material properties, the geometric properties, axial load and boundary conditions are probabilistic. Lepore and Shah [7] studied the stability of the systems under stochastic excitations. Shinozuka and Astill [8] extended the work for buckling of stochastic beam-column for metals from ref. [6]. In their study, the beam-column is supported at its ends by rotational springs. The spring supports and axial force are treated as random variables; the distributions of material and geometric properties are considered to be correlated homogeneous functions. Many other authors like Bliven and Soong [9], Vaicaitis [10] and Collins and Thomson [11] all considered the case of random elastic beams and beam-columns using the perturbation methods. Ramu and Ganesan [12] analyzed the free vibrational characteristics of a beam-column, which is having randomly varying Young's modulus and mass density and subjected to randomly distributed axial loading. In their study, Hamilton's principle is used to formulate the problem using the stochastic FEM. Vibrational frequencies and mode shapes are analyzed for their statistical descriptions. Liaw *et al* [13] studied the reliability of practical beam-column problems with complex loadings, realistic boundary conditions, arbitrary geometries, and imperfections, for which analytical solutions are difficult to obtain. Finite difference method was applied to the second-moment analysis of beams on elastic foundation with random characteristics by Grigoriu *et al* [14]. Ramu and Ganesan [15] considered a beam-column resting on

continuous Winkler foundation and discrete elastic supports. They studied the static response, free-vibration and stability behaviour of the beam-column. Jensen and Iwan [16] presented a method for the dynamic analysis of linear systems with uncertain parameters to stochastic excitation. Liu, Belytschko and Mani [17] studied the application of stochastic finite element method in elastic/plastic dynamics with random material properties in details. Ghanem and Spanos [18] proposed a new method for the solution of problems involving material variability. The material property is modeled as a stochastic process. Ganesan, Sankar and Ramu [19] developed a stochastic finite element method to solve the more general non-self-adjoint eigenvalue problems. Ramu *et al* [21] considered the Leipholz column, which is having the Young's modulus and mass per unit length as stochastic processes. The standard perturbation method is employed. Full covariance structure of the free vibration eigenvalues and critical loads is derived in terms of second order properties of input random fields characterizing the system parameter fluctuations. Ramu *et al* [22] considered a column whose material property is varying along its length stochastically and subjected to stochastic loadings in space. They derived the buckling load statistics, such as mean value and variance, and buckling mode statistics. Ahamadi *et al* [23] investigated the dynamic stability of a linear elastic column subjected to an axial stochastic load. Ramu *et al* [24] described an effective method for integrating the concepts of probabilistic structural mechanics with finite element analysis for dynamic systems.

The successful application of the mechanics of composites for achieving safer and reliable designs is hindered by the inherent uncertain distribution of material and

geometric properties. In recent years, composite structures involving random parameters have been studied by some researchers. Nakagiri *et al* [25] presented a stochastic finite element methodology and applied to the uncertain eigenvalue problem of linear vibration, which arises from the fluctuation of the overall stiffness due to uncertain variation of the stacking sequence of composite laminates. A detailed description of stochastic behaviour of composite materials is given in ref. [26]. Ganesan [27] considered fibre reinforced laminated composites, which possess a stochastic variation over mass products. He conducted vibration analysis for stability of singular non-self-adjoint beam-columns using stochastic FEM. Stochastic free-vibration analysis of composite laminated plates has been conducted by different authors [28-30]. Recently many authors studied the stochastic buckling of composite laminates [30-34].

There is wealth of literature available on buckling of thin-walled metal beam-columns. Here the literature overview on buckling of thin-walled composite beam-columns is provided. Barbero *et al* [35] investigated the global buckling and determined the critical loads experimentally for various fiber reinforced composite I-beams of long column length. Southwell's method is used to determine the critical buckling load about strong and weak axes. Kolakowski *et al* [36] studied the influence of modal interactive elastic buckling on the post-buckling behaviour of thin-walled composite beam-columns. Shield *et al* [37-39] presented the buckling of thin-walled composite I-section beams. Almanzar, and Godoy [40] presented a theory and applications to account for changes in the fundamental, buckling, and post-buckling states when design parameters of a composite material are modified. Barbero and Raftoyiannis [41-42] used pultruded composite

structural members with open or closed thin-walled sections as columns for structural applications where buckling is the main consideration in the design. Local buckling modes are developed in this work. Krolak and Marian [43] presented the overview of research done on thin-walled structures at the University of Lodz in Poland for over 30 years. Hancock and Rasmussen [44] investigated the testing of slender thin-walled I-sections bent about both the major and minor principal axes. All sections tested experienced local buckling before overall buckling. Very recently Silvestre and Camotim [45] presented the formulation of a second-order generalized beam theory developed to analyse the buckling behaviour of composite thin-walled members made of laminated plates and displaying arbitrary orthotropy. Barbero [46] developed a novel analytical model to simulate the crippling behavior of thin-wall composite beam-columns. Godoy *et al* [47] presented an analytical approximate model, leading to a closed form solution to account for buckling mode interaction in composite I section columns. Three buckling modes are considered in the analysis: a global mode (Euler mode about the weak axis); a primary local mode (rotation of the flanges and bending of the web); and a secondary local mode (bending of the flanges), which are modeled using analytical functions and four degrees of freedom. Godoy [48] studied the design sensitivity analysis of thin-walled columns made of composite materials. Barbero *et al* [49-52] investigated the global and local buckling of thin-walled pultruded FRP columns. Experimental data are presented and correlated with theoretical predictions. Kabir and Sherbourne [53] presented a theoretical view of elastic local instability of anisotropic composite beams which are treated as assemblies of symmetric angle-ply composite plates buckling under nonlinear varying, uniaxial compressive forces. Reddy and Rehfield [54] investigated the local

buckling and crippling of thin-walled graphite/epoxy I-section beams under axial compression.

During literature survey it has been observed that there is very limited work available regarding the stochastic thin-walled structures. Molnar [55] described the static and dynamic crush tests on a thin-walled prismatic column taking into account imperfections. The crushing process is regarded as a stochastic process, and the results of measurements are reduced using probability methods. Tylinkowski [56] investigated the uniform stochastic stability of thin-walled beams subjected to time and space-dependent broadband stochastic loadings. Arbocz *et al* [57] studied the collapse of axially compressed cylindrical shells with random imperfections. Poggi *et al* [58] presented the application of a probabilistic methodology to the design and analysis of cylindrical shells under axial compression. Yushanov [59] presented an analytical approach based on the theory of stochastic processes developed for the stochastic initial failure analysis and reliability predictions of thin-walled laminated composite structures. Arbocz *et al* [60] presented reliability based, probabilistic design procedure for buckling critical imperfect isotropic shells.

1.3 Scope and objectives of the thesis

In this thesis, the static buckling and dynamic response of beam-columns that have stochastic material and geometric properties, boundary conditions and external loading, and made of polymer-matrix fiber-reinforced composite materials, are determined.

In the free-vibration and global buckling problem, we assume that all coefficients of the governing differential equations and coefficients of boundary conditions have small random perturbations. Hence, perturbation method [6] is applied with good accuracy. Finally, in the local buckling of thin-walled composite beam-columns, we consider the stochastic process that corresponds to the laminate bending stiffness matrix, $[D]$. Here, the energy technique, Ritz method [1] is applied.

The objectives are:

- (1) To obtain the generalized stochastic equations for the mean value, mean square value and variance of the n^{th} natural frequency of the free-vibration of beam-columns made of polymer-matrix fiber-reinforced composite materials when damping is neglected and the axial force is less than the critical buckling load. The material properties, geometric properties and boundary conditions are random functions. Further, the theory is extended to the application to the composite thin-walled beam-columns and probabilistic characteristics of natural frequencies are determined.
- (2) To obtain the generalized stochastic equations for the mean value, mean square value and variance of the critical buckling loads of beam-columns made of polymer-matrix fiber-reinforced composite materials. The material properties, geometric properties and boundary conditions are random functions.
- (3) To obtain the stochastic equations for the mean value and variance of the critical local buckling loads of beam-columns made of polymer-matrix fiber-reinforced

composite materials. Here, we consider the stochastic process that corresponds to the laminate bending stiffness matrix, [D].

- (4) To conduct a parametric study on probabilistic free-vibration and buckling of composite beam-columns for different types of laminate configurations.
- (5) To write computer programs in MATLAB[®] to generate all numerical results in this thesis.

1.4 Organization of the thesis

The present chapter provides a brief introduction and literature survey regarding the probabilistic free vibration and buckling response of beam-columns made of polymer-matrix fiber-reinforced composite materials that were studied using perturbation method, energy methods, finite element method and finite difference method. Further, in this chapter, the scope and objectives of the thesis are provided.

In chapter 2, two different types of one-dimensional analysis i.e. cylindrical bending theory and one-dimensional laminated beam-theory, which are reduced from two-dimensional plate analysis, are summarized for buckling and free-vibration analysis. Further, in this chapter, numerical examples are presented to calculate the critical buckling loads and natural frequencies of the beam-column for different laminate configurations.

In chapter 3, the free vibration response of composite beam-columns is considered and probabilistic characteristics of natural frequencies are determined. The standard perturbation method is employed in the context of stochastic analysis [6]. Further, in this chapter, calculation of equivalent elastic constants for symmetric and un-symmetric laminates is described and also calculation of flexural rigidity for symmetrical bending is summarized. Finally, in this chapter, theory is extended to the application to the composite thin-walled beam-columns and probabilistic characteristics of natural frequencies are determined.

In chapter 4, the buckling response of composite beam-columns is considered and probabilistic characteristics of critical buckling loads are determined. Further, in this chapter, thin-wall composite beam-columns are considered. In the design of thin-walled beam-columns local buckling is of very much importance over the global buckling. Therefore, local buckling response of such composite thin-walled beam-columns is considered and probabilistic characteristics of critical buckling loads are determined. A computer program is written in MATLAB[®] to solve the eigen value problem for the critical buckling load and also to get the stochastic process that corresponds to the bending stiffness matrix, [D].

The thesis ends with chapter 5, which provides the conclusions of the present thesis work and some recommendations for the future work.

Chapter 2

ONE-DIMENSIONAL DETERMINISTIC ANALYSIS

2.1 Introduction

In the present chapter, we are dealing with two different types of one-dimensional analysis, which are reduced from two-dimensional plate analysis. The first type of analysis deals with plates that have very high length-to-width ratio so that deformation of the plate can be considered to be independent of the coordinate along the length of the plate. Such a behavior is called cylindrical bending. The second type of analysis deals with the beam considered to be very narrow in one direction and further, this theory assumes that length is much larger than the width. Such an analysis is called one-dimensional laminated beam theory.

Buckling loads and natural frequencies are calculated using both cylindrical bending and one-dimensional laminated beam theories and further, in this chapter, numerical examples are presented to calculate the critical buckling loads and free-vibration natural frequencies for different types of laminate configurations.

2.2 Cylindrical bending theory

Let us consider a laminate that has arbitrary number of layers that are very long in the y direction as shown in Figure 2.1. The plate is supported along the edges $x = 0$ and $x = a$. If the transverse load is a function of only x , $q = q(x)$, such that the plate deformation is cylindrical, i.e.,

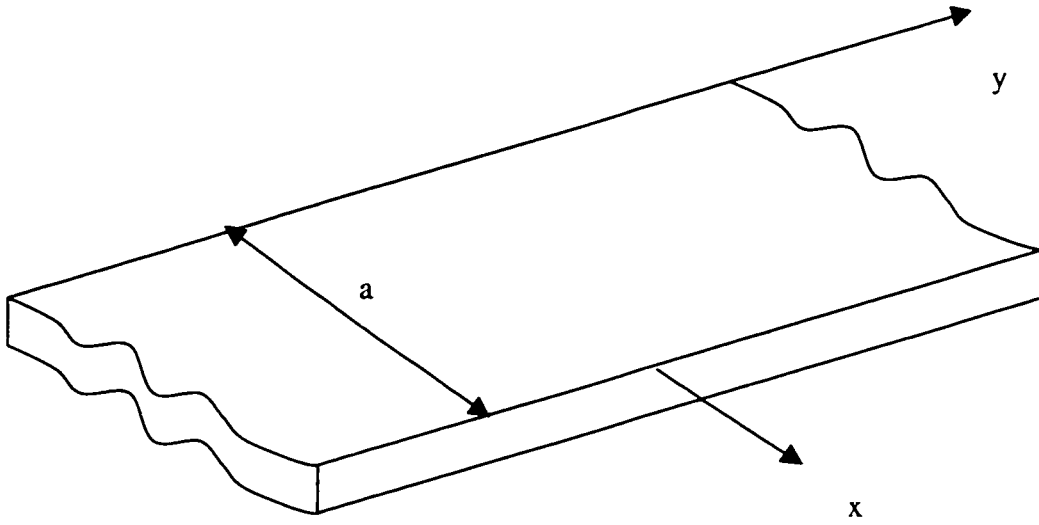


Figure 2.1 A plate with infinite length

$$u_o(x, y, t) = u_o(x, t) \quad (2.1)$$

$$v_o(x, y, t) = v_o(x, t) \quad (2.2)$$

$$w(x, y, t) = w(x, t) \quad (2.3)$$

Consider the following one-dimensional equations of motion [1].

$$A_{11} \frac{d^2 u_o}{dx^2} + A_{16} \frac{d^2 v_o}{dx^2} - B_{11} \frac{d^3 w}{dx^3} - \rho_s \omega^2 u_o = 0 \quad (2.4)$$

$$A_{16} \frac{d^2 u_o}{dx^2} + A_{66} \frac{d^2 v_o}{dx^2} - B_{16} \frac{d^3 w}{dx^3} - \rho_s \omega^2 v_o = 0 \quad (2.5)$$

$$D_{11} \frac{d^4 w}{dx^4} - B_{11} \frac{d^3 u_o}{dx^3} - B_{16} \frac{d^3 v_o}{dx^3} - N_x^i \frac{d^2 w}{dx^2} - q - \rho_s \omega^2 w = 0 \quad (2.6)$$

In the case of static bending, these equations can be uncoupled by deriving the equations for u_o and v_o from Eqs. (2.4) and (2.5) as follows:

$$\frac{d^2 u_o}{dx^2} = \frac{B}{A} \frac{d^3 w}{dx^3} \quad (2.7)$$

$$\frac{d^2 v_o}{dx^2} = \frac{C}{A} \frac{d^3 w}{dx^3} \quad (2.8)$$

Coefficients A, B and C are defined in the following:

$$\begin{aligned} A &= A_{11}A_{66} - A_{16}^2 \\ B &= A_{66}B_{11} - A_{16}B_{16} \\ C &= A_{11}B_{16} - A_{16}B_{11} \end{aligned} \quad (2.9)$$

Differentiating equations (2.7) and (2.8) and substituting the results into Eqn. (2.6), we get the differential equation in w:

$$\frac{D}{A} \frac{d^4 w}{dx^4} = q \quad (2.10)$$

The coefficient D is defined in the following:

$$D = D_{11}A - B_{11}B - B_{16}C \quad (2.11)$$

where,

coefficient A_{ij} is the Axial stiffness,

coefficient B_{ij} is the Axial-bending coupling stiffness, and

coefficient D_{ij} is the Bending stiffness.

2.3 One-dimensional laminated beam theory

Let us consider a laminated beam as shown in Figure 2.2.

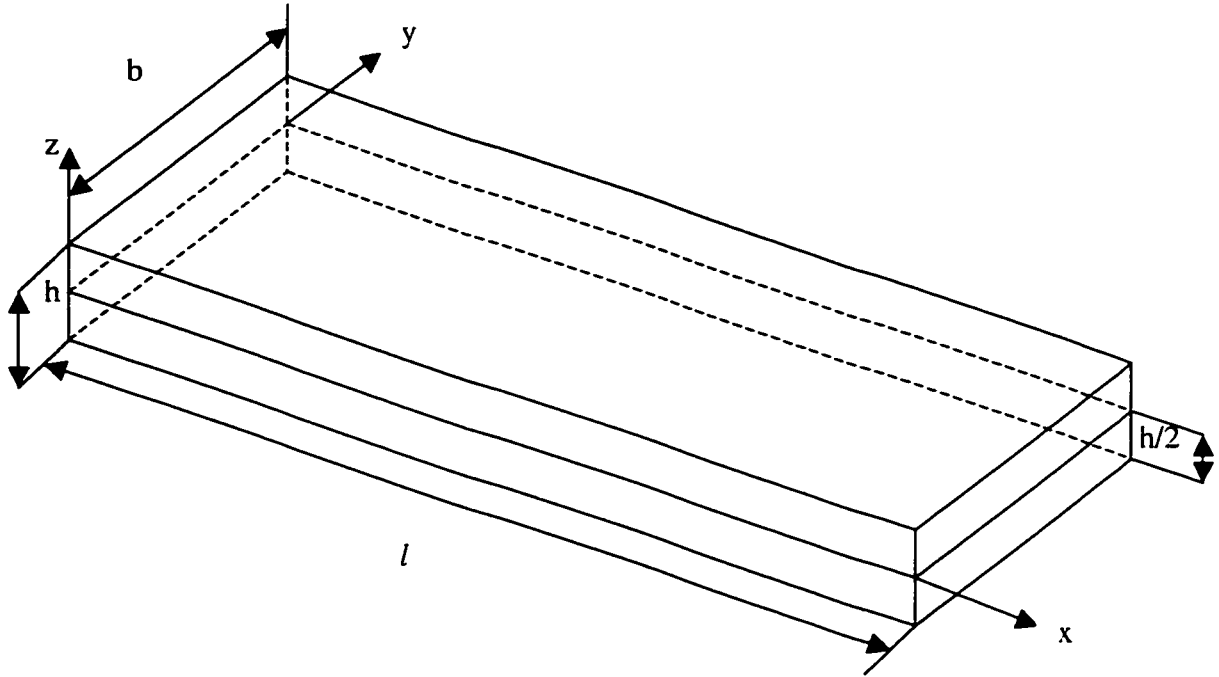


Figure 2.2 Laminated beam

The 1-D laminated beam theory assumes that length is much larger than the width, i.e.,

$$l \gg b.$$

The laminate constitutive equation is given by [1]:

$$\begin{Bmatrix} N_x \\ N_y \\ N_{xy} \\ M_x \\ M_y \\ M_{xy} \end{Bmatrix} = \begin{bmatrix} A_{11} & A_{12} & A_{16} & B_{11} & B_{12} & B_{16} \\ A_{12} & A_{22} & A_{26} & B_{12} & B_{22} & B_{26} \\ A_{16} & A_{26} & A_{66} & B_{16} & B_{26} & B_{66} \\ \hline B_{11} & B_{12} & B_{16} & D_{11} & D_{12} & D_{16} \\ B_{12} & B_{22} & B_{26} & D_{12} & D_{22} & D_{26} \\ B_{16} & B_{26} & B_{66} & D_{16} & D_{26} & D_{66} \end{bmatrix} \begin{Bmatrix} \varepsilon_x^o \\ \varepsilon_y^o \\ \gamma_{xy}^o \\ k_x \\ k_y \\ k_{xy} \end{Bmatrix} \quad (2.12)$$

In the case of pure bending of a symmetric laminate the constitutive equation reduces to:

$$\begin{bmatrix} M_x \\ M_y \\ M_{xy} \end{bmatrix} = \begin{bmatrix} D_{11} & D_{12} & D_{16} \\ D_{12} & D_{22} & D_{26} \\ D_{16} & D_{26} & D_{66} \end{bmatrix} \begin{bmatrix} \kappa_x \\ \kappa_y \\ \kappa_{xy} \end{bmatrix} \quad (2.13)$$

The inverted form of the Eqn. (2.13) can be written as:

$$\begin{bmatrix} \kappa_x \\ \kappa_y \\ \kappa_{xy} \end{bmatrix} = \begin{bmatrix} D_{11}^* & D_{12}^* & D_{16}^* \\ D_{12}^* & D_{22}^* & D_{26}^* \\ D_{16}^* & D_{26}^* & D_{66}^* \end{bmatrix} \begin{bmatrix} M_x \\ M_y \\ M_{xy} \end{bmatrix} \quad (2.14)$$

The beam theory makes the assumption that in the case of bending along the x-axis the moments M_y and M_{xy} are zero:

$$M_y = M_{xy} = 0 \quad (2.15)$$

Substituting Eqn. (2.15) into Eqn. (2.14), then Eqn. (2.14) reduces to

$$\kappa_x = -\frac{\partial^2 w}{\partial x^2} = D_{11}^* M_x \quad (2.16)$$

Further, since the beam has a high length-to-width ratio, it is assumed that

$$w = w(x) \quad (2.17)$$

Combining the equations (2.16) and (2.17), we obtain the following result:

$$\frac{d^2 w}{dx^2} = -D_{11}^* M_x \quad (2.18)$$

The above equation can be written in the form:

$$\frac{d^2 w}{dx^2} = -\frac{M}{E_x^b I} \quad (2.19)$$

where,

The effective bending modulus E_x^b of the beam:

$$E_x^b = \frac{12}{h^3 D_{11}^*} \quad (2.20)$$

The moment of inertia of the cross-section of the beam with respect to the beam (x,y) plane:

$$I = I_{xy} = \frac{bh^3}{12} \quad (2.21)$$

The bending moment M:

$$M = bM_x \quad (2.22)$$

For static bending in the absence of body moments and in-plane force effects the equation of motion becomes [1],

$$\frac{\partial^2 M_x}{\partial x^2} + 2 \frac{\partial^2 M_{xy}}{\partial x \partial y} + \frac{\partial^2 M_y}{\partial y^2} + q = 0 \quad (2.23)$$

Substituting Eqs. (2.16) and (2.17) into Eqn. (2.23), we obtain the following relationship:

$$\frac{1}{D_{11}^*} \frac{d^4 w}{dx^4} = q \quad (2.24)$$

The above equation is analogous to that of the isotropic beam theory, in the sense

that $\frac{b}{D_{11}^*}$ is analogous to the EI.

2.4 Buckling analysis using cylindrical bending theory

Considering cylindrical bending theory, neglecting the in-plane inertia effects and imposing an initial uniform compressive load $N_x^t = -N_o$, Eqn. (2.6) becomes, in the absence of transverse loading, as,

$$D_{11} \frac{d^4 w}{dx^4} - B_{11} \frac{d^3 u_o}{dx^3} - B_{16} \frac{d^3 v_o}{dx^3} + N_o \frac{d^2 w}{dx^2} = 0 \quad (2.25)$$

for the static case.

Differentiating Eqs. (2.7) and (2.8), and substituting the results in Eqn. (2.25), we get the following result:

$$\frac{d^4 w}{dx^4} + \frac{A}{D} N_o \frac{d^2 w}{dx^2} = 0 \quad (2.26)$$

The above equation is used to determine the buckling load.

For simply supported boundary conditions, the following displacements satisfy the equations (2.7), (2.8) and (2.26) and the following are the geometric boundary conditions for the simply supported case.

$$\frac{du_o}{dx} = \frac{dv_o}{dx} = w = \frac{d^2 w}{dx^2} = 0, \text{ at } x = 0, l \quad (2.27)$$

The displacements are

$$u_o = A_m \cos\left(\frac{m\pi x}{l}\right) \quad m = 1, 2, \dots \quad (2.28)$$

$$v_o = B_m \cos\left(\frac{m\pi x}{l}\right) \quad m = 1, 2, \dots \quad (2.29)$$

$$w = C_m \sin\left(\frac{m\pi x}{l}\right) \quad m = 1, 2, \dots \quad (2.30)$$

Substituting the equations (2.28),(2.29), and (2.30) into equations (2.7), (2.8) and (2.26), we get the following equations in the matrix form:

$$\begin{bmatrix} 1 & 0 & -\frac{B}{A}\left(\frac{m\pi}{l}\right) \\ 0 & 1 & -\frac{C}{A}\left(\frac{m\pi}{l}\right) \\ 0 & 0 & \frac{m^4\pi^4}{l^4} - \frac{A}{D}N_o - \frac{m^2\pi^2}{l^2} \end{bmatrix} \begin{bmatrix} A_m \\ B_m \\ C_m \end{bmatrix} = \begin{bmatrix} 0 \\ 0 \\ 0 \end{bmatrix} \quad (2.31)$$

For non-trivial solution,

$$\begin{vmatrix} 1 & 0 & -\frac{B}{A}\left(\frac{m\pi}{l}\right) \\ 0 & 1 & -\frac{C}{A}\left(\frac{m\pi}{l}\right) \\ 0 & 0 & \frac{m^4\pi^4}{l^4} - \frac{A}{D}N_o - \frac{m^2\pi^2}{l^2} \end{vmatrix} = 0 \quad (2.32)$$

Hence, we obtain,

$$\frac{m^4\pi^4}{l^4} - \frac{A}{D}N_o - \frac{m^2\pi^2}{l^2} = 0 \quad (2.33)$$

For $m = 1$, we get the critical buckling load per unit width for simply supported case:

$$N_o = \frac{D \pi^2}{A l^2} \quad (2.34)$$

The critical buckling load for the beam is

$$P_{cr} = \frac{\pi^2}{l^2} b \frac{D}{A} \quad (2.35)$$

For the clamped supports the geometric boundary conditions are:

$$u_o = v_o = w = \frac{dw}{dx} = 0, \text{ at } x = 0, l \quad (2.36)$$

The following displacements satisfy the Eqn. (2.36)

$$u_o = A_m \sin\left(\frac{m\pi x}{l}\right) \quad m = 1, 2, \dots \quad (2.37)$$

$$v_o = B_m \sin\left(\frac{m\pi x}{l}\right) \quad m = 1, 2, \dots \quad (2.38)$$

$$w = C_m \left(1 - \cos 2 \frac{m\pi x}{l}\right) \quad m = 1, 2, \dots \quad (2.39)$$

Substituting the Eqn. (2.39) in Eqn. (2.26), we obtain:

$$\left(\frac{4m^4\pi^4}{l^4} - \frac{A}{D} N_o \frac{m^2\pi^2}{l^2}\right) C_m = 0 \quad (2.40)$$

A non-zero solution of Eqn. (2.40) is obtained in the case where the coefficient of C_m vanishes, which leads to the following expression for the critical buckling load per unit width.

$$N_o = \frac{4\pi^2}{l^2} \frac{D}{A} \quad (2.41)$$

In the case of clamped-free support, the following displacement,

$$w = C_m \left(1 - \cos \frac{m\pi x}{2l} \right) \quad m = 1, 2, \dots \quad (2.42)$$

satisfies the following geometric conditions:

$$w \Big|_{x=0} = \frac{dw}{dx} \Big|_{x=0} = 0, \quad \frac{d^2 w}{dx^2} \Big|_{x=l} = \frac{d^3 w}{dx^3} \Big|_{x=l} = 0 \quad (2.43)$$

Substituting the Eqn. (2.42) in Eqn. (2.26), we obtain:

$$\left(\frac{m^4 \pi^4}{4l^4} - \frac{A}{D} N_o \frac{m^2 \pi^2}{l^2} \right) C_m = 0 \quad (2.44)$$

A non-zero solution of Eqn. (2.44) is obtained in the case where the coefficient of C_m vanishes, which leads to the following expression for the critical buckling load per unit width.

$$N_o = \frac{\pi^2}{4l^2} \frac{D}{A} \quad (2.45)$$

2.5 Buckling analysis using one-dimensional laminated beam theory

Considering the equation of motion [1],

$$\frac{\partial^2 M_x}{\partial x^2} + 2 \frac{\partial^2 M_{xy}}{\partial x \partial y} + \frac{\partial^2 M_y}{\partial y^2} + N_x \frac{\partial^2 w}{\partial x^2} + 2N_{xy} \frac{\partial^2 w}{\partial x \partial y} + N_y \frac{\partial^2 w}{\partial y^2} + q = \rho_s \frac{\partial^2 w}{\partial t^2} \quad (2.46)$$

Considering the Eqn. (2.46) for one-dimensional static case, we get the following equation:

$$\frac{d^2 M_x}{dx^2} + N_x^i \frac{d^2 w}{dx^2} = 0 \quad (2.47)$$

Substituting Eqn. (2.19) in Eqn. (2.47) and taking the in-plane load as uniform compression, $N_x^i = -N_o = \text{constant}$, we obtain the following governing equation:

$$\frac{d^4 w}{dx^4} + \frac{12}{E_x^b h^3} N_o \frac{d^2 w}{dx^2} = 0 \quad (2.48)$$

The above equation is used to determine the buckling load.

For simply supported case, geometric boundary conditions and displacements are given in Eqs. (2.27) to (2.30) respectively.

Substituting the Eqn. (2.30) in Eqn. (2.48), we obtain:

$$\left(\frac{m^4 \pi^4}{l^4} - D_{11}^* N_o \frac{m^2 \pi^2}{l^2} \right) C_m = 0 \quad (2.49)$$

A non-zero solution of Eqn. (2.49) is obtained in the case where the coefficient of C_m vanishes, which leads to the following expression for the critical buckling load per unit width.

$$N_o = \frac{\pi^2}{l^2 D_{11}^*} \quad (2.50)$$

For clamped supported case, geometric boundary conditions and displacements are given in Eqs. (2.36) to (2.39).

Substituting the Eqn. (2.39) in Eqn. (2.48), we obtain:

$$\left(\frac{4m^4\pi^4}{l^4} - D_{11}^* N_o \frac{m^2\pi^2}{l^2} \right) C_m = 0 \quad (2.51)$$

A non-zero solution of Eqn. (2.51) is obtained in the case where the coefficient of C_m vanishes, which leads to the following expression for the critical buckling load per unit width.

$$N_o = \frac{4\pi^2}{l^2 D_{11}^*} \quad (2.52)$$

For clamped-free supported case, displacement and geometric boundary conditions are given in Eqs. (2.42) and (2.43) respectively.

Substituting the Eqn. (2.42) in Eqn. (2.48), we obtain:

$$\left(\frac{m^4\pi^4}{4l^4} - D_{11}^* N_o \frac{m^2\pi^2}{l^2} \right) C_m = 0 \quad (2.53)$$

A non-zero solution of Eqn. (2.53) is obtained in the case where the coefficient of C_m vanishes, which leads to the following expression for the critical buckling load per unit width.

$$N_o = \frac{\pi^2}{4l^2 D_{11}^*} \quad (2.54)$$

2.6 Free-vibration analysis using cylindrical bending theory

Considering cylindrical bending theory, neglecting the in-plane inertia effects and imposing an initial uniform compressive load $N_x^i = -N_o$, Eqn. (2.6) becomes, in the absence of transverse loading, as,

$$D_{11} \frac{d^4 w}{dx^4} - B_{11} \frac{d^3 u_o}{dx^3} - B_{16} \frac{d^3 v_o}{dx^3} + N_o \frac{d^2 w}{dx^2} - \rho_s \omega^2 w = 0 \quad (2.56)$$

Differentiating Eqs. (2.7) and (2.8), and substituting the results in Eqn. (2.56), we get the following result:

$$\frac{d^4 w}{dx^4} + \frac{A}{D} \left(N_o \frac{d^2 w}{dx^2} - \rho_s \omega^2 w \right) = 0 \quad (2.57)$$

The above equation is used to determine the free-vibration response.

For simply supported boundary conditions, the following displacements satisfy the equations (2.7), (2.8) and (2.57) and the following are the geometric boundary conditions for the simply supported case.

$$\frac{du_o}{dx} = \frac{dv_o}{dx} = w = \frac{d^2 w}{dx^2} = 0, \text{ at } x = 0, l \quad (2.58)$$

The displacements are

$$u_o = A_m \cos\left(\frac{m\pi x}{l}\right), v_o = B_m \cos\left(\frac{m\pi x}{l}\right), w = C_m \sin\left(\frac{m\pi x}{l}\right) \quad (2.59) - (2.61)$$

$$m = 1, 2, \dots$$

Substituting the Eqn. (2.61) in Eqn. (2.57), we obtain:

$$\left[\frac{m^4 \pi^4}{l^4} - \frac{A}{D} \left(\rho_s \omega^2 + N_o \frac{m^2 \pi^2}{l^2} \right) \right] C_m = 0 \quad (2.62)$$

A non-zero solution of Eqn. (2.62) is obtained in the case where the coefficient of C_m vanishes, which leads to the following expression for the free-vibration frequency in the presence of an in-plane load N_o , where N_o is less than N_{cr} .

$$\omega_m = \frac{m\pi}{a} \sqrt{\frac{1}{\rho_s} \left(\frac{m^2 \pi^2 D}{l^2 A} - N_o \right)}, \quad N_o > 0 \quad (2.63)$$

2.7 Free-vibration analysis using one-dimensional laminated beam theory

Considering the Eqn. (2.46) for one-dimensional beam theory, we get the following equation:

$$\frac{\partial^2 M_x}{\partial x^2} + N_x^i \frac{\partial^2 w}{\partial x^2} = \rho_s \frac{\partial^2 w}{\partial t^2} \quad (2.64)$$

Substituting Eqn. (2.19) in Eqn. (2.64) and taking the in-plane load as uniform compression, $N_x^i = -N_o = \text{constant}$, we obtain the following governing equation:

$$\frac{\partial^4 w}{\partial x^4} + \frac{12}{E_x^b h^3} \left(\rho_s \frac{\partial^2 w}{\partial t^2} + N_o \frac{\partial^2 w}{\partial x^2} \right) = 0 \quad (2.65)$$

In the above equation, time can be eliminated by assuming

$$w(x,t) = w(x)e^{i\omega t} \quad (2.66)$$

Substituting the above equation in Eqn. (2.65), we obtain:

$$\frac{d^4 w}{dx^4} + \frac{12}{E_r^b h^3} \left(N_o \frac{d^2 w}{dx^2} - \rho_s \omega^2 w \right) = 0 \quad (2.67)$$

The above equation is used to determine the free-vibration response of a laminated beam.

For simply supported case, geometric boundary conditions and displacements are given in Eqs. (2.27) to (2.30).

Substituting the Eqn. (2.30) in Eqn. (2.67), we obtain:

$$\left[\frac{m^4 \pi^4}{l^4} - \frac{12}{E_r^b h^3} \left(N_o \frac{m^2 \pi^2}{l^2} + \rho_s \omega^2 \right) \right] C_m = 0 \quad (2.68)$$

A non-zero solution of Eqn. (2.68) is obtained in the case where the coefficient of C_m vanishes, which leads to the following expression for the free-vibration frequency in the presence of an in-plane load N_o .

$$\omega_n = \frac{m\pi}{l} \sqrt{\frac{1}{\rho_s} \left(\frac{m^2 \pi^2}{l^2 D_{11}^*} - N_o \right)} \quad (2.69)$$

2.8 Numerical examples

Consider a NCT-301 Graphite-Epoxy composite material and consider the material as a 'Transversely-isotropic' [61] material so that $E_2 = E_3$, $\nu_{21} = \nu_{31}$, $\nu_{23} = \nu_{32}$ and $G_{23} = E_{23}/2(1+\nu_{23})$. The deterministic material properties of the NCT-301 material [62] are given as:

$$E_1 = 129.43\text{GPa}, E_2 = 7.99\text{GPa}, \nu_{21} = 0.021 \text{ and } G_{12} = 4.28\text{GPa}.$$

A composite laminate consisting of a total of 36 plies, each having a ply thickness of 0.125 mm is considered, and the dimensions of the composite laminate are shown in the Figure 2.3.

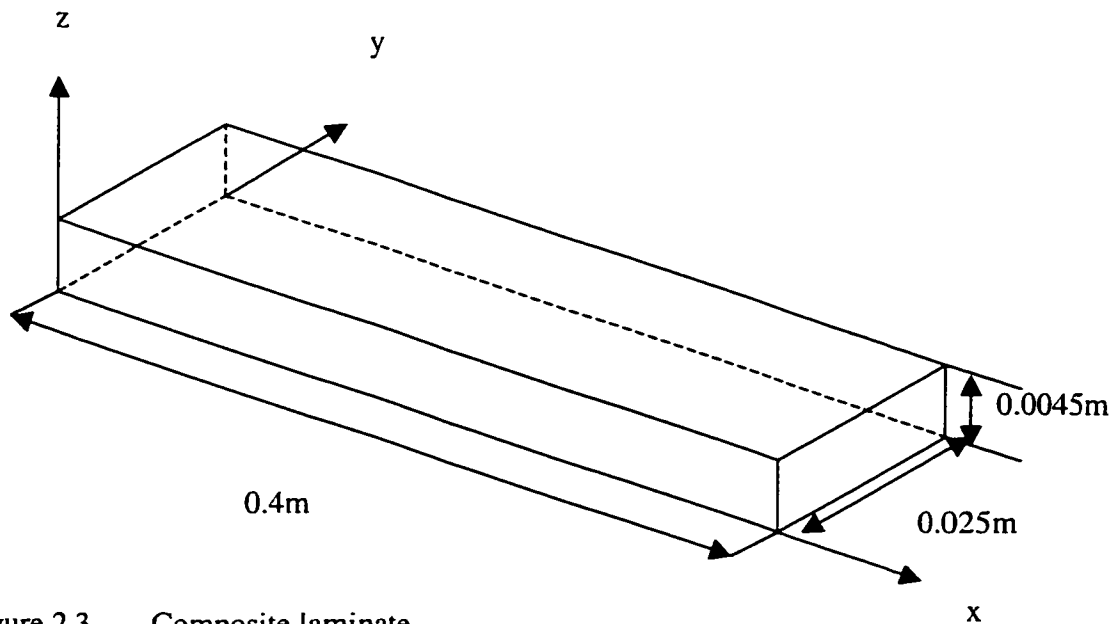


Figure 2.3 Composite laminate

The critical buckling loads and 1st natural frequencies for the different laminate configurations were calculated and they are given in the following Tables:

S.No	Type of Support	Cylindrical bending theory	1-D Laminated beam theory
1	Simply supported	869.80N	856.73N
2	Clamped-Clamped	3479.2N	3426.9N
3	Clamped-Free	217.45N	214.18N

Table 2.1 Buckling loads for symmetric cross-ply laminate $[0/90]_{9s}$

S.No	Type of Support	Cylindrical bending theory	1-D Laminated beam theory
1	Simply supported	470.83N	179.31N
2	Clamped-Clamped	1883.3N	717.26N
3	Clamped-Free	117.70N	44.829N

Table 2.2 Buckling loads for symmetric angle-ply laminate $[+45/-45]_{9s}$

S.No	Type of Support	Cylindrical bending theory	1-D Laminated beam theory
1	Simply supported	715.65N	670.48N
2	Clamped-Clamped	2862.6N	2681.9N
3	Clamped-Free	178.91N	167.62N

Table 2.3 Buckling loads for quasi-isotropic laminate $[0/-60/60]_{6s}$

S.No	Type of support	Cylindrical bending theory	1-D Laminated beam theory
1	Simply supported	996.89N	-----
2	Clamped-Clamped	3987.5N	-----
3	Clamped-Free	249.22N	-----

Table 2.4 Buckling loads for un-symmetric laminate $[0/45]_{18T}$

S.No	Laminate configuration	Cylindrical bending theory	1-D Laminated beam theory
1	$[0/90]_{9s}$	491.59	487.70
2	$[+45/-45]_{9s}$	361.61	222.86
3	$[0/-60/60]_{6s}$	445.88	431.37
4	$[0/45]_{18T}$	526.28	-----

Table 2.5 The 1st natural frequency of free-vibration for given $P_o / P_{cr} = 1/4$

S.No	Laminate configuration	Cylindrical bending theory	1-D Laminated beam theory
1	[0/90] _{9s}	401.38	398.12
2	[+45/-45] _{9s}	295.21	181.82
3	[0/-60/60] _{6s}	364.04	352.11
4	[0/45] _{18T}	429.70	-----

Table 2.6 The 1st natural frequency of free-vibration for given $P_o / P_{cr} = 1/2$

2.9 Conclusions and discussions

From the above results, we can conclude that

- For symmetric cross-ply laminate [0/90]_{9s} , for any boundary conditions, the critical buckling loads calculated using cylindrical bending and 1-D laminated beam theories are close to each other.
- For symmetric angle-ply laminate [+45/-45]_{9s} , for any boundary conditions, the critical buckling loads calculated using cylindrical bending theory are 62% more than that calculated using one-dimensional laminated beam theory.
- For quasi-isotropic laminate [0/-60/60]_{6s} , for any boundary conditions, the critical buckling loads calculated using cylindrical bending theory are 6% more than that calculated using one-dimensional laminated beam theory.

- The largest difference between the critical buckling loads calculated using both the theories is observed in the case of angle-ply laminates.
- The values of buckling loads and natural frequencies of the un-symmetric laminate are the largest.
- For symmetric cross-ply laminate $[0/90]_{9s}$, the natural frequencies calculated using cylindrical bending and 1-D laminated beam theories are close to each other.
- For symmetric angle-ply laminate $[+45/-45]_{9s}$, the natural frequencies calculated using cylindrical bending theory are 38% more than that calculated using one-dimensional laminated beam theory.
- For quasi-isotropic laminate $[0/-60/60]_{6s}$, the natural frequencies calculated using cylindrical bending theory are 3% more than that calculated using one-dimensional laminated beam theory.

Chapter 3

FREE-VIBRATION RESPONSE OF COMPOSITE BEAM-COLUMNS WITH STOCHASTIC PROPERTIES

3.1 Introduction

Composite laminates display significant variability in their material, geometric and structural properties. This variability is attributed to the variations in the properties of the fibers, matrices and interfaces, in the fiber orientations, in the void content, in the ply thickness and so on. These variations are unavoidable and are induced during manufacturing and service. Therefore, in the design and failure prediction these variations have to be taken into account. Beam-columns made of polymer-matrix fiber-reinforced composite materials are increasingly being used in automotive, aerospace, structural and mechanical engineering industries. Such structures operate in most cases in a dynamic loading environment and hence, their vibration response is of paramount importance in the design and development of high-performance composite mechanical components.

In the present chapter, the free vibration response of such composite beam-columns is considered and probabilistic characteristics of natural frequencies are determined. The standard perturbation method is employed in the context of stochastic analysis [6]. Further, in this chapter, the theory for beam-columns with solid cross-sections is

extended to the composite thin-walled beam-columns and probabilistic characteristics of natural frequencies are determined.

In section 3.2, formulation for the free vibration of composite beam-column is developed. In section 3.3, parametric study has been performed on symmetric cross-ply laminate $[0/90]_{9s}$, symmetric angle-ply laminate $[+45/-45]_{9s}$, quasi isotropic laminate $[0/-60/60]_{6s}$, and unsymmetric laminate $[0/45]_{18T}$ corresponding to cylindrical bending and one-dimensional laminated beam theories. In section 3.4, the procedures for calculating equivalent elastic constants for symmetric and unsymmetric laminates are summarized. In section 3.5, calculation of flexural rigidity for symmetric bending is summarized. In section 3.6, a general formulation for the free vibration problem is stated. In section 3.7, a parametric study is performed on symmetric I-section with flanges made up of symmetric angle-ply laminate $[+45/-45]_{9s}$ and with web made up of un-symmetric laminate $[0/45]_{18T}$.

3.2 Formulation for the free-vibration of composite beam-column

Let us consider the free vibration of composite beam-columns that have a stochastic distribution of material properties and geometric boundary conditions. A composite beam-column with axial compressive force and generalized boundary conditions is shown in Figure 3.1.

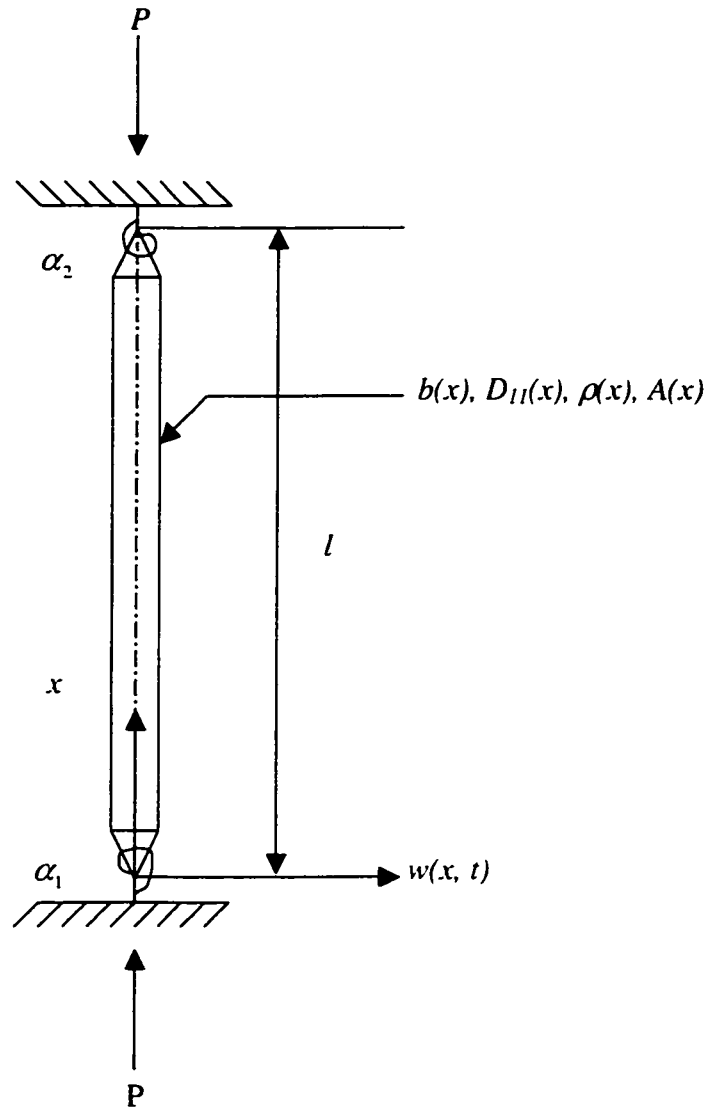


Figure 3.1 Composite beam-column

The formulation is based on the following assumptions that are customarily made in the dynamics of continuous structures.

- (1) The beam-column is initially straight.
- (2) The lateral deflection $w(x,t)$ of the beam-column axis and the cross-sectional dimensions are small compared to the length of the beam-column.

- (3) Stresses are sufficiently small to warrant the assumption of linear elasticity.
- (4) The shear and rotatory inertia effects are neglected.
- (5) The axial compressive load P is less than the critical buckling load.

With the above basic assumptions, the partial differential equation describing the free dynamic response of a beam-column made of fiber-reinforced composite laminate is given below [2]:

$$\frac{\partial^2}{\partial x^2} \left[b(x)D_{11}(x) \frac{\partial^2 w(x,t)}{\partial x^2} \right] + P \frac{\partial^2 w(x,t)}{\partial x^2} + \rho(x)A(x) \frac{\partial^2 w(x,t)}{\partial t^2} = 0 \quad (3.1)$$

The generalized boundary conditions are given by

$$\left[b(0)D_{11}(0) \frac{\partial^2 w(0,t)}{\partial x^2} \right] - \alpha_1 \frac{\partial w(0,t)}{\partial x} = 0 \quad (3.2)$$

$$w(0,t) = 0 \quad (3.3)$$

$$\left[b(l)D_{11}(l) \frac{\partial^2 w(l,t)}{\partial x^2} \right] + \alpha_2 \frac{\partial w(l,t)}{\partial x} = 0 \quad (3.4)$$

$$w(l,t) = 0 \quad (3.5)$$

In the above, $w(x,t)$ is the lateral displacement as a function of spatial coordinate x and time t , $b(x)$ is the width of the laminate as a function of x , $D_{11}(x)$ is the laminate bending

stiffness coefficient as a function of x , P is the axial compressive force, $\rho(x)$ is the density of the material as a function of x , $A(x)$ is the cross-sectional area of the laminate as a function of x , α_1 and α_2 are the coefficients of boundary rigidities and l is the length of the beam-column.

If α_1 and α_2 are zero, Eqs. (3.2) to (3.5) become simply supported boundary conditions, and if α_1 and α_2 are infinity they represent clamped end conditions. In fact, Eqs. (3.2) to (3.5) indicate that the moment is proportional to the slope at the end. Therefore they are generalized boundary conditions.

In the above equations, when the cylindrical bending theory [1] is used, the term D_{11} is set to be equal to D/A , where D/A is a function of membrane, coupling and bending stiffness terms [1]. When the one-dimensional laminated beam theory [1] is used, the term D_{11} is set to be equal to $1/D_{11}^*$, where D_{11}^* is a bending compliance coefficient [1].

Since the coefficients of Eqs. (3.1) to (3.5) are random or probabilistic, then the natural frequencies and the modes of vibration are also random. Hence the problem has to be analyzed using a probabilistic approach. The response can be evaluated in the form of mean values, mean square values and variances of natural frequencies. Such results give enough information for engineering interest.

The following assumptions are made on the stochastic coefficients and random variables:

(1) Parameters $b(x)$, $D_{11}(x)$, $\rho(x)$, $A(x)$ are stationary random functions of spatial coordinate x and can be put in the following forms:

$$D_{11}(x) = D_{11o} [1 + a(x)] \quad (3.6)$$

$$b(x) = b_o [1 + b_1(x)] \quad (3.7)$$

$$\rho(x) = \rho_o [1 + c(x)] \quad (3.8)$$

$$A(x) = A_o [1 + d(x)] \quad (3.9)$$

where $a(x), b_1(x), c(x)$ and $d(x)$ are non-dimensional stationary random functions with zero mean and very small perturbations (i.e. variance is small compared to 1) and D_{11o}, b_o, ρ_o , and A_o are the mean values that are independent of x .

(2) The random boundary rigidity coefficients α_1 and α_2 are expressed as:

$$\alpha_1 = \alpha_{1o} (1 + s) \quad (3.10)$$

$$\alpha_2 = \alpha_{2o} (1 + u) \quad (3.11)$$

where s and u are the non-dimensional random variables with zero mean and small perturbations, and α_{1o} and α_{2o} are the mean values of α_1 and α_2 respectively.

(3) P is a random variable with respect to its magnitude but independent of time with the following property:

$$P = P_o (1 + v) \quad (3.12)$$

where v is the non-dimensional random variable with zero mean and small perturbations, and P_o is the mean value of P .

(4) Random functions $b_1(x)$ and $d(x)$ are statistically independent of $a(x)$ and $c(x)$ because of obvious reason that material properties are independent of geometric properties.

(5) Similarly s , u , and v are mutually independent variables.

(6) The random variables s , u , and v are independent of the stochastic functions $a(x)$, $b_1(x)$, $c(x)$, and $d(x)$.

Since we are using the perturbation method it is essential that the variances of $a(x)$, $b_1(x)$, $c(x)$, $d(x)$, s , u and v are small compared to unity. Due to this assumption, we can neglect the terms of higher order in the series of power of the small parameters. Due to stationarity assumption for $a(x)$, $b_1(x)$, $c(x)$, and $d(x)$, the probability distribution functions for these variables are independent of x , and they are distributed over the range $(-\infty, +\infty)$.

Random variable v , which is associated with axial load P , has zero mean and very small variance compared to unity. Thus, there is almost zero probability that the axial load will exceed the critical buckling load due to randomness in P .

Let us consider now values of $D_{11}(x)$ at two different locations along the length of the beam-column. Thus, at $x = x_1$, the value of $D_{11}(x) = D_{11}(x_1)$ and at $x = x_2$, the value of $D_{11}(x) = D_{11}(x_2)$. Suppose if $(x_1 - x_2)$ is very small, then the two values $D_{11}(x_1)$ and $D_{11}(x_2)$ may be highly correlated. If $(x_1 - x_2)$ is very large, then the two values $D_{11}(x_1)$ and $D_{11}(x_2)$ will be statistically independent. Further discussions about correlation i.e. high correlation or weak correlation are given in detail in the parametric study.

3.2.1 General solution to the stochastic equation

The solution for the Eqn. (3.1) is assumed to be of the form

$$w(x, t) = \sum_{n=1}^{\infty} X_n(x) T_n(t) \quad (3.13)$$

where $T_n(t)$ are unknown time dependent functions, $X_n(x)$ are the space dependent normal modes, forming a complete set and satisfying the boundary conditions. These modes are obtained by introducing Eqn. (3.13) into the governing Eqn. (3.1):

$$\left[b(x) D_{11}(x) X_n''(x) T_n(t) \right] + P X_n'(x) T_n(t) + \rho(x) A(x) X_n(x) \ddot{T}_n(t) = 0 \quad (3.14)$$

In the above equation, the prime denotes differentiation with respect to space and the overdot symbol denotes differentiation with respect to time.

The above equation can be written as,

$$\frac{\left[b(x) D_{11}(x) X_n''(x) \right] + P X_n'(x)}{\rho(x) A(x) X_n(x)} = - \frac{\ddot{T}_n(t)}{T_n(t)} = \omega_n^2 \quad (3.15)$$

where ω_n is the natural frequency of free vibration.

Hence we have the following differential equation for $X_n(x)$

$$\left[b(x) D_{11}(x) X_n''(x) \right] + P X_n'(x) - \rho(x) A(x) \omega_n^2 X_n(x) = 0 \quad (3.16)$$

Now let us convert independent variable x to ξ using the expression $\xi = x/l$. Then we have a non-dimensionalized eigen value problem, which is given by

$$\left[b(\xi) D_{11}(\xi) X_n^-(\xi) \right]'' + Pl^2 X_n^-(\xi) - \rho(\xi) A(\xi) l^4 \omega_n^2 X_n^-(\xi) = 0 \quad (3.17)$$

and the corresponding boundary conditions are given by

$$b(0) D_{11}(0) X_n^-(0) - l\alpha_1 X_n^-(0) = 0 \quad (3.18)$$

$$X_n^-(0) = 0 \quad (3.19)$$

$$b(1) D_{11}(1) X_n^-(1) + l\alpha_2 X_n^-(1) = 0 \quad (3.20)$$

$$X_n^-(1) = 0 \quad (3.21)$$

Now substituting Eqs. (3.6) to (3.12) in the governing differential Eqn. (3.17) and boundary conditions given by Eqs. (3.18) to (3.21), we obtain the following stochastic equation

$$\left\{ [1 + R(\xi)] X_n^-(\xi) \right\}'' + P_o G(1 + \nu) X_n^-(\xi) = \lambda_n [1 + S(\xi)] X_n^-(\xi) \quad (3.22)$$

where λ_n is the non-dimensional function of the natural frequency ω_n and is given by

$$\lambda_n = \frac{\rho_o A_o l^4 \omega_n^2}{b_o D_{11o}} \quad (3.23)$$

Further,

$$G = \frac{l^2}{b_o D_{11o}} \quad (3.24)$$

$$R(\xi) = a(\xi) + b_1(\xi) + a(\xi)b_1(\xi) \quad (3.25)$$

$$S(\xi) = c(\xi) + d(\xi) + c(\xi)d(\xi) \quad (3.26)$$

The boundary conditions are given by

$$(1 + R(0))X_n''(0) - \frac{l\alpha_{1\omega}}{b_o D_{11\omega}}(1 + s)X_n'(0) = 0 \quad (3.27)$$

$$X_n(0) = 0 \quad (3.28)$$

$$(1 + R(1))X_n''(1) + \frac{l\alpha_{2\omega}}{b_o D_{11\omega}}(1 + u)X_n'(1) = 0 \quad (3.29)$$

$$X_n(1) = 0 \quad (3.30)$$

where

$$R(0) = q = a(0) + b_1(0) + a(0)b_1(0) \quad (3.31)$$

$$R(1) = r = a(1) + b_1(1) + a(1)b_1(1) \quad (3.32)$$

$R(\xi)$ and $S(\xi)$ are random functions of $a(\xi)$, $b_1(\xi)$, $c(\xi)$ and $d(\xi)$. Therefore for fixed co-coordinate ξ , they become random variables. Hence q and r are random variables. Because of our assumptions, mean values of $R(\xi)$ and $S(\xi)$ are zero, so we have zero mean for q and r .

λ_n is the non-dimensional function of the natural frequency ω_n . The probabilistic parameters of λ_n will be of interest since the probabilistic parameters of the natural frequency ω_n can be obtained from Eqn. (3.23).

It is assumed that all coefficients of the governing differential equation and boundary conditions have small random perturbations. Therefore perturbation method can be applied to the following problem with satisfactory accuracy.

Now let us consider the modified differential equation by assigning parameters for perturbation analysis, α and β to Eqn. (3.22):

$$\left\{ [1 + \alpha R(\xi)] X_n(\xi) \right\}'' + P_o G(1 + \nu) X_n(\xi) = \lambda_n [1 + \beta S(\xi)] X_n(\xi) \quad (3.33)$$

At the end of the analysis, α and β are set to be equal to 1.

Now let us assume the solutions λ_n and the corresponding modes $X_n(\xi)$ of the above Eqn. (3.33) and the boundary conditions (3.27) to (3.30) in the following expanded forms.

$$\lambda_n = \lambda_{n0} + \lambda_{n1} \alpha + \lambda_{n2} \beta + \lambda_{n3} q + \lambda_{n4} r + \lambda_{n5} s + \lambda_{n6} u + \lambda_{n7} v \quad (3.34)$$

$$X_n(\xi) = X_{n0}(\xi) + X_{n1}(\xi) \alpha + X_{n2}(\xi) \beta + X_{n3}(\xi) q + X_{n4}(\xi) r + X_{n5}(\xi) s + X_{n6}(\xi) u + X_{n7}(\xi) v \quad (3.35)$$

Now, substitute Eqs. (3.34) and (3.35) in the modified governing Eqn. (3.33) and boundary conditions (3.27) to (3.30). The coefficients of each power of $\alpha, \beta \dots$ in the resulting equations can be clubbed together and considering the linear terms only (neglecting higher order terms), this gives the differential equations for $X_i(\xi) : i=0,1 \dots 7$ which are

$$X_{no}^-(\xi) + P_o G X_{no}^-(\xi) = \lambda_{no} X_{no}(\xi) \quad (3.36)$$

$$\begin{aligned} R^-(\xi) X_{no}^-(\xi) + 2R^-(\xi) X_{no}^-(\xi) + X_{n1}^-(\xi) + R(\xi) X_{no}^-(\xi) + P_o G X_{n1}^-(\xi) \\ = \lambda_{n1} X_{no}(\xi) + \lambda_{no} X_{n1}(\xi) \end{aligned} \quad (3.37)$$

$$X_{n2}^-(\xi) + P_o G X_{n2}^-(\xi) = \lambda_{n2} X_{no}(\xi) + \lambda_{no} X_{no}(\xi) S + \lambda_{no} X_{n2}(\xi) \quad (3.38)$$

$$X_{n3}^-(\xi) + P_o G X_{n3}^-(\xi) = \lambda_{n3} X_{no}(\xi) + \lambda_{no} X_{n3}(\xi) \quad (3.39)$$

$$X_{n4}^-(\xi) + P_o G X_{n4}^-(\xi) = \lambda_{n4} X_{no}(\xi) + \lambda_{no} X_{n4}(\xi) \quad (3.40)$$

$$X_{n5}^-(\xi) + P_o G X_{n5}^-(\xi) = \lambda_5 X_{no}(\xi) + \lambda_{no} X_{n5}(\xi) \quad (3.41)$$

$$X_{n6}^-(\xi) + P_o G X_{n6}^-(\xi) = \lambda_6 X_{no}(\xi) + \lambda_{no} X_{n6}(\xi) \quad (3.42)$$

$$X_{n7}^-(\xi) + P_o G (X_{no}^-(\xi) + X_{n7}^-(\xi)) = \lambda_7 X_{no}(\xi) + \lambda_{no} X_{n7}(\xi) \quad (3.43)$$

The boundary conditions are

$$X_{no}^-(0) - \frac{\alpha_{1o} l}{b_o D_{11o}} X_{no}^-(0) = 0 \quad (3.44)$$

$$X_{n1}^-(0) - \frac{\alpha_{1o} l}{b_o D_{11o}} X_{n1}^-(0) = 0 \quad (3.45)$$

$$X_{n2}^-(0) - \frac{\alpha_{1o} l}{b_o D_{11o}} X_{n2}^-(0) = 0 \quad (3.46)$$

$$X_{no}^-(0) + X_{n3}^-(0) - \frac{\alpha_{1o} l}{b_o D_{11o}} X_{n3}^-(0) = 0 \quad (3.47)$$

$$X_{n4}^-(0) - \frac{\alpha_{1o} l}{b_o D_{11o}} X_{n4}^-(0) = 0 \quad (3.48)$$

$$X_{n5}^-(0) - \frac{\alpha_{1o} l}{b_o D_{11o}} [X_{no}^-(0) + X_{n5}^-(0)] = 0 \quad (3.49)$$

$$X_{n6}^-(0) - \frac{\alpha_{1o}l}{b_o D_{11o}} X_{n6}^{\cdot}(0) = 0 \quad (3.50)$$

$$X_{n7}^-(0) - \frac{\alpha_{1o}l}{b_o D_{11o}} X_{n7}^{\cdot}(0) = 0 \quad (3.51)$$

$$X_o(0) = X_1(0) = X_o(0) = X_2(0) = X_3(0) = X_4(0) = X_5(0) = X_6(0) \\ = X_7(0) = 0 \quad (3.52)$$

$$X_{no}^-(1) + \frac{\alpha_{2o}l}{b_o D_{11o}} X_{no}^{\cdot}(1) = 0 \quad (3.53)$$

$$X_{n1}^-(1) + \frac{\alpha_{2o}l}{b_o D_{11o}} X_{n1}^{\cdot}(1) = 0 \quad (3.54)$$

$$X_{n2}^-(1) + \frac{\alpha_{2o}l}{b_o D_{11o}} X_{n2}^{\cdot}(1) = 0 \quad (3.55)$$

$$X_{n3}^-(1) + \frac{\alpha_{2o}l}{b_o D_{11o}} X_{n3}^{\cdot}(1) = 0 \quad (3.56)$$

$$X_{no}^-(1) + X_{n4}^-(1) + \frac{\alpha_{2o}l}{b_o D_{11o}} X_{n4}^{\cdot}(1) = 0 \quad (3.57)$$

$$X_{n5}^-(1) + \frac{\alpha_{2o}l}{b_o D_{11o}} X_{n5}^{\cdot}(1) = 0 \quad (3.58)$$

$$X_{n6}^-(1) + \frac{\alpha_{2o}l}{b_o D_{11o}} [X_{n0}^{\cdot}(1) + X_{n6}^{\cdot}(1)] = 0 \quad (3.59)$$

$$X_{n7}^-(1) + \frac{\alpha_{2o}l}{b_o D_{11o}} X_{n7}^{\cdot}(1) = 0 \quad (3.60)$$

$$X_{no}(1) = X_{n1}(1) = X_{n2}(1) = X_{n3}(1) = X_{n4}(1) = X_{n5}(1) = X_{n6}(1) = \\ X_{n7}(1) = 0 \quad (3.61)$$

Now, $X_{no}(\xi)$ and λ_{no} can be determined from Eqn. (3.36) and boundary conditions (3.44), (3.52), (3.53), and (3.61). Multiplying Eqn. (3.37) by $X_{no}(\xi)$ and then integrating it from 0 to 1 leads to

$$\begin{aligned}
& \int_0^1 R^-(\xi) X_{no}^-(\xi) X_{no}(\xi) d\xi + \int_0^1 2R^-(\xi) X_{no}^-(\xi) X_{no}(\xi) d\xi + \int_0^1 X_{n1}^-(\xi) X_{no}(\xi) d\xi \\
& + \int_0^1 R^-(\xi) X_{no}^-(\xi) X_{no}(\xi) d\xi + P_o G X_{n1}^-(\xi) X_{no}(\xi) d\xi \\
& = \int_0^1 \lambda_{n1} X_{no}^2(\xi) d\xi + \int_0^1 \lambda_{no} X_{n1}(\xi) X_{no}(\xi) d\xi
\end{aligned} \tag{3.62}$$

The third and fifth terms of the left-hand side and second term of the right hand side are cancelled out because $X_{no}(\xi)$ satisfies the Eqn. (3.36). so from Eqn. (3.62) we can get the value of λ_{n1} . Hence we have

$$\lambda_{n1} = \frac{\int_0^1 R^-(\xi) X_{no}^-(\xi) X_{no}(\xi) d\xi + \int_0^1 2R^-(\xi) X_{no}^-(\xi) X_{no}(\xi) d\xi + \int_0^1 R^-(\xi) X_{no}^-(\xi) X_{no}(\xi) d\xi}{\int_0^1 X_{no}^2(\xi) d\xi} \tag{3.63}$$

Similarly if we solve for other terms $\lambda_{n1}, \lambda_{n2}, \dots, \lambda_{n7}$ one can get the non-dimensionalized natural frequencies.

$$\lambda_{n2} = -\frac{\lambda_{no} \int_0^1 S(\xi) X_{no}^2(\xi) d\xi}{\int_0^1 X_{no}^2(\xi) d\xi} \quad (3.64)$$

$$\lambda_{n3} = -\frac{X_{no}^{\cdot\cdot}(0) X_{no}^{\cdot}(0)}{\int_0^1 X_{no}^2(\xi) d\xi} \quad (3.65)$$

$$\lambda_{n4} = \frac{X_{no}^{\cdot\cdot}(1) X_{no}^{\cdot}(1)}{\int_0^1 X_{no}^2(\xi) d\xi} \quad (3.66)$$

$$\lambda_{n5} = \frac{\alpha_{1o} l}{b_o D_{11o}} \frac{[X_{no}^{\cdot}(0)]^2}{\int_0^1 X_{no}^2(\xi) d\xi} \quad (3.67)$$

$$\lambda_{n6} = \frac{\alpha_{2o} l}{b_o D_{11o}} \frac{[X_{no}^{\cdot}(1)]^2}{\int_0^1 X_{no}^2(\xi) d\xi} \quad (3.68)$$

$$\lambda_{n7} = \frac{P_o l^2}{b_o D_{11o}} \frac{\int_0^1 X_{no}^{\cdot}(\xi) X_{no}(\xi) d\xi}{\int_0^1 X_{no}^2(\xi) d\xi} \quad (3.69)$$

Substituting Eqs. (3.63) to (3.69) into Eqn. (3.34) and substituting $\alpha = \beta = 1$, after some simplification the expression for the non-dimensional natural frequency λ_n is obtained.

$$\begin{aligned} \lambda_n = & \lambda_{no} + \frac{1}{D_n} \int_0^1 R(\xi) I_n(\xi) d\xi - \frac{\lambda_{no}}{D_n} \int_0^1 S(\xi) F_n(\xi) d\xi + \frac{\alpha_{1o} l}{b_o D_{11o}} \frac{H_n(0)}{D_n} s \\ & + \frac{\alpha_{2o} l}{b_o D_{11o}} \frac{H_n(1)}{D_n} u + \frac{P_o l^2}{b_o D_{11o}} \frac{E_n}{D_n} v + \dots \end{aligned} \quad (3.70)$$

where,

$$D_n = \int_0^1 X_{no}^2(\xi) d\xi \quad (3.71)$$

$$E_n = \int_0^1 X_{no}'(\xi) X_{no}(\xi) d\xi \quad (3.72)$$

$$F_n(\xi) = X_{no}^2(\xi) \quad (3.73)$$

$$H_n(\xi) = [X_{no}'(\xi)]^2 \quad (3.74)$$

$$I_n(\xi) = [X_{no}^-(\xi)]^2 \quad (3.75)$$

From Eqn. (3.70), it can be seen that λ_n is composed of the following terms. The first term λ_{no} is independent of any random function or random variable and can be obtained by solving the deterministic eigen value problem. The second and third terms represent terms of random coefficients contained in the governing differential equation; fourth and fifth terms are for boundary rigidity and last term is for compressive axial force.

Now taking the expected value of λ_n from Eqn. (3.70), we obtain the expected value of λ_n in the following form.

$$\begin{aligned} E(\lambda_n) = & \lambda_{no} + \frac{1}{D_n} \int_0^1 E[R(\xi)] I_n(\xi) d\xi - \frac{\lambda_{no}}{D_n} \int_0^1 E[S(\xi)] F_n(\xi) d\xi + \frac{\alpha_{1o} l}{b_o D_{11o}} \frac{H_n(0)}{D_n} E(s) \\ & + \frac{\alpha_{2o} l}{b_o D_{11o}} \frac{H_n(1)}{D_n} E(u) + \frac{P_o l^2}{b_o D_{11o}} \frac{E_n}{D_n} E(v) \end{aligned} \quad (3.76)$$

According to our assumptions the mean values of $a(\xi), b_1(\xi), c(\xi), d(\xi), s, u$ and v are zero. Hence we have,

$$E[R(\xi)] = E[a(\xi)] + E[b_1(\xi)] + E[a(\xi)]E[b_1(\xi)] = 0 \quad (3.77)$$

$$E[S(\xi)] = E[c(\xi)] + E[d(\xi)] + E[c(\xi)]E[d(\xi)] = 0 \quad (3.78)$$

and also

$$E[s] = E[u] = E[v] = 0 \quad (3.79)$$

Therefore Eqn. (3.76) is simplified into

$$E[\lambda_n] = \lambda_{no} \quad (3.80)$$

We note from Eqn. (3.80) that the expected value of λ_n is independent of any random inputs.

Now we will find the expected value of ω_n . Since from Eqn. (3.23), we have

$$\omega_n = \sqrt{\left(\frac{b_o D_{11_o}}{\rho_o A_o l^4}\right)} \lambda_n \quad (3.81)$$

Let

$$k = \frac{\rho_o A_o l^4}{b_o D_{11_o}} \quad (3.82)$$

Therefore Eqn. (3.81) becomes

$$\omega_n = \sqrt{\frac{\lambda_n}{k}} \quad (3.83)$$

From reference [63], we have the following relation:

$$E[\sqrt{\lambda_n}] \approx \sqrt{\frac{1}{2} \left[E[\lambda_n] + \sqrt{(E[\lambda_n])^2 - \text{var}[\lambda_n]} \right]} \quad (3.84)$$

Now by performing expectation operation on both sides of Eqn. (3.83) and using the above Eqn. (3.84), we obtain the following expected value of natural frequency.

$$E[\omega_n] \approx \sqrt{\frac{b_o D_{11_o}}{\rho_o A_o l^4}} * \sqrt{\frac{1}{2} \left[E[\lambda_n] + \sqrt{(E[\lambda_n])^2 - \text{var}[\lambda_n]} \right]} \quad (3.85)$$

By using Eqn. (3.70), we calculate λ_n^2 . Then introducing the statistical treatment to λ_n^2 , we obtain the following relation for mean square value.

$$\begin{aligned} E(\lambda_n^2) &= \lambda_{no}^2 + \frac{1}{D_n^2} \int_0^1 \int_0^1 E[R(\xi_1)R(\xi_2)]I_n(\xi_1)I_n(\xi_2)d\xi_1d\xi_2 \\ &+ \frac{\lambda_{no}^2}{D_n^2} \int_0^1 \int_0^1 E[S(\xi_1)S(\xi_2)]F_n(\xi_1)F_n(\xi_2)d\xi_1d\xi_2 \\ &- \frac{2\lambda_{no}}{D_n^2} \int_0^1 \int_0^1 E[R(\xi_1)S(\xi_2)]U_n(\xi_1)F_n(\xi_2)d\xi_1d\xi_2 + \left(\frac{\alpha_{1o}l}{b_o D_{11_o}} \right)^2 \frac{H_n^2(0)}{D_n^2} \sigma_s^2 + \\ &\left(\frac{\alpha_{2o}l}{b_o D_{11_o}} \right)^2 \frac{H_n^2(1)}{D_n^2} \sigma_u^2 + \left(\frac{P_o l^2}{b_o D_{11_o}} \right)^2 \frac{E_n^2}{D_n^2} \sigma_v^2 \end{aligned} \quad (3.86)$$

In obtaining the above Eqn. (3.86), the following equations have been used.

$$\begin{aligned} E[sR(\xi)] &= E[s]E[R(\xi)] = 0 \\ E[uR(\xi)] &= E[vR(\xi)] = E[sS(\xi)] = E[uS(\xi)] = E[vS(\xi)] = 0 \\ E[su] &= E[sv] = E[uv] = 0 \end{aligned} \quad (3.87)$$

The above equations arise due to the property of statistical independence.

The variance of λ_n is given by

$$\begin{aligned}
\text{var}[\lambda_n] &= E[\lambda_n^2] - [E(\lambda_n)]^2 \\
&= \frac{1}{D_n^2} \int_0^1 \int_0^1 E[R(\xi_1)R(\xi_2)]I_n(\xi_1)I_n(\xi_2)d\xi_1d\xi_2 \\
&\quad + \frac{\lambda_{no}^2}{D_n^2} \int_0^1 \int_0^1 E[S(\xi_1)S(\xi_2)]F_n(\xi_1)F_n(\xi_2)d\xi_1d\xi_2 \\
&\quad - \frac{2\lambda_{no}}{D_n^2} \int_0^1 \int_0^1 E[R(\xi_1)S(\xi_2)]I_n(\xi_1)F_n(\xi_2)d\xi_1d\xi_2 \\
&\quad \left(\frac{\alpha_{o1}l}{b_o D_{11_o}} \right)^2 \frac{H_n^2(0)}{D_n^2} \sigma_s^2 + \left(\frac{\alpha_{o2}l}{b_o D_{11_o}} \right)^2 \frac{H_n^2(1)}{D_n^2} \sigma_u^2 + \left(\frac{P_o l^2}{b_o D_{11_o}} \right)^2 \frac{E_n^2}{D_n^2} \sigma_v^2
\end{aligned} \tag{3.88}$$

From reference [63], we have the following relation:

$$\sigma[\sqrt{\lambda_n}] \approx \frac{1}{2} \left(\frac{\sigma[\lambda_n]}{E[\lambda_n]} \right) \tag{3.89}$$

By performing the operations leading to variance values on both sides of Eqn. (3.83) and using the above Eqn. (3.89), we obtain the following relation for variance of natural frequency.

$$\text{var}[\omega_n] \approx \text{var} \left[\sqrt{\frac{\lambda_n}{k}} \right] = \frac{b_o D_{11_o}}{\rho_o A_o l^4} \text{var}[\sqrt{\lambda_n}] \tag{3.90}$$

Note: According the properties of variance,

$$\text{var}[cX] = c^2 \text{var}[X] \tag{3.91}$$

where c is a constant and X is a random variable

In Eqn. (3.88) for variance the terms σ_s^2, σ_u^2 and σ_v^2 are the variances of s, u and v respectively. Terms $E[R(\xi_1)R(\xi_2)]$ and $E[S(\xi_1)S(\xi_2)]$ are auto-correlation functions and term $E[R(\xi_1)S(\xi_2)]$ is cross-correlation function.

Since we assumed the stationarity property of random processes, the above terms are functions of $(\xi_1 - \xi_2)$ instead of ξ_1 and ξ_2 . Using the Eqs. (3.25) and (3.26), we obtain the following equations for the auto-correlation and cross-correlation functions.

$$E[R(\xi_1)R(\xi_2)] = R_a(\xi_1 - \xi_2) + R_{b_1}(\xi_1 - \xi_2) + R_a(\xi_1 - \xi_2)R_{b_1}(\xi_1 - \xi_2) \quad (3.92)$$

$$E[S(\xi_1)S(\xi_2)] = R_c(\xi_1 - \xi_2) + R_d(\xi_1 - \xi_2) + R_c(\xi_1 - \xi_2)R_d(\xi_1 - \xi_2) \quad (3.93)$$

$$E[R(\xi_1)S(\xi_2)] = R_{ac}(\xi_1 - \xi_2) + R_{b_1d}(\xi_1 - \xi_2) + R_{ad}(\xi_1 - \xi_2) + R_{ac}(\xi_1 - \xi_2)R_{b_1d}(\xi_1 - \xi_2) \quad (3.94)$$

In which $R_a(\xi_1 - \xi_2)$ indicates the auto-correlation function of $a(\xi)$ and term $R_{ac}(\xi_1 - \xi_2)$ indicates the cross-correlation function of $a(\xi)$ and $c(\xi)$. Other terms can also be interpreted in a similar manner.

3.3 Parametric study

In the following sections, parametric study is performed on four different types of laminates i.e. (a) Symmetric Cross-ply Laminate: $[0/90]_{9s}$, (b) Symmetric Angle-ply Laminate: $[+45/-45]_{9s}$, (c) Quasi-isotropic Laminate: $[0/-60/60]_{6s}$, and (d) Un-Symmetric Laminate: $[0/45]_{18T}$ using both the cylindrical bending and one-dimensional laminated beam theories.

3.3.1 Random axial load

First of all, let us consider the composite beam-column that is simply supported at both ends for which the axial force, P , is random and all other parameters are deterministic.

Governing differential Eqn. (2.1), gives

$$\left[bD_{11} \frac{\partial^4 w(x,t)}{\partial x^4} \right] + P \frac{\partial^2 w(x,t)}{\partial x^2} + \rho A \frac{\partial^2 w(x,t)}{\partial t^2} = 0 \quad (3.95)$$

The corresponding boundary conditions can be obtained by substituting $\alpha_1 = 0$ and $\alpha_2 = 0$ in Eqs. (3.2) to (3.5).

$$w(0,t) = \frac{\partial^2 w(0,t)}{\partial x^2} = 0 \quad (3.96)$$

$$w(l,t) = \frac{\partial^2 w(l,t)}{\partial x^2} = 0 \quad (3.97)$$

Eigen value problem is given by the following equation

$$bD_{11} X_n''''(\xi) + Pl^2 X_n''(\xi) - \rho Al^4 \omega_n^2 X_n(\xi) = 0 \quad (3.98)$$

and corresponding boundary conditions are given by

$$X_n(0) = X_n''(0) = X_n(l) = X_n''(l) = 0 \quad (3.99)$$

Using the deterministic counterpart of Eqn. (3.23), the above Eqn. (3.98) can be written as,

$$X_n^-(\xi) + PGX_n^-(\xi) - \lambda_n X_n(\xi) = 0 \quad (3.100)$$

Since there exists only one random variable P , it is possible to solve the problem using two methods: (1) Direct method and (2) Perturbation method.

(1) Direct method:

For simply supported beam-column the following function satisfies the boundary conditions given by Eqn. (3.99).

$$X_n(\xi) = w_m \sin(n\pi\xi) \quad (3.101)$$

Substituting Eqn. (3.101), in Eqn. (3.98), we get the following non-dimensionalized natural frequency.

$$\lambda_n = n^2\pi^2(n^2\pi^2 - PG) \quad (3.102)$$

Applying the expectation operation on both sides, we obtain the following expected value:

$$E[\lambda_n] = n^2\pi^2(n^2\pi^2 - E[P]G) \quad (3.103)$$

Since

$$E[P] = E[P_o(1 + \nu)] = E[P_o] = P_o \quad (3.104)$$

$$\therefore E[\lambda_n] = n^2\pi^2[n^2\pi^2 - P_oG] \quad (3.105)$$

From Eqn. (3.102), we have

$$\lambda_n^2 = n^4 \pi^4 [n^4 \pi^4 - 2n^2 \pi^2 PG + (PG)^2] \quad (3.106)$$

Applying the expectation operation on both sides, we obtain the following mean square value:

$$E[\lambda_n^2] = n^4 \pi^4 [n^4 \pi^4 - 2n^2 \pi^2 P_o G + (P_o G)^2 (1 + \sigma_v^2)] \quad (3.107)$$

Since the variance is given by the following:

$$\text{var}[\lambda_n] = E[\lambda_n^2] - (E[\lambda_n])^2 \quad (3.108)$$

$$\therefore \text{var}[\lambda_n] = n^4 \pi^4 [P_o G]^2 \sigma_v^2 \quad (3.109)$$

Since from Eqn. (3.85), we have

$$E[\omega_n] \approx \sqrt{\frac{b_o D_{l_1}}{\rho_o A_o l^4}} * \sqrt{\frac{1}{2} [E[\lambda_n] + \sqrt{(E[\lambda_n])^2 - \text{var}[\lambda_n]}]} \quad (3.110)$$

Substituting Eqn. (3.105) and (3.109) in Eqn. (3.110), we obtain the following equation for the natural frequency.

$$E[\omega_n] \approx n^2 \pi^2 \sqrt{\frac{bD_{l1}}{\rho A l^4}} \left[\frac{1}{2} \left\{ \left(1 - \frac{P_o G}{n^2 \pi^2} \right) + \sqrt{\left(1 - \frac{P_o G}{n^2 \pi^2} \right)^2 - \frac{P_o^2 G^2 \sigma_v^2}{n^4 \pi^4}} \right\} \right]^{1/2} \quad (3.111)$$

Since

$$\sigma[\sqrt{\lambda_n}] \approx \frac{1}{2} \left(\frac{\sigma[\lambda_n]}{E[\lambda_n]} \right) \quad (3.112)$$

$$\therefore \text{var}[\omega_n] \approx \frac{bD_{11}}{4\rho Al^4} \frac{P_o^2 G^2 \sigma_v^2}{n^4 \pi^4} \frac{1}{\left(1 - \frac{P_o G}{n^2 \pi^2}\right)^2} \quad (3.113)$$

(2) Perturbation Method:

The solution can be obtained from Eqs. (3.80), (3.86), (3.88), by substituting zero for all terms associated with variance and auto-correlation functions of material and geometric properties.

$$\therefore E[\lambda_n] = \lambda_{no} \quad (3.114)$$

$$E[\lambda_n^2] = \lambda_{no}^2 + (P_o G)^2 \frac{E_n^2}{D_n^2} \sigma_v^2 \quad (3.115)$$

$$\text{var}[\lambda_n] = (P_o G)^2 \frac{E_n^2}{D_n^2} \sigma_v^2 \quad (3.116)$$

λ_{no} and X_{no} are determined by using Eqs. (3.36),(3.44),(3.52),(3.53) and (3.61) in which $\alpha_{1o} = \alpha_{2o} = 0$ for simple supports.

The solutions for λ_{no} and X_{no} are as follows:

$$\lambda_{no} = n^2 \pi^2 (n^2 \pi^2 - P_o G) \quad (3.117)$$

$$X_{no}(\xi) = w_m \sin(n\pi\xi) \quad (3.118)$$

D_n and E_n are given by substituting Eqn. (3.118) in Eqs. (3.71) and (3.72) respectively.

Thus simplified Eqs. (3.114), (3.115) and (3.116) are given by

$$E[\lambda_n] = n^2 \pi^2 [n^2 \pi^2 - P_o G] \quad (3.119)$$

$$E[\lambda_n^2] = n^4 \pi^4 [n^4 \pi^4 - 2n^2 \pi^2 P_o G + (P_o G)^2 (1 + \sigma_v^2)] \quad (3.220)$$

$$\text{var}[\lambda_n] = n^4 \pi^4 [P_o G]^2 \sigma_v^2 \quad (3.221)$$

From the above solutions, we can conclude that the perturbation solution exactly coincides with that of the direct method. However, this is a particular case, and, if more than one random coefficients are involved, the solutions from these two methods will differ. By the direct method it is almost impossible to get the solutions, since outputs are generally non-linear functions of these random inputs. Hence other techniques have to be followed to solve the problem.

The deterministic free vibration frequency is given by [2]:

For cylindrical bending theory:

$$\omega_n^* = \frac{n\pi}{l} \sqrt{\frac{1}{\rho h} \left[\frac{D}{A} * \frac{n\pi^2}{l^2} - N_x \right]} \quad (3.122)$$

For one-dimensional laminated beam theory:

$$\omega_n^{**} = \frac{n\pi}{l} \sqrt{\frac{1}{\rho h} \left[\frac{n^2 \pi^2 E_x^b h^3}{12l^2} - N_x \right]} \quad (3.123)$$

3.3.1.1 Numerical examples

A composite laminate consisting of a total of 36 plies made of NCT-301 Graphite-Epoxy composite material, each having a ply thickness of 0.125 mm is considered. The width of the laminate is 0.025m and length of the laminate is 0.4m as shown in the Figure 2.3. P_{cr} is calculated using the one-dimensional deterministic analysis as explained in chapter 2.

In the present examples, four different types of laminates i.e. symmetric cross-ply laminate $[0/90]_{9s}$, symmetric angle-ply laminate $[+45/-45]_{9s}$, quasi-isotropic laminate $[0/-60/60]_{6s}$ and un-symmetric laminate $[0/45]_{18T}$ are considered. Results that correspond to the cylindrical bending theory and 1-D laminated beam theory are obtained.

Tables 3.1 to 3.7 show the deterministic, expected and variance values of first natural frequency ω_1 for four different types of laminates corresponding to cylindrical bending and 1-D analysis for given input σ_v^2 and axial load.

Figures 3.2 and 3.3 show the variance of natural frequencies for four different types of laminates i.e. $[0/90]_{9s}$ laminate, $[+45/-45]_{9s}$ laminate, $[0/-60/60]_{6s}$ laminate and $[0/45]_{18T}$ laminate corresponding to cylindrical bending theory and 1-D laminated beam theory.

Input, σ_v^2	Cylindrical Bending Analysis			1-D Analysis		
	$^* \omega_1$	$E[\omega_1]$	$\text{var}[\omega_1]$	$^{**} \omega_1$	$E[\omega_1]$	$\text{var}[\omega_1]$
0.01	491.61	491.51	0.919	487.90	487.66	0.905
0.05		491.23	4.597		487.39	4.525
0.09		490.96	8.275		487.11	8.146
0.13		490.68	11.95		486.84	11.76

Table 3.1 Mean value and variance of 1st natural frequency for the [0/90]_{9s} laminate with

$$P_o / P_{cr} = 1/4$$

Input, σ_v^2	Cylindrical Bending Analysis			1-D Analysis		
	$^* \omega_1$	$E[\omega_1]$	$\text{var}[\omega_1]$	$^{**} \omega_1$	$E[\omega_1]$	$\text{var}[\omega_1]$
0.01	401.40	400.92	8.264	398.37	397.78	8.1357
0.05		398.87	41.32		395.75	40.67
0.09		396.77	74.38		393.66	73.22
0.13		394.62	107.44		391.52	105.76

Table 3.2 Mean value and variance of 1st natural frequency for the [0/90]_{9s} laminate with

$$P_o / P_{cr} = 1/2$$

Input, σ_v^2	Cylindrical Bending Analysis			1-D Analysis		
	$^*\omega_1$	$E[\omega_1]$	$\text{var}[\omega_1]$	$^{**}\omega_1$	$E[\omega_1]$	$\text{var}[\omega_1]$
0.01	361.70	361.56	0.497	223.22	222.90	0.189
0.05		361.36	2.487		222.78	0.945
0.09		361.16	4.478		222.65	1.702
0.13		360.96	6.468		222.53	2.458

Table 3.3 Mean value and variance of 1st natural frequency for the [45/-45]_{9s} laminate
with $P_o / P_{cr} = 1/4$

Input, σ_v^2	Cylindrical Bending Analysis			1-D Analysis		
	$^*\omega_1$	$E[\omega_1]$	$\text{var}[\omega_1]$	$^{**}\omega_1$	$E[\omega_1]$	$\text{var}[\omega_1]$
0.01	295.33	294.92	4.472	182.26	181.82	1.699
0.05		293.42	22.36		180.89	8.499
0.09		291.87	40.25		179.94	15.29
0.13		290.28	58.13		178.96	22.09

Table 3.4 Mean value and variance of 1st natural frequency for the [45/-45]_{9s} laminate
with $P_o / P_{cr} = 1/2$

Input, σ_v^2	Cylindrical Bending Analysis			1-D Analysis		
	$^* \omega_1$	$E[\omega_1]$	$\text{var}[\omega_1]$	$^{**} \omega_1$	$E[\omega_1]$	$\text{var}[\omega_1]$
0.01	445.93	445.81	0.756	431.62	431.36	0.708
0.05		445.56	3.782		431.12	3.541
0.09		445.31	6.808		430.87	6.373
0.13		445.06	9.833		430.63	9.206

Table 3.5 Mean value and variance of 1st natural frequency for the $[0/-60/60]_{6s}$ laminate
with $P_o / P_{cr} = 1/4$

Input, σ_v^2	Cylindrical Bending Analysis			1-D Analysis		
	$^* \omega_1$	$E[\omega_1]$	$\text{var}[\omega_1]$	$^{**} \omega_1$	$E[\omega_1]$	$\text{var}[\omega_1]$
0.01	364.10	363.64	6.799	352.42	351.85	6.365
0.05		361.79	33.99		350.06	31.82
0.09		359.88	61.19		348.21	57.28
0.13		357.93	88.39		346.32	82.75

Table 3.6 Mean value and variance of 1st natural frequency for the $[0/-60/60]_{6s}$ laminate
with $P_o / P_{cr} = 1/2$

Input, σ_v^2	$P_o / P_{cr} = 1/4$			$P_o / P_{cr} = 1/2$		
	* ω_1	$E[\omega_1]$	$\text{var}[\omega_1]$	** ω_1	$E[\omega_1]$	$\text{var}[\omega_1]$
0.01	526.85	526.19	1.053	430.39	429.20	9.472
0.05		525.90	5.269		427.02	47.36
0.09		525.60	9.484		424.77	85.24
0.13		525.31	13.69		422.77	123.1

Table 3.7 Mean value and variance of 1st natural frequency for [0/45]_{18T} laminate using cylindrical bending analysis

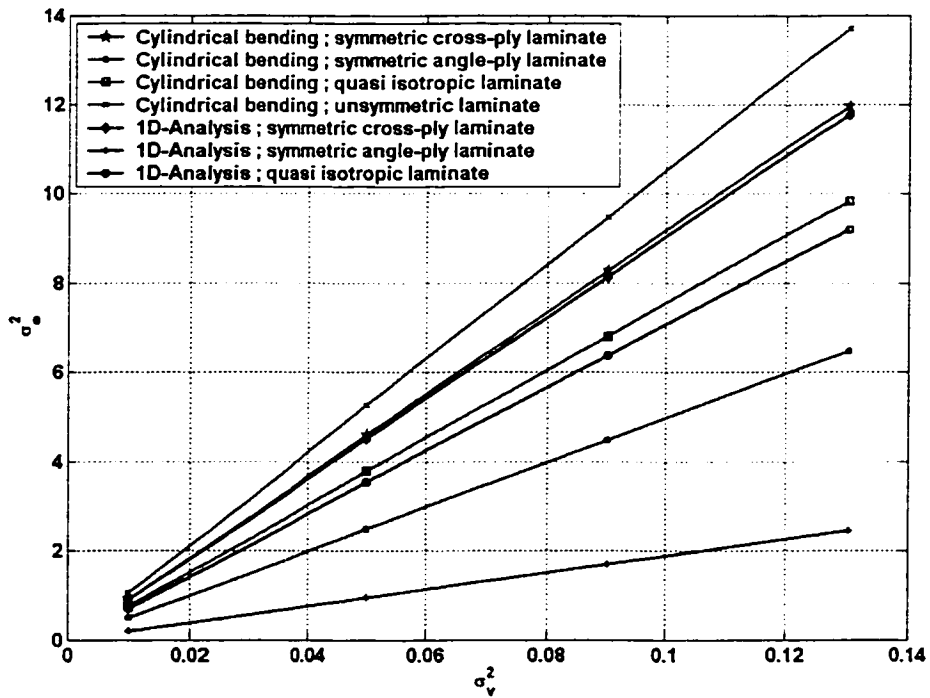


Figure 3.2 Variance of 1st natural frequency vs σ_v^2 for $P_o / P_{cr} = 1/4$

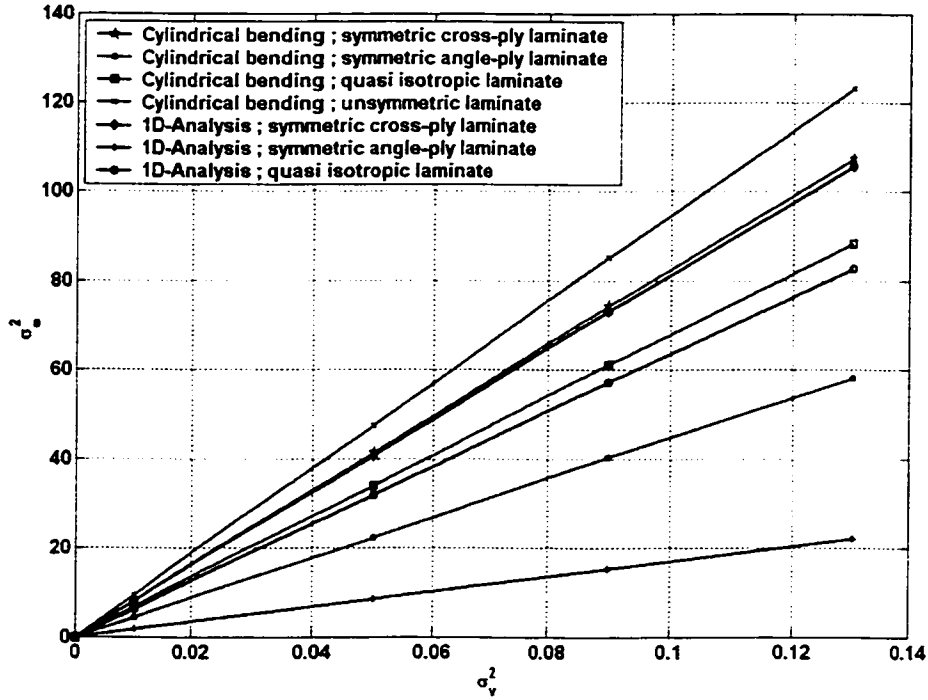


Figure 3.3 Variance of 1st natural frequency vs σ_v^2 for $P_o / P_{cr} = 1/2$

Observations:

It can be observed from Tables 3.1, 3.3, and 3.5 that the expected values of natural frequency ω_1 are almost the same as the deterministic natural frequency $\bar{\omega}_1$, whereas in Tables 3.2, 3.4, 3.6 and 3.7 it can be seen that the expected values of natural frequency ω_1 are slightly different from the deterministic natural frequency $\bar{\omega}_1$ and their values decrease as the input random variable v and axial load increase. Also it can be observed from Eqn. (3.111) and Table 3.2 that the input variance term σ_v^2 has more effect on the expected value when axial load reaches the critical buckling load.

It can be observed from Tables 3.1 to 3.7 that the variance value increases quite significantly and this significant increase was observed when the axial load reaches the critical buckling load. Also we note that the variance of natural frequency ω_1 takes on quite a big value compared to the small variance of the input σ_v^2 .

The mean square value and variance of ω_n are linear functions of the variance of v . The variation of the variance of ω_1 with the given input σ_v^2 is illustrated in Figures 3.2 and 3.3. The graphs show that they are linearly related.

It can be observed from Figures 3.2 and 3.3 that an un-symmetric laminate possesses the highest variance values of natural frequency whereas symmetric angle-ply laminate has the lowest variance values of natural frequency. It can also be seen that the expected and variance values of natural frequency corresponding to both the theories are almost same in the cases of symmetric cross-ply laminate and quasi-isotropic laminate, and that the largest difference occurs in the case of symmetric angle-ply laminate.

3.3.2 Ratio of the coefficients of variation of input and output

Coefficient of variation is defined as the ratio of standard deviation to the mean value.

Input coefficient of variation is given by

$$V_P = \frac{\sigma_P}{E[P]} \quad (3.124)$$

Expected value of P is given by using Eqn. (3.12)

$$E[P] = P_o E[1 + v] \quad (3.125)$$

and since according to our assumption

$$E(v) = 0 \quad (3.126)$$

The expected value of P is given as follows:

$$E[P] = P_o \quad (3.127)$$

Mean square value is given by

$$E[P^2] = E[P_o(1 + v)]^2 = P_o^2(1 + \sigma_v^2 + 2v) \quad (3.128)$$

According to the assumption of Eqn. (3.126), mean square value simplifies to

$$E[P^2] = P_o^2(1 + \sigma_v^2) \quad (3.129)$$

Variance is given by the following equation:

$$\text{var}[P] = E[P^2] - (E[P])^2 \quad (3.130)$$

$$\therefore \text{var}[P] = P_o^2 \sigma_v^2 \quad (3.131)$$

Thus the coefficient of variation of P is given by substituting Eqs. (3.127) and (3.131) in Eqn. (3.124)

$$V_p = \frac{P_o \sigma_v}{P_o} = \sigma_v \quad (3.132)$$

Output coefficient of variation is given by

$$V_{\omega_n} = \frac{\sigma_{\omega_n}}{E[\omega_n]} \quad (3.133)$$

Expected value and variance of ω_n are given by Eqs. (3.85) and (3.90) respectively.

The coefficient of variation of ω_n is given by substituting Eqs. (3.85) and (3.90) in Eqn.

(3.133)

$$V_{\omega_n} = \frac{\sqrt{\frac{1}{k} \text{var}[\sqrt{\lambda_n}]}}{\frac{1}{\sqrt{k}} E[\sqrt{\lambda_n}]} = \frac{\sqrt{\text{var}[\sqrt{\lambda_n}]}}{E[\sqrt{\lambda_n}]} \quad (3.134)$$

Thus the ratio of coefficient of variation of input and output is given as follows:

$$\frac{V_p}{V_{\omega_n}} = \frac{E[\sqrt{\lambda_n}]}{\sqrt{\text{var}[\sqrt{\lambda_n}]}} \sigma_v = \frac{\sqrt{\frac{1}{2} \left[E[\sqrt{\lambda_n}] + \sqrt{(E[\sqrt{\lambda_n}])^2 - \text{var}[\sqrt{\lambda_n}]} \right]}}{\frac{1}{2} \left(\frac{\sigma[\lambda_n]}{E[\lambda_n]} \right)} \sigma_v \quad (3.135)$$

The coefficient of variation quantifies the degree of variation of a random variable.

Therefore the ratio given by Eqn. (3.135) indicates the comparative degree of variation

between the input and output parameters. It can be observed from Eqn. (3.135) that the

ratio is independent of material and geometric properties and depends on P_o and σ_v^2 .

Tables 3.8 and 3.9 show the ratio of coefficients of variation of input and output when $n = 1$ and $n = 2$. Figure 3.4 shows the ratio of coefficients of variation of the 1st and 2nd natural frequencies.

Input, σ_v^2	$\frac{V_P}{V_{\omega_1}}$ for $\frac{P_o}{P_{cr}} = \frac{1}{4}$	$\frac{V_P}{V_{\omega_1}}$ for $\frac{P_o}{P_{cr}} = \frac{1}{2}$	$\frac{V_P}{V_{\omega_1}}$ for $\frac{P_o}{P_{cr}} = 1$
0.01	51.258	13.945	all values are almost zero
0.05	51.229	13.874	
0.09	51.201	13.801	
0.13	51.172	13.726	

Table 3.8 Ratio of the coefficients of variation of input and output when $n = 1$

Input, σ_v^2	$\frac{V_P}{V_{\omega_1}}$ for $\frac{P_o}{P_{cr}} = \frac{1}{4}$	$\frac{V_P}{V_{\omega_1}}$ for $\frac{P_o}{P_{cr}} = \frac{1}{2}$	$\frac{V_P}{V_{\omega_1}}$ for $\frac{P_o}{P_{cr}} = 1$
0.01	205.126	55.826	all values are almost zero
0.05	205.012	55.541	
0.09	204.897	55.249	
0.13	204.782	54.950	

Table 3.9 Ratio of the coefficients of variation of input and output when $n = 2$

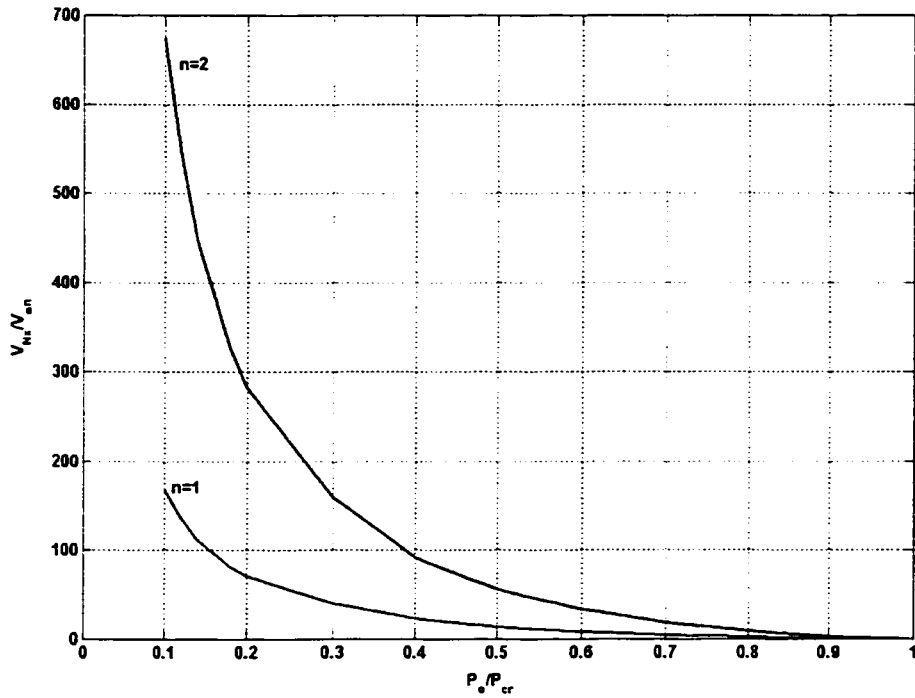


Figure 3.4 Ratio of the coefficients of variation of P and ω_n for given P_o / P_{cr}

Observations:

It can be observed from Eqn. (3.135) and Tables 3.8 and 3.9 that the input variance v has almost negligible effect on the ratio of coefficients of variation and further, it can be observed from Figure 3.4 that the ratio of coefficients of variation significantly decreases when $P_o / P_{cr} > 1/2$.

3.3.3 Random material and geometric properties

Now let us consider that the composite beam-column is simply supported at both ends and further the axial force, stiffness term, material properties and geometric coefficients are random.

For simply supported ends substitute $\alpha_{1o} = \alpha_{2o} = 0$ in Eqn. (3.70), which gives

$$\lambda_n = \lambda_{no} + \frac{1}{D_n} \int_0^1 R(\xi) I_n(\xi) d\xi - \frac{\lambda_{no}}{D_n} \int_0^1 S(\xi) F_n(\xi) d\xi + \frac{P_o l^2}{b_o D_{11o}} \frac{E_n}{D_n} v \quad (3.136)$$

Applying the expectation operator on both sides, we have the following expected value of non-dimensionalized natural frequency.

$$E[\lambda_n] = \lambda_{no} \quad (3.137)$$

From Eqn. (3.85), we have the following expression for the expected value of ω_n .

$$E[\omega_n] \approx \sqrt{\frac{b_o D_{11o}}{\rho_o A_o l^4}} * \sqrt{\frac{1}{2} \left[E[\lambda_n] + \sqrt{(E[\lambda_n])^2 - \text{var}[\lambda_n]} \right]} \quad (3.138)$$

From Eqn. (3.86), for simply supported case, we obtain the following expression:

$$\begin{aligned} E[\lambda_n^2] &= \lambda_{no}^2 + \frac{1}{D_n^2} \int_0^1 \int_0^1 E[R(\xi_1)R(\xi_2)] I_n(\xi_1) I_n(\xi_2) d\xi_1 d\xi_2 \\ &+ \frac{\lambda_{no}^2}{D_n^2} \int_0^1 \int_0^1 E[S(\xi_1)S(\xi_2)] F_n(\xi_1) F_n(\xi_2) d\xi_1 d\xi_2 \\ &- \frac{2\lambda_{no}}{D_n^2} \int_0^1 \int_0^1 E[R(\xi_1)S(\xi_2)] I_n(\xi_1) F_n(\xi_2) d\xi_1 d\xi_2 + \left(\frac{P_o l^2}{b_o D_{11o}} \right)^2 \frac{E_n^2}{D_n^2} \sigma_v^2 \end{aligned} \quad (3.139)$$

Therefore variance of λ_n is given by the following expression:

$$\begin{aligned} \text{var}[\lambda_n] &= \frac{1}{D_n^2} \int_0^1 \int_0^1 E[R(\xi_1)R(\xi_2)]I_n(\xi_1)I_n(\xi_2)d\xi_1d\xi_2 \\ &+ \frac{\lambda_{no}^2}{D_n^2} \int_0^1 \int_0^1 E[S(\xi_1)S(\xi_2)]F_n(\xi_1)F_n(\xi_2)d\xi_1d\xi_2 \\ &- \frac{2\lambda_{no}}{D_n^2} \int_0^1 \int_0^1 E[R(\xi_1)S(\xi_2)]I_n(\xi_1)F_n(\xi_2)d\xi_1d\xi_2 + \left(\frac{P_o l^2}{b_o D_{11_o}} \right)^2 \frac{E_n^2}{D_n^2} \sigma_v^2 \end{aligned} \quad (3.140)$$

We obtain the following expression for the variance of ω_n from Eqn. (3.90).

$$\text{var}[\omega_n] \approx \text{var} \left[\sqrt{\frac{\lambda_n}{k}} \right] = \frac{b_o D_{11_o}}{\rho_o A_o l^4} \text{var}[\sqrt{\lambda_n}] \quad (3.141)$$

3.3.3.1 Case 1: Uniform auto-correlation and cross-correlation functions

Let us consider the case where all auto-correlation and cross-correlation functions have uniform distribution and their constant values are equal to the variance or product of standard deviations respectively. In other words, we have complete statistical dependence between random functions at any two arbitrary locations.

Hence we have the following equations:

$$R_a(\xi_1 - \xi_2) = \sigma_a^2 \quad (3.142)$$

$$R_b(\xi_1 - \xi_2) = \sigma_b^2 \quad (3.143)$$

$$R_c(\xi_1 - \xi_2) = \sigma_c^2 \quad (3.144)$$

$$R_d(\xi_1 - \xi_2) = \sigma_d^2 \quad (3.145)$$

$$R_{ac}(\xi_1 - \xi_2) = \sigma_a \sigma_c \quad (3.146)$$

$$R_{bd}(\xi_1 - \xi_2) = \sigma_b \sigma_d \quad (3.147)$$

$$R_{ad}(\xi_1 - \xi_2) = \sigma_a \sigma_d \quad (3.148)$$

Thus, the correlation coefficient is given by the following equation:

$$\gamma_{ac} = \frac{C_{ac}}{\sigma_a \sigma_c} \quad (3.149)$$

where C_{ac} is the covariance.

But according to our assumption

$$E[a] = E[c] = 0. \quad (3.150)$$

Therefore we can equate covariance to correlation.

$$\gamma_{ac} = \frac{E[a(\xi_1)c(\xi_2)]}{\sigma_a \sigma_c} = \frac{\sigma_a \sigma_c}{\sigma_a \sigma_c} = 1 \quad (3.151)$$

It can be shown from [64] that $-1 \leq \gamma_{ac} \leq 1$.

Correlation coefficient γ_{ac} measures the degree of linear statistical dependence between random functions a and c .

Similarly

$$\gamma_{aa} = \gamma_{b_1 b_1} = \gamma_{cc} = \gamma_{dd} = \gamma_{b_1 d} = \gamma_{ad} = 1 \quad (3.152)$$

Substituting Eqs. (3.142) to (3.148) in Eqn. (3.140) and after simplification, we obtain the following equation for the variance of λ_n .

$$\begin{aligned} \text{var}[\lambda_n] = & n^8 \pi^8 (\sigma_a^2 + \sigma_{b_1}^2 + \sigma_a^2 \sigma_{b_1}^2) + \lambda_{no}^2 [\sigma_c^2 + \sigma_d^2 + \sigma_c^2 \sigma_d^2] \\ & - 2\lambda_{no} n^4 \pi^4 (\sigma_a \sigma_c + \sigma_{b_1} \sigma_d + \sigma_a \sigma_d + \sigma_a \sigma_c \sigma_{b_1} \sigma_d + n^4 \pi^4 (P_o G)^2 \sigma_v^2 \end{aligned} \quad (3.153)$$

3.3.3.1.1 Numerical examples

Laminate dimensions and configurations are the same as explained in section 3.3.1.1

Tables 3.10 to 3.16 show the deterministic, expected and variance values of first natural frequency ω_1 for four different types of laminates corresponding to cylindrical bending and 1-D analysis for given input $\sigma_a^2 = \sigma_{b_1}^2 = \sigma_c^2 = \sigma_d^2 = \sigma_v^2 = \sigma^2$ and axial load.

Figure 3.5 shows the variance of 1st natural frequency when material and geometric properties have uniform correlation for [0/90]_{9s} laminate, [+45/-45]_{9s} laminate, [0/-60/60]_{6s} laminate and [0/45]_{18T} laminate corresponding to cylindrical bending theory and 1-D laminated beam theory.

Note: $\sigma_a^2 = \sigma_b^2 = \sigma_c^2 = \sigma_d^2 = \sigma_v^2 = \sigma^2$

Input, σ^2	Cylindrical Bending Analysis			1-D Analysis		
	$^* \omega_1$	$E[\omega_1]$	$\text{var}[\omega_1]$	$^{**} \omega_1$	$E[\omega_1]$	$\text{var}[\omega_1]$
0.01	491.61	491.38	2.76	487.90	487.68	2.72
0.05		490.54	14.0		486.84	13.8
0.09		489.67	25.5		485.98	25.1
0.13		488.77	37.4		485.08	36.8

Table 3.10 Mean value and variance of 1st natural frequency for the [0/90]_{9s} laminate

with $P_o / P_{cr} = 1/4$

Input, σ^2	Cylindrical Bending Analysis			1-D Analysis		
	$^* \omega_1$	$E[\omega_1]$	$\text{var}[\omega_1]$	$^{**} \omega_1$	$E[\omega_1]$	$\text{var}[\omega_1]$
0.01	401.40	390.91	24.87	398.37	396.89	24.48
0.05		393.39	126.0		390.42	124.0
0.09		386.06	229.8		383.14	226.2
0.13		377.67	336.2		374.82	331.0

Table 3.11 Mean value and variance of 1st natural frequency for the [0/90]_{9s} laminate

with $P_o / P_{cr} = 1/2$

Input, σ^2	Cylindrical Bending Analysis			1-D Analysis		
	$^*\omega_1$	$E[\omega_1]$	$\text{var}[\omega_1]$	$^{**}\omega_1$	$E[\omega_1]$	$\text{var}[\omega_1]$
0.01	361.70	361.53	1.497	223.22	223.10	0.56
0.05		360.91	7.587		222.72	2.88
0.09		360.26	13.83		222.32	5.25
0.13		359.60	20.24		221.91	7.69

Table 3.12 Mean value and variance of 1st natural frequency for the [45/-45]_{9s} laminate with $P_o / P_{cr} = 1/4$

Input, σ^2	Cylindrical Bending Analysis			1-D Analysis		
	$^*\omega_1$	$E[\omega_1]$	$\text{var}[\omega_1]$	$^{**}\omega_1$	$E[\omega_1]$	$\text{var}[\omega_1]$
0.01	295.33	294.22	13.46	182.26	181.57	5.116
0.05		289.42	68.20		178.61	25.92
0.09		284.03	124.3		175.28	47.27
0.13		277.87	181.9		171.47	69.16

Table 3.13 Mean value and variance of 1st natural frequency for the [45/-45]_{9s} laminate with $P_o / P_{cr} = 1/2$

Input, σ^2	Cylindrical Bending Analysis			1-D Analysis		
	$^* \omega_1$	$E[\omega_1]$	$\text{var}[\omega_1]$	$^{**} \omega_1$	$E[\omega_1]$	$\text{var}[\omega_1]$
0.01	445.93	445.72	2.276	431.62	431.42	2.131
0.05		444.96	11.53		430.68	10.80
0.09		444.16	21.03		429.68	19.69
0.13		443.35	30.78		429.13	28.81

Table 3.14 Mean value and variance of 1st natural frequency for the $[0/-60/60]_{6s}$

laminate with $P_o / P_{cr} = 1/4$

Input, σ^2	Cylindrical Bending Analysis			1-D Analysis		
	$^* \omega_1$	$E[\omega_1]$	$\text{var}[\omega_1]$	$^{**} \omega_1$	$E[\omega_1]$	$\text{var}[\omega_1]$
0.01	364.10	362.74	20.46	352.42	351.11	19.16
0.05		356.83	103.6		345.38	97.07
0.09		350.18	189.0		338.95	177.0
0.13		342.58	276.6		331.59	259.0

Table 3.15 Mean value and variance of 1st natural frequency for the $[0/-60/60]_{6s}$

laminate with $P_o / P_{cr} = 1/2$

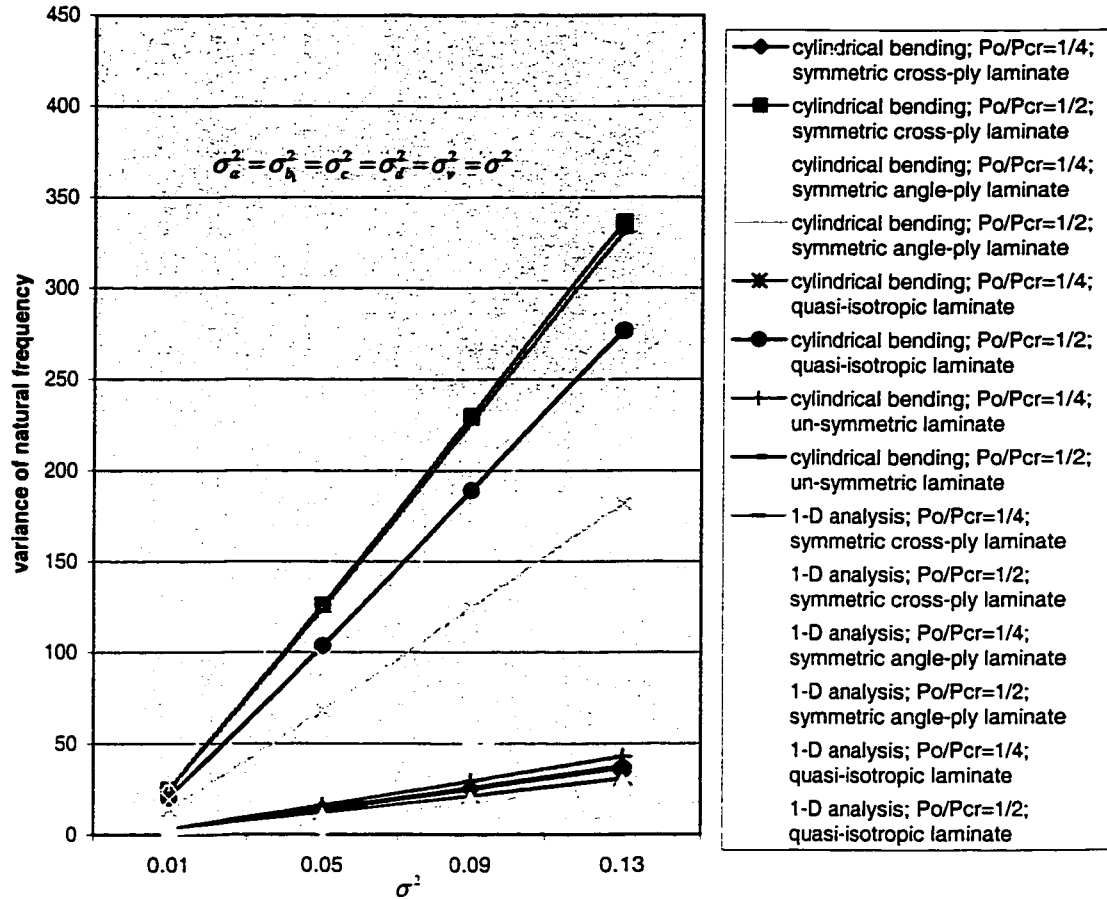


Figure 3.5 The variance of 1st natural frequency vs σ^2

Input, σ^2	$P_o / P_{cr} = 1/4$			$P_o / P_{cr} = 1/2$		
	* ω_1	$E[\omega_1]$	$\text{var}[\omega_1]$	** ω_1	$E[\omega_1]$	$\text{var}[\omega_1]$
0.01	526.85	526.47	3.172	430.39	428.46	28.510
0.05		525.57	16.07		421.47	144.44
0.09		524.63	29.30		413.62	263.41
0.13		523.69	42.87		404.64	385.41

Table 3.16 Mean value and variance of 1st natural frequency for $[0/45]_{18T}$ laminate

corresponding to cylindrical bending analysis

It can be observed from the Tables 3.10 to 3.16 that the expected values of natural frequency ω_1 vary more from the deterministic natural frequency when the input random variable ν and axial load increase.

The Figure 3.5 represents that the variance of ω_n increases linearly with σ^2 . It can also be observed that the variance of natural frequency ω_n takes on quite a large value compared to small input of σ^2 .

Further, it can be observed from the Figure 3.5 that an un-symmetric laminate possesses the highest variance values of natural frequency whereas symmetric angle-ply laminate has the lowest variance values of natural frequency. It can be seen that the expected and variance values of natural frequency corresponding to both the theories are almost same in the cases of $[0/90]_{9s}$ laminate and $[0/-60/60]_{6s}$ laminate. The largest difference occurs in the case of $[45/-45]_{9s}$ laminate.

3.3.3.2 Case 2: Exponential auto and cross-correlation functions

Let us consider the case where all auto-correlation and cross-correlation functions have exponential distribution. Hence we have auto-correlation and cross-correlation functions as

$$R_a(\xi_1 - \xi_2) = \sigma_a^2 e^{-k_1|\xi_1 - \xi_2|} \quad (3.154)$$

$$R_{b_i}(\xi_1 - \xi_2) = \sigma_{b_i}^2 e^{-k_2|\xi_1 - \xi_2|} \quad (3.155)$$

$$R_c(\xi_1 - \xi_2) = \sigma_c^2 e^{-k_3|\xi_1 - \xi_2|} \quad (3.156)$$

$$R_d(\xi_1 - \xi_2) = \sigma_d^2 e^{-k_4|\xi_1 - \xi_2|} \quad (3.157)$$

$$R_{ac}(\xi_1 - \xi_2) = \sigma_a \sigma_c e^{-k_5|\xi_1 - \xi_2|} \quad (3.158)$$

$$R_{b_d}(\xi_1 - \xi_2) = \sigma_b \sigma_d e^{-k_6|\xi_1 - \xi_2|} \quad (3.159)$$

$$R_{ad}(\xi_1 - \xi_2) = \sigma_a \sigma_d e^{-k_7|\xi_1 - \xi_2|} \quad (3.160)$$

where k_i 's are positive constants. The constants k_i 's govern the interval over which appreciable correlation occurs. If we introduce a correlation length ε_i for each k_i in such a way that auto-correlation and cross-correlation functions are negligible for $|\xi_1 - \xi_2| > \varepsilon_i$, then the correlation length ε_i describes the degree of the input randomness. Suppose that the auto-correlation and cross-correlation functions are reduced to 5% of their maximum values within the distances ε_i , then we have the following equations:

$$R_a(\varepsilon_1) = 0.05\sigma_a^2 \quad (3.161)$$

$$R_{b_1}(\varepsilon_2) = 0.05\sigma_{b_1}^2 \quad (3.162)$$

$$R_c(\varepsilon_3) = 0.05\sigma_c^2 \quad (3.163)$$

$$R_d(\varepsilon_4) = 0.05\sigma_d^2 \quad (3.164)$$

$$R_{ac}(\varepsilon_5) = 0.05\sigma_a \sigma_c \quad (3.165)$$

$$R_{b_1d}(\varepsilon_6) = 0.05\sigma_{b_1} \sigma_d \quad (3.166)$$

$$R_{ad}(\varepsilon_7) = 0.05\sigma_a \sigma_d \quad (3.167)$$

Now equating (3.154) and (3.161), we have

$$\sigma_a^2 e^{-k_1 \varepsilon_1} = 0.05 \sigma_a^2 \quad (3.168)$$

which gives

$$k_1 \varepsilon_1 = 2.99 \quad (3.169)$$

In a similar manner the values of $k_2 \varepsilon_2, k_3 \varepsilon_3, k_4 \varepsilon_4, k_5 \varepsilon_5, k_6 \varepsilon_6$, and $k_7 \varepsilon_7$ can also be obtained.

Let us assume that the correlation length ε_i is the same for all random inputs, then we have

$$\varepsilon = \varepsilon_1 = \varepsilon_2 = \varepsilon_3 = \varepsilon_4 = \varepsilon_5 = \varepsilon_6 = \varepsilon_7 \quad (3.170)$$

$$k = k_1 = k_2 = k_3 = k_4 = k_5 = k_6 = k_7 \quad (3.171)$$

Hence

$$k \varepsilon = 2.99 \quad (3.172)$$

Now substituting Eqn. (3.171) in Eqs. (3.154) to (3.160) and then introducing the results into Eqn. (3.140), we obtain the variance of λ_n .

$$\begin{aligned}
\text{var}[\lambda_n] = & 4n^8 \pi^8 (\sigma_a^2 + \sigma_{b_1}^2) \int_0^1 \int_0^1 e^{-k|\epsilon_1 - \epsilon_2|} \sin^2 n\pi\epsilon_1 \sin^2 n\pi\epsilon_2 d\xi_1 d\xi_2 \\
& + 4n^8 \pi^8 \sigma_a^2 \sigma_{b_1}^2 \int_0^1 \int_0^1 e^{-2k|\epsilon_1 - \epsilon_2|} \sin^2 n\pi\epsilon_1 \sin^2 n\pi\epsilon_2 d\xi_1 d\xi_2 \\
& + 4\lambda_{no}^2 (\sigma_c^2 + \sigma_d^2) \int_0^1 \int_0^1 e^{-k|\epsilon_1 - \epsilon_2|} \sin^2 n\pi\epsilon_1 \sin^2 n\pi\epsilon_2 d\xi_1 d\xi_2 \\
& + 4\lambda_{no}^2 \sigma_c^2 \sigma_d^2 \int_0^1 \int_0^1 e^{-2k|\epsilon_1 - \epsilon_2|} \sin^2 n\pi\epsilon_1 \sin^2 n\pi\epsilon_2 d\xi_1 d\xi_2 \\
& - 8\lambda_{no} n^4 \pi^4 (\sigma_a \sigma_c + \sigma_{b_1} \sigma_d) \int_0^1 \int_0^1 e^{-k|\epsilon_1 - \epsilon_2|} \sin^2 n\pi\epsilon_1 \sin^2 n\pi\epsilon_2 d\xi_1 d\xi_2 \\
& - 8\lambda_{no} n^4 \pi^4 \sigma_a \sigma_d \int_0^1 \int_0^1 e^{-k|\epsilon_1 - \epsilon_2|} \sin^2 n\pi\epsilon_1 \sin^2 n\pi\epsilon_2 d\xi_1 d\xi_2 \\
& - 8\lambda_{no} n^4 \pi^4 \sigma_a \sigma_c \sigma_{b_1} \sigma_d \int_0^1 \int_0^1 e^{-k|\epsilon_1 - \epsilon_2|} \sin^2 n\pi\epsilon_1 \sin^2 n\pi\epsilon_2 d\xi_1 d\xi_2 \\
& + n^4 \pi^4 (P_o G)^2 \sigma_v^2
\end{aligned} \tag{3.173}$$

3.3.3.2.1 Numerical examples

Laminate dimensions and configurations are the same the as explained in section 3.3.1.1.

Figures 3.6 and 3.7 represent the variance of 1st natural frequency when material and geometric properties have exponential correlation for [0/90]_{9s} laminate, [+45/-45]_{9s} laminate, [0/-60/60]_{6s} laminate and [0/45]_{18T} laminate corresponding to cylindrical bending theory and 1-D laminated beam theory.

Figures 3.8 to 3.11 show the variance of 1st natural frequency vs correlation length for given P_o/P_{cr} corresponding to cylindrical bending theory.

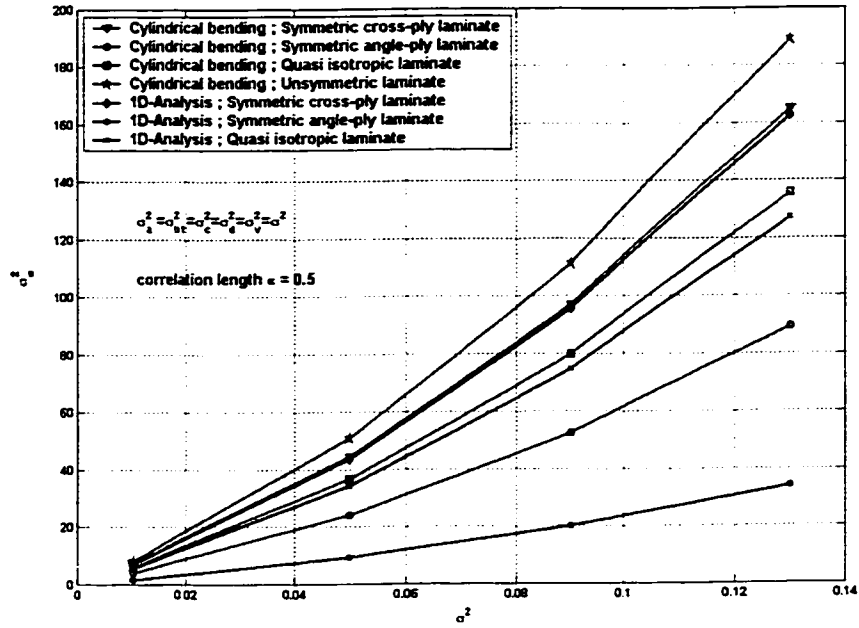


Figure 3.6 The variance of 1st natural frequency vs σ^2 for $P_0/P_{cr} = 1/4$

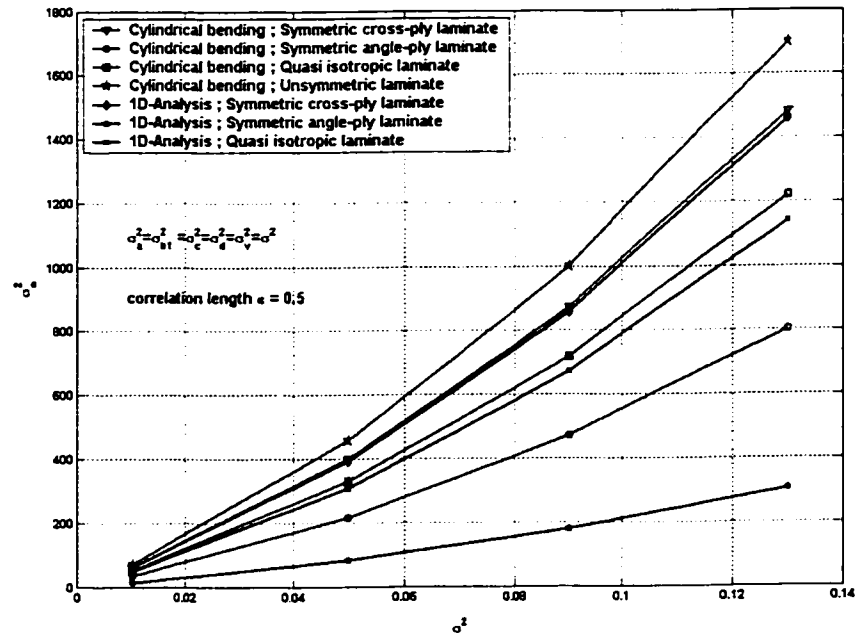


Figure 3.7 The variance of 1st natural frequency vs σ^2 for $P_0/P_{cr} = 1/2$

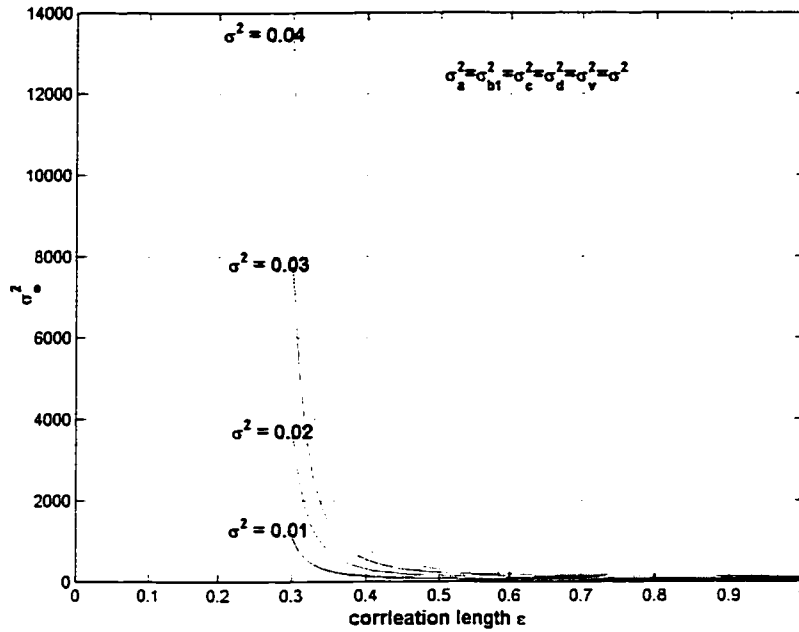


Figure 3.8 Variance of 1st natural frequency corresponding to cylindrical bending analysis for $[0/90]_{9s}$ laminate when $P_o/P_{cr} = 1/2$

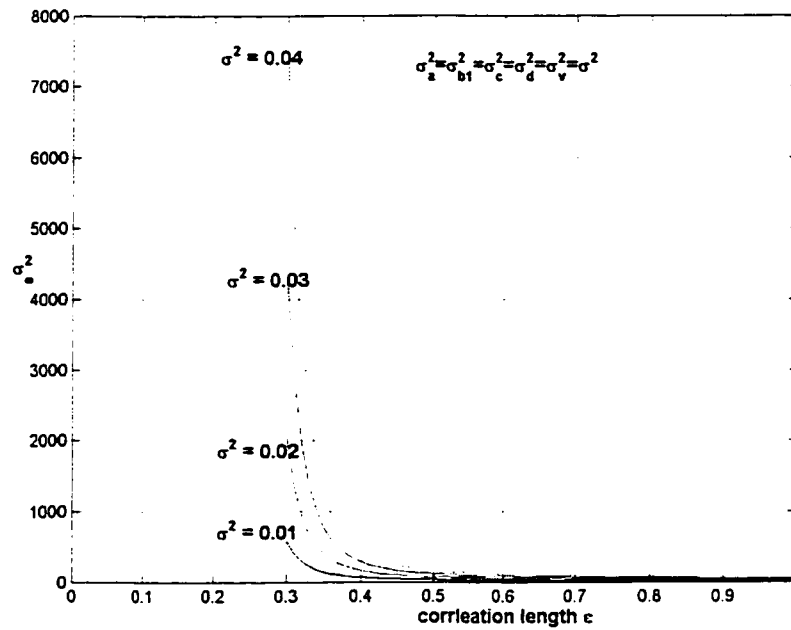


Figure 3.9 Variance of 1st natural frequency corresponding to cylindrical bending analysis for $[+45/-45]_{9s}$ laminate when $P_o/P_{cr} = 1/2$

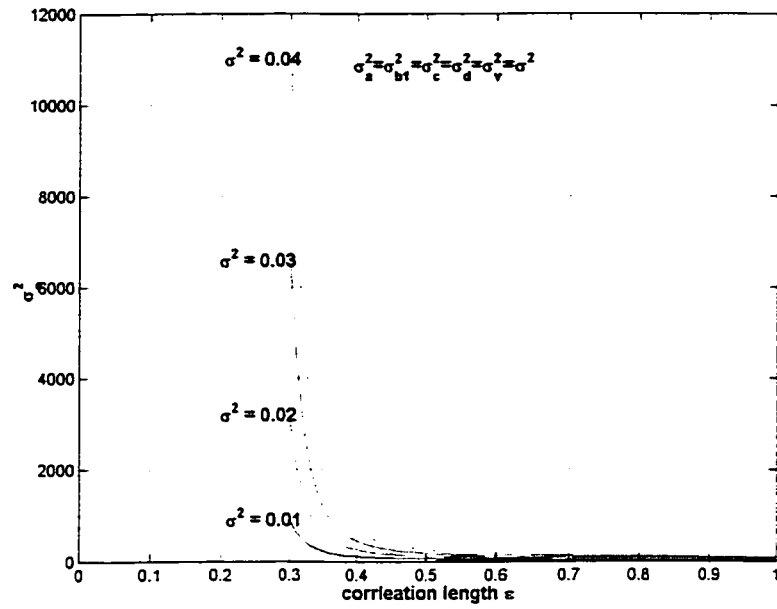


Figure 3.10 Variance of 1st natural frequency corresponding to cylindrical bending analysis for $[0/-60/60]_{6s}$ laminate when $P_o/P_{cr} = 1/2$

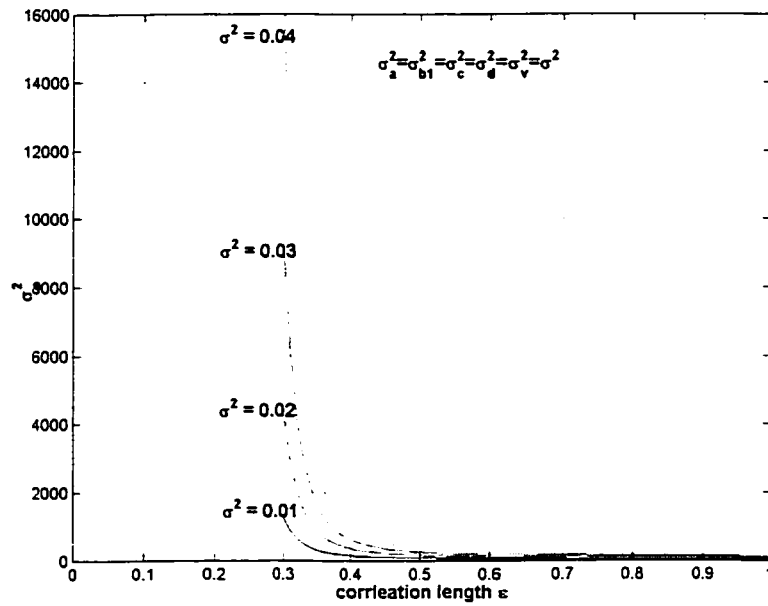


Figure 3.11 Variance of 1st natural frequency corresponding to cylindrical bending analysis for $[0/45]_{18T}$ laminate when $P_o/P_{cr} = 1/2$

The Figures 3.6 and 3.7 show that the variances of natural frequencies increase in a piecewisely linear manner. Further, It can be observed from these figures that the $[0/45]_{18T}$ laminate possesses the highest variance values of natural frequency whereas $[+45/-45]_{9s}$ laminate has the lowest variance values of natural frequency. It can also be seen that the expected and variance values of natural frequency corresponding to both the theories are almost same in the cases of $[0/-90]_{9s}$ laminate and $[0/-60/60]_{6s}$ laminate. The largest difference occurs in the case of symmetric $[+45/-45]_{9s}$ laminate.

In Figures 3.8 to 3.11, it can be observed that the variance of ω_1 increases exponentially as the correlation length, ε , decreases. The variance of ω_1 is almost infinity when the correlation length is very small. This means that if the inputs at any two locations are almost uncorrelated, the variance of output becomes infinity.

3.4 Equivalent elastic constants

In the following sections, the equivalent elastic constants for symmetric and un-symmetric laminates are presented. The following section follows that of ref. [65] and ref. [66].

3.4.1 Equivalent elastic constants for symmetric laminates

The laminate constitutive equation is given by [65]

$$\begin{Bmatrix} N_x \\ N_y \\ N_{xy} \\ M_x \\ M_y \\ M_{xy} \end{Bmatrix} = \begin{bmatrix} A_{11} & A_{12} & A_{16} & B_{11} & B_{12} & B_{16} \\ A_{12} & A_{22} & A_{26} & B_{12} & B_{22} & B_{26} \\ A_{16} & A_{26} & A_{66} & B_{16} & B_{26} & B_{66} \\ \hline B_{11} & B_{12} & B_{16} & D_{11} & D_{12} & D_{16} \\ B_{12} & B_{22} & B_{26} & D_{12} & D_{22} & D_{26} \\ B_{16} & B_{26} & B_{66} & D_{16} & D_{26} & D_{66} \end{bmatrix} \begin{Bmatrix} \varepsilon_x^o \\ \varepsilon_y^o \\ \gamma_{xy}^o \\ k_x \\ k_y \\ k_{xy} \end{Bmatrix} \quad (3.174)$$

where,

$$A_{ij} = \sum_{k=1}^n [\bar{Q}_{ij}]_k (h_k - h_{k-1}) \quad (\text{Axial stiffness}) \quad (3.175)$$

$$B_{ij} = \frac{1}{2} \sum_{k=1}^n [\bar{Q}_{ij}]_k (h_k^2 - h_{k-1}^2) \quad (\text{Axial-Bending coupling stiffness}) \quad (3.176)$$

$$D_{ij} = \frac{1}{3} \sum_{k=1}^n [\bar{Q}_{ij}]_k (h_k^3 - h_{k-1}^3) \quad (\text{Bending stiffness}) \quad (3.177)$$

For symmetric laminates, all the coupling terms B_{ij} will be zero. As a consequence, the full laminate constitutive equation can be uncoupled, that is, with coupling terms equal to zero, the force intensities will induce membrane strains only without an associated coupling of any curvatures and in a similar manner, moment intensities will induce curvatures only without any coupling of membrane strains. Thus Eqn. (3.174) can be simplified as

$$\begin{Bmatrix} N_x \\ N_y \\ N_{xy} \end{Bmatrix} = \begin{bmatrix} A_{11} & A_{12} & A_{16} \\ A_{12} & A_{22} & A_{26} \\ A_{16} & A_{26} & A_{66} \end{bmatrix} \begin{Bmatrix} \varepsilon_x^o \\ \varepsilon_y^o \\ \gamma_{xy}^o \end{Bmatrix} \quad (3.178)$$

$$\begin{Bmatrix} M_x \\ M_y \\ M_{xy} \end{Bmatrix} = \begin{bmatrix} D_{11} & D_{12} & D_{16} \\ D_{12} & D_{22} & D_{26} \\ D_{16} & D_{26} & D_{66} \end{bmatrix} \begin{Bmatrix} k_x \\ k_y \\ k_{xy} \end{Bmatrix} \quad (3.179)$$

The Eqs. (3.178) and (3.179), give the laminate constitutive equation for a symmetric laminate, that is load-deformation expression related by the A_{ij} and D_{ij} terms, which are extensional and bending stiffnesses, respectively.

Inversion of Eqs. (3.178) and (3.179) gives

$$\begin{Bmatrix} \varepsilon_x^o \\ \varepsilon_y^o \\ \gamma_{xy}^o \end{Bmatrix} = \begin{bmatrix} a_{11} & a_{12} & a_{16} \\ a_{12} & a_{22} & a_{26} \\ a_{16} & a_{26} & a_{66} \end{bmatrix} \begin{Bmatrix} N_x \\ N_y \\ N_{xy} \end{Bmatrix} \quad (3.180)$$

$$\begin{Bmatrix} k_x \\ k_y \\ k_{xy} \end{Bmatrix} = \begin{bmatrix} d_{11} & d_{12} & d_{16} \\ d_{12} & d_{22} & d_{26} \\ d_{16} & d_{26} & d_{66} \end{bmatrix} \begin{Bmatrix} M_x \\ M_y \\ M_{xy} \end{Bmatrix} \quad (3.181)$$

where $[a]$ is the membrane compliance matrix, which is the inverse of the corresponding stiffness matrix, as given below

$$[a]=[A]^{-1} \quad (3.182)$$

and $[d]$ is the bending compliance matrix, which is the inverse of the corresponding stiffness matrix, as given below.

$$[d]=[D]^{-1} \quad (3.183)$$

Considering a symmetric layered laminate of arbitrary length in the x-direction, unit width in the y-direction and thickness h, subjected to membrane direct force intensity N_x only, as shown in the Figure 3.12, then membrane force intensities can be simplified as follows

$$N_x \neq 0 \text{ and } N_y = N_{xy} = 0 \quad (3.184)$$

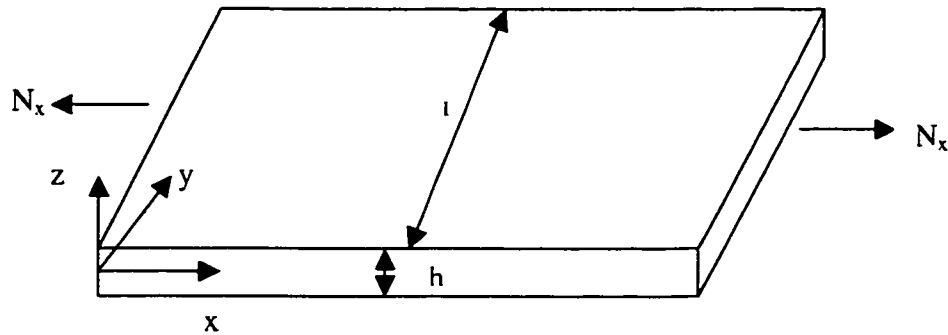


Figure 3.12 Laminate subjected to N_x only

In the above, N_x is the membrane direct force intensity in x-direction, N_y is the membrane direct force intensity in y-direction and N_{xy} is the membrane shear force intensity in xy-plane.

Substituting the Eqn. (3.184), in Eqn. (3.180), we obtain the following strains:

$$\varepsilon_x^o = a_{11} N_x \quad (3.185)$$

$$\varepsilon_y^o = a_{12} N_x \quad (3.186)$$

$$\gamma_{xy}^o = a_{16} N_x \quad (3.187)$$

Considering the average direct stress [65], which is given by

$$f_x = \frac{N_x}{h} \quad (3.188)$$

Substituting N_x from Eqn. (3.188) into Eqn. (3.185), we obtain

$$\frac{f_x}{\varepsilon_x^o} = \frac{1}{ha_{11}} \quad (3.189)$$

By definition of Hooke's law, we have

$$\frac{f_x}{\varepsilon_x^o} = E_x \quad (3.190)$$

Therefore substituting f_x / ε_x^o for E_x , we obtain the equivalent Young's modulus in x-direction in membrane mode, which is given by

$$E_x = \frac{1}{ha_{11}} \quad (3.191)$$

In the above, a_{11} is the extensional compliance term and h is the thickness of the laminate.

In a similar manner, an equivalent Young's modulus in y-direction in membrane mode is given by

$$E_y = \frac{1}{ha_{22}} \quad (3.192)$$

Equivalent shear modulus in x-y plane in membrane mode is given by

$$G_{xy} = \frac{1}{ha_{66}} \quad (3.193)$$

Now, considering a symmetric layered laminate of arbitrary length in the x-direction, unit width in the y- direction, and thickness h, subjected to moment intensity M_x only, as shown in the Figure 3.13, then bending moment intensities can be simplified as follows:

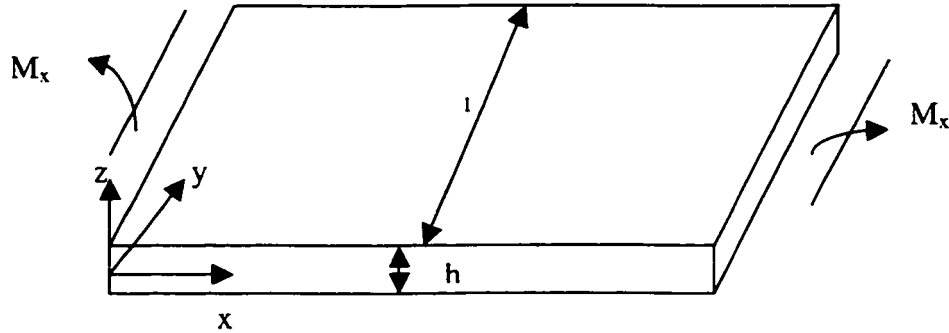


Figure 3.13 Laminate subjected to M_x only

$$M_x \neq 0 \text{ and } M_y = M_{xy} = 0 \quad (3.194)$$

In the above, M_x is the moment intensity about the y-axis, M_y is the moment intensity about the x-axis and M_{xy} is the twisting moment intensity.

Substituting Eqn. (3.194) in Eqn. (3.181), we get

$$k_x = d_{11}M_x \quad (3.195)$$

$$k_y = d_{12}M_x \quad (3.196)$$

$$k_{xy} = d_{16}M_x \quad (3.197)$$

From engineer's theory of bending [65], we have

$$\frac{M}{k} = EI \quad (3.198)$$

where $I = h^3 / 12$ per unit width across the y-axis and so moment about the y-axis is given by

$$M_x = k_x E_x \frac{h^3}{12} \quad (3.199)$$

Substituting Eqn. (3.199) in Eqn. (3.195), we get

$$E_x = \frac{12}{h^3 d_{11}} \quad (3.200)$$

where E_x is the equivalent Young's modulus in x-direction in bending mode, d_{11} is the bending compliance term and h is the thickness of the laminate.

In a similar manner, an equivalent Young's modulus in y-direction in bending mode is given by

$$E_y = \frac{12}{h^3 d_{22}} \quad (3.201)$$

Equivalent shear modulus in x-y plane in bending mode is given by

$$G_{xy} = \frac{12}{h^3 d_{66}} \quad (3.202)$$

3.4.2 Equivalent elastic constants for un-symmetric laminates

In symmetric laminates since the coupling terms are zero, it is easy to get the equivalent engineering constants, whereas in un-symmetrical laminates, coupling terms, B_{ij} are not equal to zero, and therefore the calculation of equivalent engineering constants becomes complicated. However the same basic procedure is followed as for symmetric laminates.

Considering an un-symmetric layered laminate of arbitrary length in the x-direction, unit width in the y-direction, and thickness h, subjected to membrane direct force intensity N_x only as shown in Figure 3.12, then the membrane force and bending moment intensities can be simplified as follows:

$$N_x \neq 0 \text{ and } N_y = N_{xy} = M_x = M_y = M_{xy} = 0 \quad (3.203)$$

Substituting Eqn. (3.203) in laminate constitutive Eqn. (3.1), we obtain

$$\begin{Bmatrix} N_x \\ 0 \\ 0 \\ 0 \\ 0 \\ 0 \end{Bmatrix} = \begin{bmatrix} A_{11} & A_{12} & A_{16} & B_{11} & B_{12} & B_{16} \\ A_{12} & A_{22} & A_{26} & B_{12} & B_{22} & B_{26} \\ A_{16} & A_{26} & A_{66} & B_{16} & B_{26} & B_{66} \\ \hline B_{11} & B_{12} & B_{16} & D_{11} & D_{12} & D_{16} \\ B_{12} & B_{22} & B_{26} & D_{12} & D_{22} & D_{26} \\ B_{16} & B_{26} & B_{66} & D_{16} & D_{26} & D_{66} \end{bmatrix} \begin{Bmatrix} \varepsilon_x^o \\ \varepsilon_y^o \\ \gamma_{xy}^o \\ k_x \\ k_y \\ k_{xy} \end{Bmatrix} \quad (3.204)$$

Using the Cramer's rule to solve for ε_x^o , we obtain

$$\varepsilon_x^o = \frac{\begin{vmatrix} N_x & A_{12} & A_{16} & B_{11} & B_{12} & B_{16} \\ 0 & A_{22} & A_{26} & B_{12} & B_{22} & B_{26} \\ 0 & A_{26} & A_{66} & B_{16} & B_{26} & B_{66} \\ 0 & B_{12} & B_{16} & D_{11} & D_{12} & D_{16} \\ 0 & B_{22} & B_{26} & D_{12} & D_{22} & D_{26} \\ 0 & B_{26} & B_{66} & D_{16} & D_{26} & D_{66} \end{vmatrix}}{\begin{vmatrix} A_{11} & A_{12} & A_{16} & B_{11} & B_{12} & B_{16} \\ A_{12} & A_{22} & A_{26} & B_{12} & B_{22} & B_{26} \\ A_{16} & A_{26} & A_{66} & B_{16} & B_{26} & B_{66} \\ B_{11} & B_{12} & B_{16} & D_{11} & D_{12} & D_{16} \\ B_{12} & B_{22} & B_{26} & D_{12} & D_{22} & D_{26} \\ B_{16} & B_{26} & B_{66} & D_{16} & D_{26} & D_{66} \end{vmatrix}} \quad (3.205)$$

To obtain the solution of Eqn. (3.205), cofactor expansion can be used in the numerator for simplification, and then the Eqn. (3.205) can be simplified as follows:

$$\varepsilon_x^o = \frac{N_x \begin{vmatrix} A_{22} & A_{26} & B_{12} & B_{22} & B_{26} \\ A_{26} & A_{66} & B_{16} & B_{26} & B_{66} \\ B_{12} & B_{16} & D_{11} & D_{12} & D_{16} \\ B_{22} & B_{26} & D_{12} & D_{22} & D_{26} \\ B_{26} & B_{66} & D_{16} & D_{26} & D_{66} \end{vmatrix}}{\begin{vmatrix} A_{11} & A_{12} & A_{16} & B_{11} & B_{12} & B_{16} \\ A_{12} & A_{22} & A_{26} & B_{12} & B_{22} & B_{26} \\ A_{16} & A_{26} & A_{66} & B_{16} & B_{26} & B_{66} \\ B_{11} & B_{12} & B_{16} & D_{11} & D_{12} & D_{16} \\ B_{12} & B_{22} & B_{26} & D_{12} & D_{22} & D_{26} \\ B_{16} & B_{26} & B_{66} & D_{16} & D_{26} & D_{66} \end{vmatrix}} \quad (3.206)$$

Considering the average direct stress [65], which is given by

$$f_x = \frac{N_x}{h} \quad (3.207)$$

Substituting N_x from Eqn. (3.207) into Eqn. (3.206), we obtain the equivalent Young's modulus in x-direction in membrane mode:

$$\frac{f_x}{\varepsilon_x^o} = E_x = \frac{\begin{vmatrix} A_{11} & A_{12} & A_{16} & B_{11} & B_{12} & B_{16} \\ A_{12} & A_{22} & A_{26} & B_{12} & B_{22} & B_{26} \\ A_{16} & A_{26} & A_{66} & B_{16} & B_{26} & B_{66} \\ B_{11} & B_{12} & B_{16} & D_{11} & D_{12} & D_{16} \\ B_{12} & B_{22} & B_{26} & D_{12} & D_{22} & D_{26} \\ B_{16} & B_{26} & B_{66} & D_{16} & D_{26} & D_{66} \end{vmatrix}}{\begin{vmatrix} A_{22} & A_{26} & B_{12} & B_{22} & B_{26} \\ A_{26} & A_{66} & B_{16} & B_{26} & B_{66} \\ B_{12} & B_{16} & D_{11} & D_{12} & D_{16} \\ B_{22} & B_{26} & D_{12} & D_{22} & D_{26} \\ B_{26} & B_{66} & D_{16} & D_{26} & D_{66} \end{vmatrix}} \frac{1}{h} \quad (3.208)$$

In a similar manner, an equivalent Young's modulus in y-direction in membrane mode is given by

$$\frac{f_y}{\varepsilon_y^o} = E_y = \frac{\begin{vmatrix} A_{11} & A_{12} & A_{16} & B_{11} & B_{12} & B_{16} \\ A_{12} & A_{22} & A_{26} & B_{12} & B_{22} & B_{26} \\ A_{16} & A_{26} & A_{66} & B_{16} & B_{26} & B_{66} \\ B_{11} & B_{12} & B_{16} & D_{11} & D_{12} & D_{16} \\ B_{12} & B_{22} & B_{26} & D_{12} & D_{22} & D_{26} \\ B_{16} & B_{26} & B_{66} & D_{16} & D_{26} & D_{66} \end{vmatrix}}{\begin{vmatrix} A_{11} & A_{16} & B_{11} & B_{12} & B_{16} \\ A_{16} & A_{66} & B_{16} & B_{26} & B_{66} \\ B_{11} & B_{16} & D_{11} & D_{12} & D_{16} \\ B_{12} & B_{26} & D_{12} & D_{22} & D_{26} \\ B_{16} & B_{66} & D_{16} & D_{26} & D_{66} \end{vmatrix}} \frac{1}{h} \quad (3.209)$$

Equivalent shear modulus in x-y plane in membrane mode is given by

$$\frac{f_{xy}}{\gamma_{xy}^o} = G_{xy} = \frac{\begin{vmatrix} A_{11} & A_{12} & A_{16} & B_{11} & B_{12} & B_{16} \\ A_{12} & A_{22} & A_{26} & B_{12} & B_{22} & B_{26} \\ A_{16} & A_{26} & A_{66} & B_{16} & B_{26} & B_{66} \\ B_{11} & B_{12} & B_{16} & D_{11} & D_{12} & D_{16} \\ B_{12} & B_{22} & B_{26} & D_{12} & D_{22} & D_{26} \\ B_{16} & B_{26} & B_{66} & D_{16} & D_{26} & D_{66} \end{vmatrix}}{\begin{vmatrix} A_{11} & A_{12} & B_{11} & B_{12} & B_{16} \\ A_{12} & A_{22} & B_{12} & B_{22} & B_{26} \\ B_{11} & B_{12} & D_{11} & D_{12} & D_{16} \\ B_{12} & B_{22} & D_{12} & D_{22} & D_{26} \\ B_{16} & B_{26} & D_{16} & D_{26} & D_{66} \end{vmatrix}} \frac{1}{h} \quad (3.210)$$

Now, considering a un-symmetric layered laminate arbitrary length in the x-direction, unit width in the y- direction, and thickness h, subjected to moment intensity M_x only, as shown in the Figure 3.13, then bending moment intensities can be simplified as follows

$$M_x \neq 0 \text{ and } M_y = M_{xy} = 0 \quad (3.211)$$

Substituting Eqn. (3.211) in laminate constitutive Eqn. (3.1), we obtain

$$\begin{Bmatrix} 0 \\ 0 \\ 0 \\ M_x \\ 0 \\ 0 \end{Bmatrix} = \begin{bmatrix} A_{11} & A_{12} & A_{16} & B_{11} & B_{12} & B_{16} \\ A_{12} & A_{22} & A_{26} & B_{12} & B_{22} & B_{26} \\ A_{16} & A_{26} & A_{66} & B_{16} & B_{26} & B_{66} \\ \hline B_{11} & B_{12} & B_{16} & D_{11} & D_{12} & D_{16} \\ B_{12} & B_{22} & B_{26} & D_{12} & D_{22} & D_{26} \\ B_{16} & B_{26} & B_{66} & D_{16} & D_{26} & D_{66} \end{bmatrix} \begin{Bmatrix} \epsilon_x^o \\ \epsilon_y^o \\ \gamma_{xy}^o \\ k_x \\ k_y \\ k_{xy} \end{Bmatrix} \quad (3.212)$$

Using the Cramer's rule to solve for k_x , we obtain

$$k_x = \frac{\begin{vmatrix} A_{11} & A_{12} & A_{16} & 0 & B_{12} & B_{16} \\ A_{12} & A_{22} & A_{26} & 0 & B_{22} & B_{26} \\ A_{16} & A_{26} & A_{66} & 0 & B_{26} & B_{66} \\ B_{11} & B_{12} & B_{16} & M_x & D_{12} & D_{16} \\ B_{12} & B_{22} & B_{26} & 0 & D_{22} & D_{26} \\ B_{16} & B_{26} & B_{66} & 0 & D_{26} & D_{66} \end{vmatrix}}{\begin{vmatrix} A_{11} & A_{12} & A_{16} & B_{11} & B_{12} & B_{16} \\ A_{12} & A_{22} & A_{26} & B_{12} & B_{22} & B_{26} \\ A_{16} & A_{26} & A_{66} & B_{16} & B_{26} & B_{66} \\ B_{11} & B_{12} & B_{16} & D_{11} & D_{12} & D_{16} \\ B_{12} & B_{22} & B_{26} & D_{12} & D_{22} & D_{26} \\ B_{16} & B_{26} & B_{66} & D_{16} & D_{26} & D_{66} \end{vmatrix}} \quad (3.213)$$

To obtain the solution of Eqn. (3.213), cofactor expansion can be used in the numerator for simplification, and then the Eqn. (3.213) can be simplified as follows:

$$k_x = \frac{M_x \begin{vmatrix} A_{11} & A_{12} & A_{16} & B_{12} & B_{16} \\ A_{12} & A_{22} & A_{26} & B_{22} & B_{26} \\ A_{16} & A_{26} & A_{66} & B_{26} & B_{66} \\ B_{12} & B_{22} & B_{26} & D_{22} & D_{26} \\ B_{16} & B_{26} & B_{66} & D_{26} & D_{66} \end{vmatrix}}{\begin{vmatrix} A_{11} & A_{12} & A_{16} & B_{11} & B_{12} & B_{16} \\ A_{12} & A_{22} & A_{26} & B_{12} & B_{22} & B_{26} \\ A_{16} & A_{26} & A_{66} & B_{16} & B_{26} & B_{66} \\ B_{11} & B_{12} & B_{16} & D_{11} & D_{12} & D_{16} \\ B_{12} & B_{22} & B_{26} & D_{12} & D_{22} & D_{26} \\ B_{16} & B_{26} & B_{66} & D_{16} & D_{26} & D_{66} \end{vmatrix}} \quad (3.214)$$

From engineer's theory of bending [65], we have

$$\frac{M}{I} = Ek \quad (3.215)$$

where $I = h^3/12$ per unit width across the y-axis and so moment about the y-axis is given by

$$M_x = k_x E_x \frac{h^3}{12} \quad (3.216)$$

Substituting Eqn. (3.215) in Eqn. (3.216), we obtain the equivalent Young's modulus in x-direction in bending mode.

$$E_x = \frac{\begin{vmatrix} A_{11} & A_{12} & A_{16} & B_{11} & B_{12} & B_{16} \\ A_{12} & A_{22} & A_{26} & B_{12} & B_{22} & B_{26} \\ A_{16} & A_{26} & A_{66} & B_{16} & B_{26} & B_{66} \\ B_{11} & B_{12} & B_{16} & D_{11} & D_{12} & D_{16} \\ B_{12} & B_{22} & B_{26} & D_{12} & D_{22} & D_{26} \\ B_{16} & B_{26} & B_{66} & D_{16} & D_{26} & D_{66} \end{vmatrix}}{h^3} \quad (3.217)$$

In a similar manner, an equivalent Young's modulus in y-direction in bending mode is given by

$$E_y = \frac{\begin{vmatrix} A_{11} & A_{12} & A_{16} & B_{11} & B_{12} & B_{16} \\ A_{12} & A_{22} & A_{26} & B_{12} & B_{22} & B_{26} \\ A_{16} & A_{26} & A_{66} & B_{16} & B_{26} & B_{66} \\ B_{11} & B_{12} & B_{16} & D_{11} & D_{12} & D_{16} \\ B_{12} & B_{22} & B_{26} & D_{12} & D_{22} & D_{26} \\ B_{16} & B_{26} & B_{66} & D_{16} & D_{26} & D_{66} \end{vmatrix}}{h^3} \quad (3.218)$$

Equivalent shear modulus in x-y plane in bending mode is given by

$$G_{xy} = \frac{\begin{vmatrix} A_{11} & A_{12} & A_{16} & B_{11} & B_{12} & B_{16} \\ A_{12} & A_{22} & A_{26} & B_{12} & B_{22} & B_{26} \\ A_{16} & A_{26} & A_{66} & B_{16} & B_{26} & B_{66} \\ B_{11} & B_{12} & B_{16} & D_{11} & D_{12} & D_{16} \\ B_{12} & B_{22} & B_{26} & D_{12} & D_{22} & D_{26} \\ B_{16} & B_{26} & B_{66} & D_{16} & D_{26} & D_{66} \end{vmatrix}}{h^3} \quad (3.219)$$

3.5 Calculation of flexural rigidity for symmetrical bending

In the following section, calculation of flexural rigidity for symmetric bending is presented. The following section follows that of ref. [65] and ref. [67].

Symmetrical bending of a section is said to occur when the section has single (C-section) or double (I-section) axis of symmetry and for this case, the neutral planes lie along the X and Y-axes, for the corresponding moments about X and Y-axes, respectively as shown in the Figure 3.14.

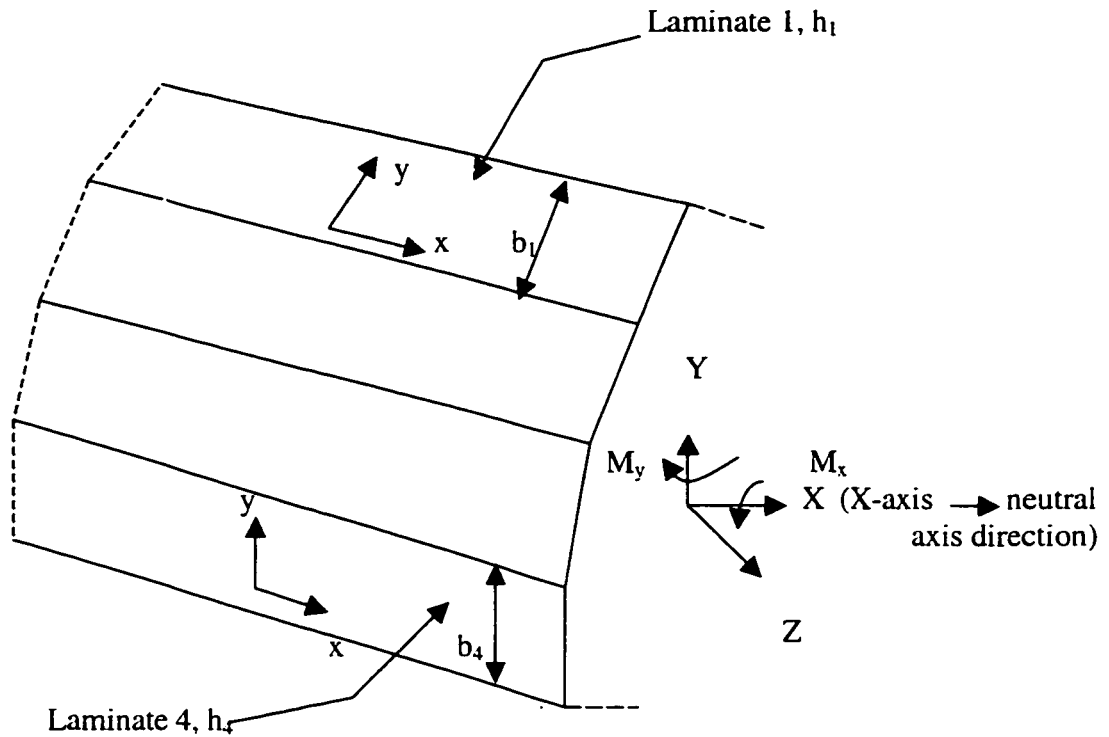


Figure 3.14 Symmetrical bending of a composite section

Overall flexural rigidities of a structure in x and y axes are given by the following equations [67], by assuming the bending mode for the flanges and axial mode for the web since the web bending mode is in the orthogonal direction to the bending mode of the overall beam:

$$E_X I_X = E_{x_1} I_{x_1} + E_{x_2} I_{x_2} + E_{x_3} I_{x_3} + \dots + E_{x_n} I_{x_n} \quad (3.220)$$

$$E_Y I_Y = E_{y_1} I_{y_1} + E_{y_2} I_{y_2} + E_{y_3} I_{y_3} + \dots + E_{y_n} I_{y_n} \quad (3.221)$$

In the above, E_x is the equivalent Young's modulus in x-direction, E_y is the equivalent Young's modulus in y-direction, I_x is the centroidal moment of inertia about the x-axis of the section and I_y is the centroidal moment of inertia about the y-axis of the section.

3.6 Formulation for thin-walled beam-columns

Considering the beam-column as shown in Figure 3.1, making the conventional assumptions as given in section 3.2, one obtains the following governing differential equation and boundary conditions:

$$\frac{\partial^2}{\partial x^2} \left[E(x)I(x) \frac{\partial^2 w(x,t)}{\partial x^2} \right] + P \frac{\partial^2 w(x,t)}{\partial x^2} + \rho(x)A(x) \frac{\partial^2 w(x,t)}{\partial t^2} = 0 \quad (3.222)$$

$$\left[E(0)I(0) \frac{\partial^2 w(0,t)}{\partial x^2} \right] - \alpha_1 \frac{\partial w(0,t)}{\partial x} = 0 \quad (3.223)$$

$$w(0,t) = 0 \quad (3.224)$$

$$\left[E(l)I(l) \frac{\partial^2 w(l,t)}{\partial x^2} \right] + \alpha_2 \frac{\partial w(l,t)}{\partial x} = 0 \quad (3.225)$$

$$w(l,t) = 0 \quad (3.226)$$

where $\alpha_1 = \alpha_2 = 0$ for simple supports and $\alpha_1 = \alpha_2 = \infty$ for fixed supports. The motion of vibration is assumed to be simple harmonic with circular frequency ω , so that the term $\partial^2 w / \partial t^2$ is replaced by $-\omega^2 w$.

The assumptions regarding the statistical properties of the beam-column can be restated as:

- (1) $a(x)$, $b_1(x)$, $c(x)$, and $d(x)$ are non-dimensional stationary random functions with zero mean and very small perturbations.
- (2) s and u are non-dimensional random variables that correspond to spring constants with zero mean and very small perturbations.
- (3) v is non-dimensional random variable that corresponds to axial load with zero mean and very small perturbations.
- (4) All random variables and random functions, except $a(\xi)$ and $c(\xi)$, and $b_1(\xi)$ and $d(\xi)$, are considered to be statistically independent.

Further, with the following substitutions,

$$x = \xi l \tag{3.227}$$

$$E(\xi) = E_o [1 + a(\xi)] \tag{3.228}$$

$$I(\xi) = I_o [1 + b_1(\xi)] \tag{3.229}$$

$$\rho(\xi) = \rho_o [1 + c(\xi)] \tag{3.230}$$

$$A(\xi) = A_o [1 + d(\xi)] \tag{3.231}$$

$$\alpha_1 = \alpha_{1o}(1+s) \quad (3.232)$$

$$\alpha_2 = \alpha_{2o}(1+u) \quad (3.233)$$

$$P = P_o(1+v) \quad (3.234)$$

$$\lambda_n = \frac{\rho_o A_o l^4 \omega_n^2}{E_o I_o} \quad (3.235)$$

$$R(\xi) = a(\xi) + b(\xi) + a(\xi)b(\xi) \quad (3.236)$$

$$S(\xi) = c(\xi) + d(\xi) + c(\xi)d(\xi) \quad (3.237)$$

The differential equation and boundary conditions reduce to,

$$\{[1 + R(\xi)]X_n^-(\xi)\}'' + P_o \frac{l^2}{E_o I_o} (1+v)X_n^-(\xi) = \lambda_n [1 + S(\xi)]X_n^-(\xi) \quad (3.238)$$

$$[1 + R(0)]X_n^-(0) - \frac{\alpha_{o1}l}{E_o I_o} (1+s)X_n^-(0) = 0 \quad X_n^-(0) = 0 \quad (3.239)$$

$$[1 + R(1)]X_n^-(1) - \frac{\alpha_{o2}l}{E_o I_o} (1+u)X_n^-(1) = 0 \quad X_n^-(1) = 0 \quad (3.240)$$

The solution to the above problem is given by using standard perturbation analysis [6] as:

$$\begin{aligned} \lambda_n = & \lambda_{no} + \frac{1}{D_n} \int_0^1 R(\xi) I_n(\xi) d\xi - \frac{\lambda_{no}}{D_n} \int_0^1 S(\xi) F_n(\xi) d\xi + \frac{\alpha_{1o}l}{E_o I_o} \frac{H_n(0)}{D_n} s \\ & + \frac{\alpha_{2o}l}{E_o I_o} \frac{H_n(1)}{D_n} u + \frac{P_o l^2}{E_o I_o} \frac{E_n}{D_n} v \end{aligned} \quad (3.241)$$

Terms D_n, E_n, F_n, H_n , and I_n are given in Eqs. (3.71) to (3.75).

Using the assumptions made with regard to statistical independence of the random variables and random functions and by taking the expected values of λ_n and λ_n^2 using Eqn. (3.75), we obtain

$$E[\lambda_n] = \lambda_{no} \quad (3.242)$$

$$\begin{aligned} \text{var}[\lambda_n] &= \frac{1}{D_n^2} \int_0^1 \int_0^1 E[R(\xi_1)R(\xi_2)]I_n(\xi_1)I_n(\xi_2)d\xi_1d\xi_2 \\ &+ \frac{\lambda_{no}^2}{D_n^2} \int_0^1 \int_0^1 E[S(\xi_1)S(\xi_2)]F_n(\xi_1)F_n(\xi_2)d\xi_1d\xi_2 \\ &- \frac{2\lambda_{no}}{D_n^2} \int_0^1 \int_0^1 E[R(\xi_1)S(\xi_2)]U_n(\xi_1)F_n(\xi_2)d\xi_1d\xi_2 \\ &\left(\frac{\alpha_{1o}l}{E_oI_o}\right)^2 \frac{H_n^2(0)}{D_n^2} \sigma_s^2 + \left(\frac{\alpha_{2o}l}{E_oI_o}\right)^2 \frac{H_n^2(1)}{D_n^2} \sigma_u^2 + \left(\frac{P_o l^2}{E_o I_o}\right)^2 \frac{E_n^2}{D_n^2} \sigma_v^2 \end{aligned} \quad (3.243)$$

Now by performing expectation operation on both sides in Eqn. (3.235) and using the Eqn. (3.84), we obtain the expected value of natural frequency.

$$E[\omega_n] \approx \sqrt{\frac{E_o I_o}{\rho_o A_o l^4}} * \sqrt{\frac{1}{2} \left[E[\lambda_n] + \sqrt{(E[\lambda_n])^2 - \text{var}[\lambda_n]} \right]} \quad (3.244)$$

Now by performing the operation for variance on both sides in Eqn. (3.235) and using the Eqn. (3.89), we obtain the following relation for variance of natural frequency.

$$\text{var}[\omega_n] \approx \frac{E_o I_o}{\rho_o A_o l^4} \text{var}[\sqrt{\lambda_n}] \quad (3.245)$$

3.7 Parametric study

In the following sections, parametric study is performed on symmetrical I-section with flanges made up of symmetric angle-ply laminate $[+45/-45]_{9s}$ and web made up of un-symmetric laminate $[0/45]_{18T}$.

3.7.1 Random axial force

First of all, let us consider that the composite beam-column is simply supported at both ends and all coefficients in the governing differential equation are deterministic except for the compressive axial force, P .

After performing the standard perturbation analysis, we have non-dimensionalized expected value and variance value given as,

$$E[\lambda_n] = n^2\pi^2(n^2\pi^2 - P_oG) \quad (3.246)$$

$$\text{var}[\lambda_n] = n^4\pi^4(P_oG)^2\sigma_v^2 \quad (3.247)$$

Substituting Eqn. (3.246) and (3.247) in Eqn. (3.110) and Eqn. (3.112), we obtain expected value and variance value of natural frequency ω_n , which are given by,

$$E[\omega_n] \approx \sqrt{\frac{n^4\pi^4 EI}{\rho A l^4} \left[\frac{1}{2} \left\{ \left(1 - \frac{P_oG}{n^2\pi^2} \right) + \sqrt{\left(1 - \frac{P_oG}{n^2\pi^2} \right)^2 - \frac{P_o^2 G^2 \sigma_v^2}{n^4\pi^4}} \right\} \right]^{1/2}} \quad (3.248)$$

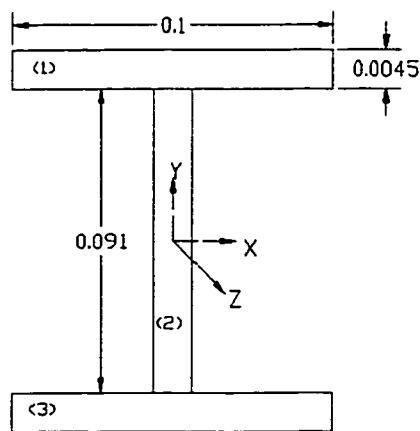
$$\text{var}[\omega_n] \approx \frac{EI}{4\rho A l^4} \frac{P_o^2 G^2 \sigma_v^2}{n^4 \pi^4} \frac{1}{\left(1 - \frac{P_o G}{n^2 \pi^2}\right)^2} \quad (3.249)$$

Deterministic free vibration frequency for the beam-column with compressive axial load is given by [68]:

$$^* \omega_n = \frac{n^2 \pi^2}{l^2} \sqrt{\frac{EI}{\rho A}} \sqrt{1 - \frac{Pl^2}{n^2 \pi^2 EI}} \quad (3.250)$$

3.7.1.1 Numerical examples

A composite laminate consisting of a total of 36 plies made of NCT-301 Graphite-Epoxy composite material, each having a ply thickness of 0.125 mm is considered. The length of the laminate is 1.2 m and the cross-sectional dimensions are as shown in Figure 3.15.



Flanges (1) and (3) [+45/-45]_{9s}
 Web (2) [0/45]_{18τ}

All dimensions are in meters

Figure 3.15 Symmetric I-section

The flexural rigidity is given by,

$$E_x I_x = (E_{x_1} I_{x_1})_{bending_mode} + (E_{x_2} I_{x_2})_{membrane_mode} + (E_{x_3} I_{x_3})_{bending_mode} \quad (3.251)$$

where, (1) and (3) corresponds to flange and (2) corresponds to web, and $Z = x$.

The calculated values of EI, for the I-section is given in the following:

$$E_x I_x = 11.49 \times 10^3 \text{ N-m}^2 \text{ and } E_y I_y = 53.41 \times 10^3 \text{ N-m}^2$$

One of the interesting problems in engineering applications is the calculation of the lowest frequency and critical buckling load. Therefore the lower value of EI is considered for the following parametric study.

P_{cr} is calculated using the one-dimensional deterministic analysis as explained in chapter 2.

Table 3.17 shows the deterministic, expected and variance values of first natural frequency ω_1 for given input σ_v^2 and axial load.

The graph of the variance of ω_1 for given input σ_v^2 is illustrated in Figure 3.16.

Input, σ_v^2	$P_o / P_{cr} = 1/4$			$P_o / P_{cr} = 1/2$		
	$\# \omega_1$	$E[\omega_1]$	$\text{var}[\omega_1]$	$\# \omega_1$	$E[\omega_1]$	$\text{var}[\omega_1]$
0.01	457.01	456.94	0.794	373.19	372.72	7.143
0.05		456.69	3.973		370.82	35.71
0.09		456.43	7.152		368.87	64.28
0.13		456.18	10.33		366.86	92.86

Table 3.17 Mean value and variance of 1st natural frequency for given P_o / P_{cr}

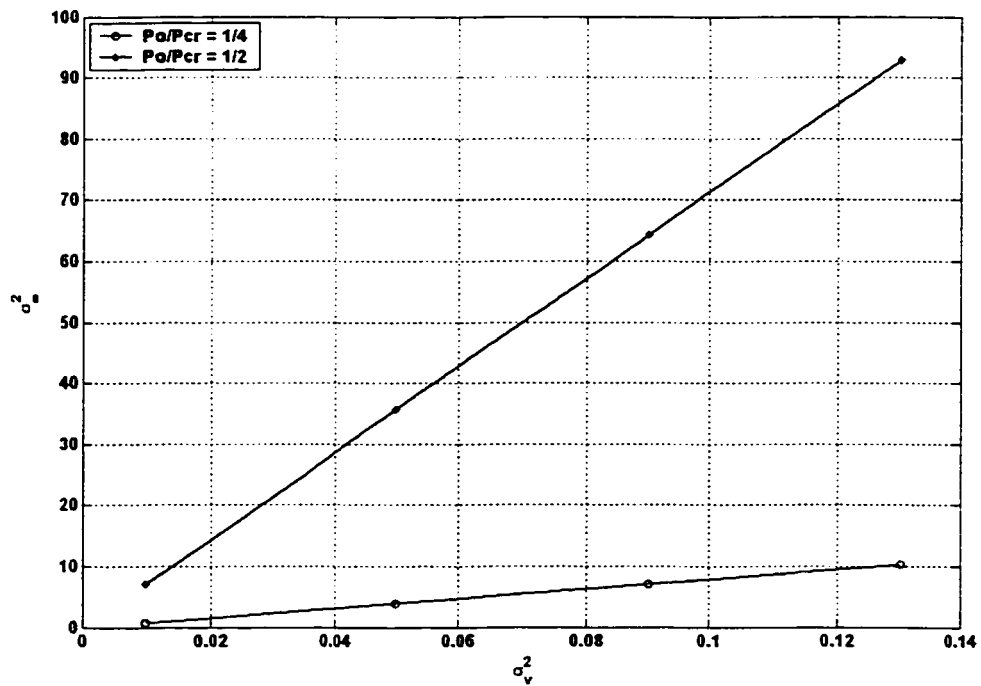


Figure 3.16 The variance of 1st natural frequency vs σ_v^2

Observations:

It can be observed from Table 3.17 that the expected values of natural frequency ω_i are almost the same as the deterministic natural frequency ${}^*\omega_i$ when the given input axial load is $\frac{1}{4}$ of the critical buckling load and it can be seen that the expected values of natural frequency ω_i are slightly different from the deterministic natural frequency ${}^*\omega_i$ when the given input axial load is $\frac{1}{2}$ of the critical buckling load. The expected value decrease as the input random variable v and axial load increase. Also it can be observed from Eqn. (3.248) and Tables 3.17 that the input variance term σ_v^2 has more effect on the expected value when axial load reaches the critical buckling load.

It can be observed from Tables 3.17 that the variance value increases quite significantly and this significant increase was observed when the axial load reaches the critical buckling load and also we note that the variance of natural frequency ω_i takes on quite a large value compared to the small variance of the input σ_v^2 .

The mean square value and variance of ω_n are linear functions of the variance of v . The Figure 3.16 shows that they are linearly related.

3.7.2 Random material and geometric properties

Now let us consider that the composite beam-column is simply supported at both ends and further the axial force, stiffness term, material properties and geometric coefficients are random.

3.7.2.1 Case 1: Uniform auto-correlation and cross-correlation functions

Let us consider the case where all auto-correlation and cross-correlation functions have a uniform distribution and their constant values are equal to the variance or product of standard deviations respectively. In other words, we have complete statistical dependence between random functions at any two arbitrary locations. After performing the standard perturbation analysis [6], we have non-dimensionalized expected value and variance value, which are obtained by solving equations (3.242) and (3.243),

$$E[\lambda_n] = n^2 \pi^2 (n^2 \pi^2 - P_o G) \quad (3.252)$$

$$\begin{aligned} \text{var}[\lambda_n] = & n^8 \pi^8 (\sigma_a^2 + \sigma_b^2 + \sigma_a^2 \sigma_b^2) + n^4 \pi^4 (n^2 \pi^2 - P_o G)^2 [\sigma_c^2 + \sigma_d^2 + \sigma_c^2 \sigma_d^2] \\ & - 2n^6 \pi^6 (n^2 \pi^2 - P_o G) (\sigma_a \sigma_c + \sigma_b \sigma_d + \sigma_a \sigma_c \sigma_b \sigma_d) + n^4 \pi^4 (P_o G)^2 \sigma_v^2 \end{aligned} \quad (3.253)$$

Substituting Eqs. (3.251) and (3.253) in Eqn. (3.110) and Eqn. (3.112), we obtain expected value and variance value of natural frequency ω_n , which are given by,

$$E[\omega_n] \approx \sqrt{\frac{E_o I_o}{\rho_o A_o l^4}} * \sqrt{\frac{1}{2} \left[E[\lambda_n] + \sqrt{(E[\lambda_n])^2 - \text{var}[\lambda_n]} \right]} \quad (3.254)$$

$$\text{var}[\omega_n] \approx \frac{E_o I_o}{\rho_o A_o l^4} \text{var}[\sqrt{\lambda_n}] \quad (3.255)$$

3.7.2.1.1 Numerical examples

Laminate sectional dimensions and configurations are the same as explained in section 3.7.1.1.

Table 3.18 shows the deterministic, expected and variance values of first natural frequency ω_1 for given input $\sigma_a^2 = \sigma_{b_1}^2 = \sigma_c^2 = \sigma_d^2 = \sigma_v^2 = \sigma^2$ and axial load.

Figure 3.17 shows the variance of 1st natural frequency when material and geometric properties have uniform correlation.

Note: $\sigma_a^2 = \sigma_{b_1}^2 = \sigma_c^2 = \sigma_d^2 = \sigma_v^2 = \sigma^2$

Input, σ^2	$P_o / P_{cr} = 1/4$			$P_o / P_{cr} = 1/2$		
	$\# \omega_1$	$E[\omega_1]$	$\text{var}[\omega_1]$	$\# \omega_1$	$E[\omega_1]$	$\text{var}[\omega_1]$
0.01	457.01	456.81	2.3921	373.19	371.77	21.500
0.05		456.03	12.119		365.71	108.93
0.09		455.22	22.100		358.90	198.64
0.13		454.38	32.336		351.10	290.65

Table 3.18 Mean value and variance of 1st natural frequency when material and geometric properties have uniform correlation

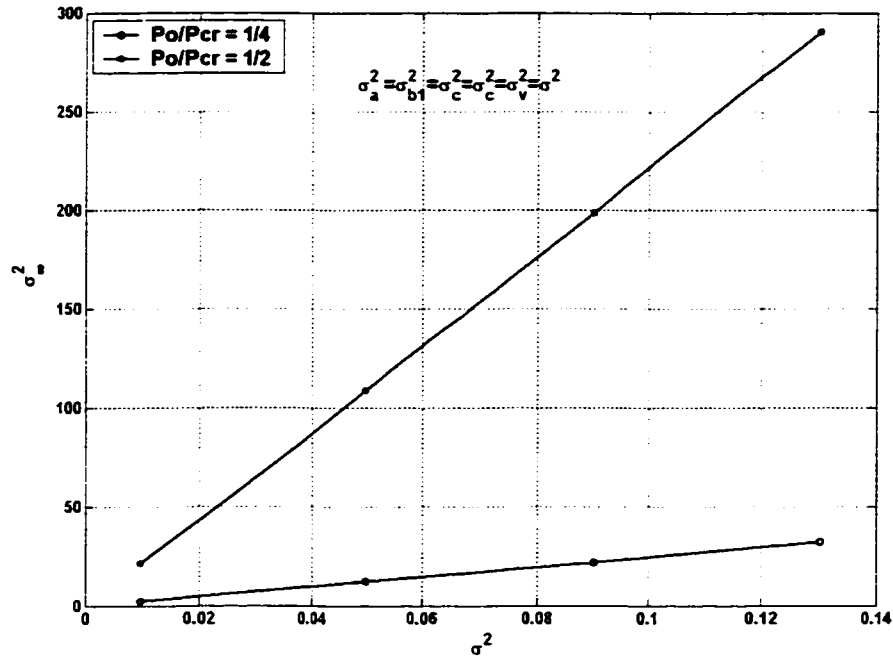


Figure 3.17 The variance of 1st natural frequency vs σ^2

Observations:

It can be observed from the Table 3.18 that the difference between the expected value of natural frequency ω_i and deterministic natural frequency is more when the input σ^2 increases and also when the axial load approaches the critical buckling load.

The Figure 3.17 represents that the variance of ω_n increases linearly with σ^2 and also it can be observed that variance of natural frequency ω_n takes on quite a large value compared to small input of σ^2 .

3.7.2.2 Case 2: Exponential auto and cross-correlation functions

Let us consider the case where all auto-correlation and cross-correlation functions have exponential distribution. After performing the standard perturbation analysis [6], using the auto-correlation and cross-correlation functions given, the non-dimensional expected and variance values are obtained as follows:

$$R_a(\xi_1 - \xi_2) = \sigma_a^2 e^{-k_1|\xi_1 - \xi_2|} ; \quad R_{b_1}(\xi_1 - \xi_2) = \sigma_{b_1}^2 e^{-k_2|\xi_1 - \xi_2|} \quad (3.256)$$

$$R_c(\xi_1 - \xi_2) = \sigma_c^2 e^{-k_3|\xi_1 - \xi_2|} ; \quad R_d(\xi_1 - \xi_2) = \sigma_d^2 e^{-k_4|\xi_1 - \xi_2|} \quad (3.257)$$

$$R_{ac}(\xi_1 - \xi_2) = \sigma_a \sigma_c e^{-k_3|\xi_1 - \xi_2|} ; \quad R_{b_1d}(\xi_1 - \xi_2) = \sigma_{b_1} \sigma_d e^{-k_4|\xi_1 - \xi_2|} \quad (3.258)$$

$$E[\lambda_n] = n^2 \pi^2 (n^2 \pi^2 - P_o G) \quad (3.259)$$

$$\begin{aligned} \text{var}(\lambda_n) &= 4n^8 \pi^8 (\sigma_a^2 + \sigma_{b_1}^2) \int_0^1 \int_0^1 e^{-k|\epsilon_1 - \epsilon_2|} \sin^2 n\pi\epsilon_1 \sin^2 n\pi\epsilon_2 d\xi_1 d\xi_2 \\ &+ 4n^8 \pi^8 \sigma_a^2 \sigma_{b_1}^2 \int_0^1 \int_0^1 e^{-2k|\epsilon_1 - \epsilon_2|} \sin^2 n\pi\epsilon_1 \sin^2 n\pi\epsilon_2 d\xi_1 d\xi_2 \\ &+ 4\lambda_{no}^2 (\sigma_c^2 + \sigma_d^2) \int_0^1 \int_0^1 e^{-k|\epsilon_1 - \epsilon_2|} \sin^2 n\pi\epsilon_1 \sin^2 n\pi\epsilon_2 d\xi_1 d\xi_2 \\ &+ 4\lambda_{no}^2 (\sigma_c^2 \sigma_d^2) \int_0^1 \int_0^1 e^{-2k|\epsilon_1 - \epsilon_2|} \sin^2 n\pi\epsilon_1 \sin^2 n\pi\epsilon_2 d\xi_1 d\xi_2 \\ &- 8\lambda_{no} n^4 \pi^4 (\sigma_a \sigma_c + \sigma_{b_1} \sigma_d) \int_0^1 \int_0^1 e^{-k|\epsilon_1 - \epsilon_2|} \sin^2 n\pi\epsilon_1 \sin^2 n\pi\epsilon_2 d\xi_1 d\xi_2 \\ &- 8\lambda_{no} n^4 \pi^4 \sigma_a \sigma_c \sigma_{b_1} \sigma_d \int_0^1 \int_0^1 e^{-2k|\epsilon_1 - \epsilon_2|} \sin^2 n\pi\epsilon_1 \sin^2 n\pi\epsilon_2 d\xi_1 d\xi_2 \\ &+ n^4 \pi^4 (P_o G)^2 \sigma_v^2 \end{aligned} \quad (3.260)$$

Substituting Eqn. (3.259) and (3.260) in Eqn. (3.110) and Eqn. (3.112), we obtain expected value and variance value of natural frequency ω_n as follows:

$$E[\omega_n] \approx \sqrt{\frac{E_o I_o}{\rho_o A_o l^4}} * \sqrt{\frac{1}{2} \left[E[\lambda_n] + \sqrt{(E[\lambda_n])^2 - \text{var}[\lambda_n]} \right]} \quad (3.261)$$

$$\text{var}[\omega_n] \approx \frac{E_o I_o}{\rho_o A_o l^4} \text{var}[\sqrt{\lambda_n}] \quad (3.262)$$

3.7.2.2.1 Numerical examples

Laminate sectional dimensions and configurations are the same as explained in section 3.7.1.1.

Figure 3.18 provides the variance of 1st natural frequency when material and geometric properties have exponential correlation.

Figure 3.19 shows the variance of 1st natural frequency vs correlation length for given input variance and P_o/P_{cr} .

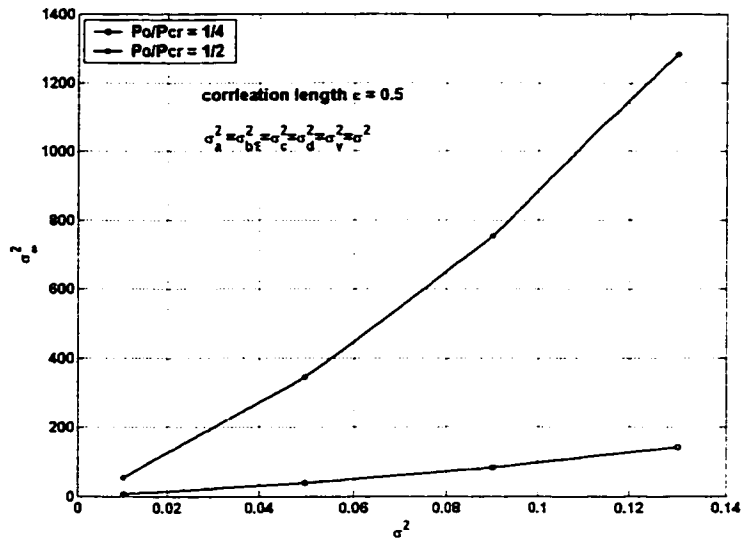


Figure 3.18 The variance of 1st natural frequency vs σ^2 for given correlation length and P_0 / P_{cr} when material and geometric properties have exponential correlation

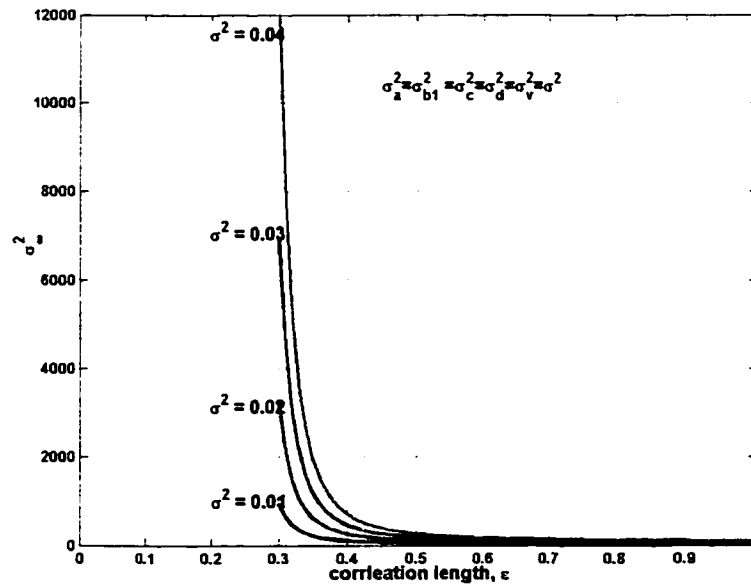


Figure 3.19 The variance of 1st natural frequency vs ϵ for given variance and $P_0 / P_{cr} = 1/2$

Observations:

The Figure 3.18 shows the relation between input variance ν and output variance ω_1 and the graph shows that the variances of natural frequencies increase in a piecewisely linear manner.

In Figure 3.19, it can be observed that the variance of ω_1 increases exponentially as the correlation length, ε , decreases. The variance of ω_1 is almost infinity when the correlation length is very small. This means that if the inputs at any two locations are almost uncorrelated, the variance of output becomes infinity.

3.8 Conclusions and discussions

In this chapter, the formulation for the free vibration of composite beam-columns with stochastic properties is developed using standard perturbation analysis. Three cases are considered i.e. (1) Random axial load (2) Random material and geometric properties having uniform correlation, and (3) Random material and geometric properties having exponential correlation. Expected, Mean square and Variance values of 1st natural frequency for $[0/90]_{9s}$, $[+45/-45]_{9s}$, $[0/-60/60]_{6s}$, and $[0/45]_{18T}$ NCT-301 composite laminates are determined corresponding to cylindrical bending and one-dimensional laminated beam theories. Further, the formulation is extended to the composite thin-walled beam-columns and the probabilistic characteristics are obtained.

From the results, it is observed that the expected value of natural frequency ω_1 differs more from the deterministic natural frequency when the input random variable ν increases and also when the axial load approaches the critical buckling load. Also it can be seen that the variance of ω_1 and given input σ^2 are linearly related when random properties have uniform correlation, whereas the corresponding graph for exponential correlation shows that the variation is piecewisely linear.

It can be observed that the ratio of coefficients of variation of input and output is independent of material and geometric properties and depends on P_c and σ_ν^2 .

Comparing the results for various composite laminates, it is observed that un-symmetric laminate possesses the highest mean and variance values of natural frequency whereas symmetric angle-ply laminate has the lowest mean and variance values of natural frequency.

Chapter 4

BUCKLING OF COMPOSITE BEAM-COLUMNS WITH STOCHASTIC PROPERTIES

4.1 Introduction

In recent years, the applications of composite materials in various automotive, aerospace, structural, marine and mechanical engineering industries have increased tremendously. The main advantages of composite materials over the conventional high strength metals are: high strength, high stiffness, low cost, low density, wear resistance and, thermal and acoustic insulation. Composite laminates display significant variability in their material, geometric and structural properties. This variability is attributed to the variations in the properties of the fibers, matrices and interfaces, in the fiber orientations, in the void content and in the ply thickness. These variations are unavoidable and are induced during manufacturing and service. Therefore, in the design and failure prediction these variations have to be taken into account. Beam-columns made of polymer-matrix fiber-reinforced composite materials are increasingly being used in many engineering industries. The buckling is of paramount importance in the design and development of high-performance composite mechanical components.

In the present chapter, the buckling of such composite beam-columns is considered and probabilistic characteristics of critical buckling loads are determined. Further, in this chapter, thin-walled composite beam-columns are considered. In the design of thin-walled beam-columns local buckling is a priority over the global buckling. Therefore, the

theoretical view of elastic local instability of anisotropic composite beam-columns, in which they are treated as assemblies of generally laminated composite plates buckling under uniaxial compressive forces, is presented, and probabilistic characteristics of critical buckling loads are determined.

In section 4.2, the formulation for the buckling of composite beam-column is developed. In section 4.3, parametric study has been performed on symmetric cross-ply laminate $[0/90]_{9s}$, symmetric angle-ply laminate $[+45/-45]_{9s}$, quasi isotropic laminate $[0/-60/60]_{6s}$, and unsymmetric laminate $[0/45]_{18T}$ corresponding to cylindrical bending and one-dimensional laminated beam theories for various boundary conditions. Further, in this chapter, in section 4.4, deterministic local buckling of thin-walled composite beam-columns is described for various boundary conditions. In section 4.5, stochastic local buckling of thin-walled composite beam-columns is considered. Further, in this section, stochastic simulation of laminate bending stiffness matrix is described. Finally, in section 4.6, parametric study is performed for various types of laminate configurations by changing the aspect ratio and loading edge boundary conditions.

4.2 Formulation for the buckling of composite beam-column

Let us consider the buckling of composite beam-columns that have a stochastic distribution of stiffness properties and geometric boundary conditions. A composite beam-column with axial compressive force and generalized boundary conditions is shown in Figure 4.1.

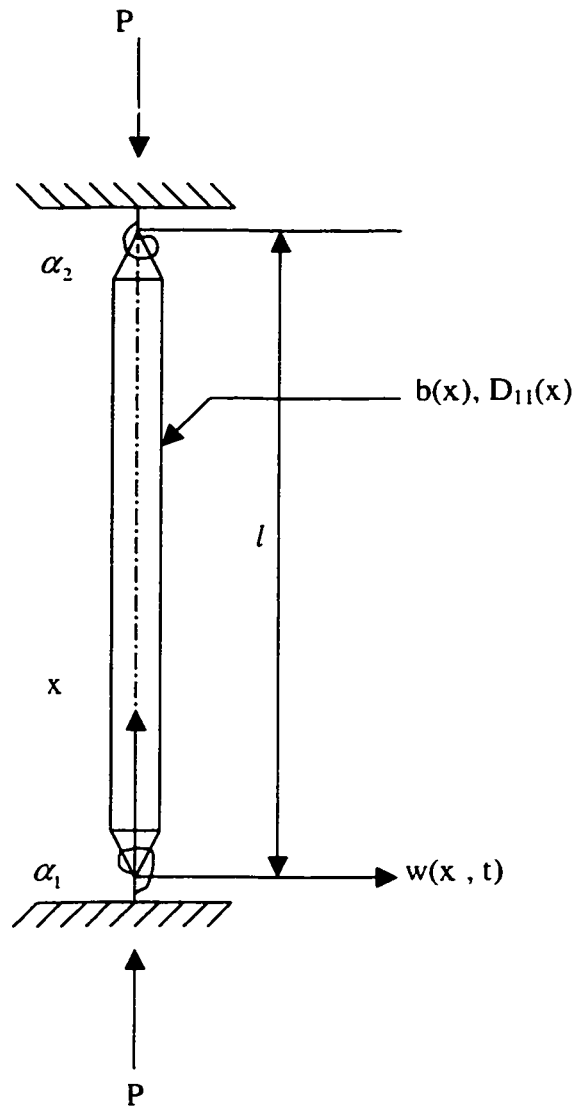


Figure 4.1 Composite beam-column

Making the basic assumptions, as mentioned in previous chapter, the partial differential equation describing the response of a beam-column made of fiber-reinforced composite laminate is given below:

$$\frac{\partial^2}{\partial x^2} \left[b(x) D_{11}(x) \frac{\partial^2 w(x, t)}{\partial x^2} \right] + P \frac{\partial^2 w(x, t)}{\partial x^2} + \rho(x) A(x) \frac{\partial^2 w(x, t)}{\partial t^2} = 0 \quad (4.1)$$

The generalized boundary conditions are given by

$$\left[b(0)D_{11}(0) \frac{\partial^2 w(0,t)}{\partial x^2} \right] - \alpha_1 \frac{\partial w(0,t)}{\partial x} = 0 \quad (4.2)$$

$$w(0,t) = 0 \quad (4.3)$$

$$\left[b(l)D_{11}(l) \frac{\partial^2 w(l,t)}{\partial x^2} \right] + \alpha_2 \frac{\partial w(l,t)}{\partial x} = 0 \quad (4.4)$$

$$w(l,t) = 0 \quad (4.5)$$

In the above, $w(x,t)$ is the lateral displacement as a function of spatial coordinate x and time t , $b(x)$ is the width of the laminate as a function of x , $D_{11}(x)$ is the laminate bending stiffness coefficient as a function of x , P is the axial compressive force, α_1 and α_2 are the coefficients of boundary rigidities and l is the length of the beam-column.

In the above equations, when the cylindrical bending theory [1] is used, the term D_{11} is set to be equal to D/A , where D/A is a function of membrane, coupling and bending stiffness terms [1]. When the one-dimensional laminated beam theory [1] is used, the term D_{11} is set to be equal to $1/D_{11}^*$, where D_{11}^* is bending compliance coefficient [1].

Since the coefficients of Eqs. (4.1) to (4.5) are random or probabilistic, then the buckling load is also random. Hence the problem has to be analyzed using a probabilistic approach. The response can be evaluated in the form of mean values, mean square values

and variances of buckling loads. Such results give enough information for engineering interest.

The assumptions made about the stochastic coefficients and random variables except assumptions 4 and 6, in the previous chapter, for the free-vibration case, are again made here. Hence the coefficients in the governing differential equation and boundary conditions are given by

$$D_{11}(x) = D_{11o}[1 + a(x)] \quad (4.6)$$

$$b(x) = b_o[1 + b_1(x)] \quad (4.7)$$

$$\alpha_1 = \alpha_{1o}(1 + s) \quad (4.8)$$

$$\alpha_2 = \alpha_{2o}(1 + u) \quad (4.9)$$

4.2.1 General solution to the stochastic equation

The solution for the Eqn. (4.1) is assumed to be of the form

$$w(x, t) = \sum_{n=1}^{\infty} W_n X_n(x) \quad (4.10)$$

where $X_n(x)$ are the space dependent buckling modes, forming a complete set and satisfying the boundary conditions, and W_n are the amplitudes. For buckling problem W_n will be set to be equal to 1.

These modes are obtained by introducing Eqn. (4.10) into governing Eqn. (4.1):

$$\left[b(x)D_{11}(x)X_n^-(x) \right]'' + PX_n^-(x) = 0 \quad (4.11)$$

In the above equation, the prime denotes d/dx .

Now let us convert the independent variable x to ξ using the expression $\xi = x/l$. Then we have a non-dimensionalized eigen value problem, which is given by

$$\left[b(\xi)D_{11}(\xi)X_n^-(\xi) \right]'' + Pl^2X_n^-(\xi) = 0 \quad (4.12)$$

and the corresponding boundary conditions are given by

$$b(0)D_{11}(0)X_n^-(0) - l\alpha_1 X_n^-(0) = 0 \quad ; \quad X_n^-(0) = 0 \quad (4.13)$$

$$b(1)D_{11}(1)X_n^-(1) + l\alpha_2 X_n^-(1) = 0 \quad ; \quad X_n^-(1) = 0 \quad (4.14)$$

Now substituting Eqs. (4.6) to (4.9) in the governing differential Eqn. (4.12) and boundary conditions given by Eqs. (4.13) and (4.14), we obtain the following stochastic equation:

$$\left\{ [1 + R(\xi)]X_n^-(\xi) \right\}'' + \frac{Pl^2}{b_o D_{11_o}} X_n^-(\xi) = 0 \quad (4.15)$$

Let

$$\mu_n = \frac{P_n l^2}{b_o D_{11_o}} \quad (4.16)$$

where μ is the non-dimensional function of the static buckling load P .

Now, Eqn. (4.15) can be written as

$$\{[1 + R(\xi)]X_n^-(\xi)\}'' + \mu X_n^-(\xi) = 0 \quad (4.17)$$

and the boundary conditions are

$$(1 + R(0))X_n^-(0) - \frac{l\alpha_{o1}}{b_o D_{11_o}}(1 + s)X_n^-(0) = 0 \quad ; \quad X_n^-(0) = 0 \quad (4.18)$$

$$(1 + R(1))X_n^-(1) + \frac{l\alpha_{o2}}{b_o D_{11_o}}(1 + u)X_n^-(1) = 0 \quad ; \quad X_n^-(1) = 0 \quad (4.19)$$

where

$$R(\xi) = a(\xi) + b_1(\xi) + a(\xi)b_1(\xi) \quad (4.20)$$

$$R(0) = q = a(0) + b_1(0) + a(0)b_1(0) \quad (4.21)$$

$$R(1) = r = a(1) + b_1(1) + a(1)b_1(1) \quad (4.22)$$

$R(\xi)$ is a random function of $a(\xi)$ and $b_1(\xi)$. Therefore for fixed co-coordinate ξ , it becomes a random variable. Hence q and r are random variables. Because of our assumptions, mean value of $R(\xi)$ is zero, so we have zero mean for q and r .

It is assumed that all coefficients of the governing differential equation and boundary conditions have small random perturbations. Therefore perturbation method can be applied to the following problem with satisfactory accuracy.

Now let us consider the modified differential equation obtained by assigning a perturbation parameter α to Eqn. (4.18):

$$\left\{ [1 + \alpha R(\xi)] X_n''(\xi) \right\} + \mu_n X_n''(\xi) = 0 \quad (4.23)$$

At the end of the analysis, α is set to be equal to 1.

Now let us assume the solutions μ_n and the corresponding modes $X_n(\xi)$ of the above Eqn. (4.23) and the boundary conditions given by Eqs. (4.18) and (4.19) in the following expanded forms.

$$\mu_n = \mu_{n0} + \mu_{n1}\alpha + \mu_{n2}q + \mu_{n3}r + \mu_{n4}s + \mu_{n5}u \quad (4.24)$$

$$\begin{aligned} X_n(\xi) = & X_{n0}(\xi) + X_{n1}(\xi)\alpha + X_{n2}(\xi)q + X_{n3}(\xi)r \\ & + X_{n4}(\xi)s + X_{n5}(\xi)u \end{aligned} \quad (4.25)$$

Now, substitute Eqs. (4.24) and (4.25) in modified governing Eqn. (4.23) and boundary conditions given by the Eqs. (4.18) and (4.19).

The perturbation procedure followed from here onwards is similar to that followed in the free-vibration problem. Further, substitute $\beta = 0$ in the procedure followed in the free-vibration problem.

After some simplifications, the expression for the non-dimensional static buckling load μ_n is obtained as follows:

$$\mu_n = \mu_{n0} + \frac{1}{D_n} \int_0^1 R(\xi) I_n(\xi) d\xi + \frac{\alpha_{10} l}{b_o D_{11_o}} \frac{H_n(0)}{D_n} s + \frac{\alpha_{20} l}{b_o D_{11_o}} \frac{H_n(1)}{D_n} u \quad (4.26)$$

where

$$D_n = \int_0^1 [X_o'(\xi)]^2 d\xi \quad (4.27)$$

$$I_n(\xi) = [X_o^-(\xi)]^2 \quad (4.28)$$

$$H_n(\xi) = [X_o^+(\xi)]^2 \quad (4.29)$$

From Eqn. (4.26), it can be seen that μ_n is composed of the following terms. The first term μ_{no} is independent of any random function or random variable and can be obtained by solving the deterministic eigen value problem. The second term on the right hand side represents the effects of random coefficients contained in the governing differential equation, and the third and fourth terms are for boundary rigidity.

Now applying the expectation operator on both sides in Eqn. (4.26), we obtain

$$E[\mu_n] = \mu_{no} + \frac{1}{D_n} \int_0^1 E[R(\xi)] I_n(\xi) d\xi + \frac{\alpha_{1o} l}{b_o D_{11o}} \frac{H_n(0)}{D_n} E(s) + \frac{\alpha_{2o} l}{b_o D_{11o}} \frac{H_n(1)}{D_n} E(u) \quad (4.30)$$

Using the assumptions made with regard to statistical independence of the random variables and random functions, we obtain

$$E[\mu_n] = \mu_{no} \quad (4.31)$$

We note from the above equation that the expected value of μ_n is independent of any random inputs and coincides with the solution of the corresponding deterministic buckling problem.

Substituting the value of μ_n from Eqn. (4.16), we have

$$E\left[\frac{P_n l^2}{b_o D_{1l_o}}\right] = E[\mu_n] \quad (4.32)$$

$$\therefore E[P_n] = \mu_{no} \frac{b_o D_{1l_o}}{l^2} \quad (4.33)$$

By using Eqn. (4.26), we calculate μ_n^2 . Then introducing the statistical treatment to μ_n^2 , we obtain the following relation for mean square value.

$$\begin{aligned} E[\mu_n^2] &= \mu_{no}^2 + \frac{1}{D_n^2} \int_0^1 \int_0^1 E[R(\xi_1)R(\xi_2)]V_n(\xi_1)I_n(\xi_2)d\xi_1 d\xi_2 + \left(\frac{\alpha_{1o}l}{b_o D_{1l_o}}\right)^2 \frac{H_n^2(0)}{D_n^2} \sigma_s^2 \\ &+ \left(\frac{\alpha_{2o}l}{b_o D_{1l_o}}\right)^2 \frac{H_n^2(1)}{D_n^2} \sigma_u^2 \end{aligned} \quad (4.34)$$

In obtaining the above equation, the following assumptions of statistical independency have been used.

$$E[sR(\xi)] = E[uR(\xi)] = E[su] = 0 \quad (4.35)$$

The variance of μ_n is given by

$$\begin{aligned} \text{var}[\mu_n] &= E[\mu_n^2] - E[\mu_n]^2 \\ &= \frac{1}{D_n^2} \int_0^1 \int_0^1 E[R(\xi_1)R(\xi_2)]V_n(\xi_1)I_n(\xi_2)d\xi_1 d\xi_2 \\ &+ \left(\frac{\alpha_{1o}l}{b_o D_{1l_o}}\right)^2 \frac{H_n^2(0)}{D_n^2} \sigma_s^2 + \left(\frac{\alpha_{2o}l}{b_o D_{1l_o}}\right)^2 \frac{H_n^2(1)}{D_n^2} \sigma_u^2 \end{aligned} \quad (4.36)$$

Now by using the Eqn. (4.16), we obtain the variance of buckling load P_n .

$$\begin{aligned} \text{var}[P_n] = & \left[\frac{1}{D_n^2} \int_0^1 \int_0^1 E[R(\xi_1)R(\xi_2)]I_n(\xi_1)I_n(\xi_2)d\xi_1d\xi_2 \right. \\ & \left. + \left(\frac{\alpha_{1o}l}{b_o D_{11o}} \right)^2 \frac{H_n^2(0)}{D_n^2} \sigma_s^2 + \left(\frac{\alpha_{2o}l}{b_o D_{11o}} \right)^2 \frac{H_n^2(1)}{D_n^2} \sigma_u^2 \right] \left[\frac{b_o D_{11o}}{l^2} \right]^2 \end{aligned} \quad (4.37)$$

In the above Eqn. (4.37), the terms σ_s^2 and σ_u^2 are the variances of s and u respectively, and the term $E[R(\xi_1)R(\xi_2)]$ is the auto-correlation function.

Since we assumed the stationarity property of random processes, the above terms are functions of $(\xi_1 - \xi_2)$ instead of ξ_1 and ξ_2 . Using the Eqn. (4.20), we obtain the following equation for the auto-correlation function.

$$E[R(\xi_1)R(\xi_2)] = R_a(\xi_1 - \xi_2) + R_{b_1}(\xi_1 - \xi_2) + R_a(\xi_1 - \xi_2)R_{b_1}(\xi_1 - \xi_2) \quad (4.38)$$

In the above, $R_a(\xi_1 - \xi_2)$ indicates the auto-correlation function of $a(\xi)$.

4.3 Parametric study

In the following sections, parametric study is performed on four different types of laminates i.e. (a) Symmetric Cross-ply Laminate: $[0/90]_{9s}$, (b) Symmetric Angle-ply Laminate: $[+45/-45]_{9s}$, (c) Quasi-isotropic Laminate: $[0/-60/60]_{6s}$, and (d) Un-Symmetric Laminate: $[0/45]_{18T}$ using both the cylindrical bending and one-dimensional laminated beam theories.

4.3.1 Random stiffness and geometric properties

Now, let us consider that the composite beam-column is simply supported at both ends and further the stiffness term and geometric coefficient are random.

As explained before the expected value of μ_n is independent of any random inputs and coincides with the solution of a deterministic buckling problem.

$$\therefore E[\mu_n] = \mu_{no} \quad (4.39)$$

For simply supported ends substituting $\alpha_{1o} = \alpha_{2o} = 0$ in Eqn. (4.36), we obtain

$$\text{var}[\mu_n] = \frac{1}{D_n^2} \int_0^1 \int_0^1 E[R(\xi_1)R(\xi_2)]I_n(\xi_1)I_n(\xi_2)d\xi_1d\xi_2 \quad (4.40)$$

4.3.1.1 Case 1: Uniform auto-correlation function

Let us consider the case where all auto-correlation functions have uniform distribution and their constant values are equal to the respective values of variance or product of standard deviations. In other words, we have the same(or comparable) statistical dependence between random functions at any two arbitrary locations.

Hence we have the following equations:

$$R_a(\xi_1 - \xi_2) = \sigma_a^2 \quad (4.41)$$

$$R_b(\xi_1 - \xi_2) = \sigma_b^2 \quad (4.42)$$

Now, let us determine the expressions for the expected value and variance of buckling loads for three types of support conditions.

(a) For simply supports, as mentioned in chapter 2, the following displacement function, $X_o(\xi) = \sin(n\pi\xi)$, satisfies the geometric boundary conditions.

Since from Eqn. (4.33), the expected value of buckling load P_n is given as

$$E[P_n] = \mu_{no} \frac{b_o D_{11_o}}{l^2} \quad (4.43)$$

Substituting the above mentioned displacement function $X_o(\xi) = \sin(n\pi\xi)$ in the eigen value problem of Eqn. (4.12), we obtain

$$E[P_n] = n^2 \pi^2 \frac{b_o D_{11_o}}{l^2} \quad (4.44)$$

Substituting the displacement function $X_o(\xi)$ in Eqs. (4.27) and (4.28) and simplifying, we obtain

$$D_n = \int_0^l [X_o(\xi)]^2 d\xi = \frac{n^2 \pi^2}{2} \quad (4.45)$$

$$I_n(\xi) = [X_o(\xi)]^2 = n^4 \pi^4 \sin^2 n\pi\xi \quad (4.46)$$

Substituting Eqs. (4.41), (4.42), (4.45) and (4.46) in Eqn. (4.40), we obtain the variance of buckling load as follows:

$$\text{var}[\mu_n] = n^4 \pi^4 (\sigma_a^2 + \sigma_{b_1}^2 + \sigma_a^2 \sigma_{b_1}^2) \quad (4.47)$$

Applying the variance operation on both sides in Eqn. (4.16), we obtain the variance of P_n as follows:

$$\text{var}[P_n] = n^4 \pi^4 (\sigma_a^2 + \sigma_{b_1}^2 + \sigma_a^2 \sigma_{b_1}^2) \left[\frac{b_o D_{11_o}}{l^2} \right]^2 \quad (4.48)$$

(b) For clamped-clamped support, as mentioned in chapter 2, the following displacement function, $X_o(\xi) = 1 - \cos(2n\pi\xi)$, satisfies the geometric boundary conditions.

Substituting the above mentioned displacement function $X_o(\xi)$ in the eigen value problem of Eqn. (4.12), we obtain

$$E[P_n] = 4n^2 \pi^2 \frac{b_o D_{11_o}}{l^2} \quad (4.49)$$

Substituting the displacement function $X_o(\xi)$ in Eqs. (4.27) and (4.28) and simplifying, we obtain

$$D_n = \int_0^1 [X_o'(\xi)]^2 d\xi = 2n^2 \pi^2 \quad (4.50)$$

$$I_n(\xi) = [X_o''(\xi)]^2 = 16n^4 \pi^4 \cos^2(2n\pi\xi) \quad (4.51)$$

Substituting Eqs. (4.41), (4.42), (4.50) and (4.51) in Eqn. (4.40), we obtain the variance of buckling load as follows:

$$\text{var}[\mu_n] = 16n^4 \pi^4 (\sigma_a^2 + \sigma_{b_1}^2 + \sigma_a^2 \sigma_{b_1}^2) \quad (4.52)$$

Applying the variance operation on both sides in Eqn. (4.16), we obtain the variance of P_n as follows:

$$\text{var}[P_n] = 16n^4 \pi^4 (\sigma_a^2 + \sigma_{b_1}^2 + \sigma_a^2 \sigma_{b_1}^2) \left[\frac{b_o D_{11_o}}{l^2} \right]^2 \quad (4.53)$$

(c) For clamped-free support, as mentioned in chapter 2, the following displacement function, $X_o(\xi) = 1 - \cos\left(\frac{n\pi\xi}{2}\right)$, satisfies the geometric boundary conditions.

Substituting the above mentioned displacement function $X_o(\xi)$ in the eigen value problem of Eqn. (4.12), we obtain

$$E[P_n] = \frac{n^2 \pi^2 b_o D_{11_o}}{4 l^2} \quad (4.54)$$

Substituting the displacement function $X_o(\xi)$ in Eqs. (4.27) and (4.28) and simplifying, we obtain

$$D_n = \int_0^l [X_o(\xi)]^2 d\xi = \frac{n^2 \pi^2}{8} \quad (4.55)$$

$$I_n(\xi) = [X_o(\xi)]^2 = \frac{n^4 \pi^4}{16} \cos^2\left(\frac{n\pi\xi}{2}\right) \quad (4.56)$$

Substituting Eqs. (4.41), (4.42), (4.55) and (4.56) in Eqn. (4.40), we obtain the variance of buckling load as follows:

$$\text{var}[\mu_n] = \frac{n^4 \pi^4}{16} (\sigma_a^2 + \sigma_{b_1}^2 + \sigma_a^2 \sigma_{b_1}^2) \quad (4.57)$$

Applying the variance operation on both sides in Eqn. (4.16), we obtain the variance of P_n as follows:

$$\text{var}[P_n] = \frac{n^4 \pi^4}{16} (\sigma_a^2 + \sigma_{b_1}^2 + \sigma_a^2 \sigma_{b_1}^2) \left[\frac{b_a D_{11_n}}{l^2} \right]^2 \quad (4.58)$$

4.3.1.1.1 Numerical examples

A composite laminate consisting of a total of 36 plies made of NCT-301 Graphite-Epoxy composite material, each having a ply thickness of 0.125 mm is considered. The width of the laminate is 0.025m and length of the laminate is 0.4m as shown in the Figure 2.3.

In the present examples, four different types of laminates i.e. symmetric cross-ply laminate $[0/90]_{9s}$, symmetric angle-ply laminate $[+45/-45]_{9s}$, quasi-isotropic laminate $[0/-60/60]_{6s}$ and un-symmetric laminate $[0/45]_{18T}$ are considered and results that correspond to the cylindrical bending theory and 1-D laminated beam theory are obtained.

Tables 4.1 to 4.7 show the expected and variance values of critical buckling load P_1 for four different types of laminates corresponding to cylindrical bending and 1-D analysis for given input $\sigma_a^2 = \sigma_{b_1}^2 = \sigma^2$.

Figure 4.2 shows the variance of critical buckling load when stiffness and geometric properties have uniform correlation for four different types of laminates.

Note: $\sigma_a^2 = \sigma_b^2 = \sigma^2$; $E[P_1]$ is given in N units.

Input	Simply supported		Clamped-clamped		Clamped-free	
σ^2	$E[P_1]$	$\text{var}[P_1] \times 10^4$	$E[P_1]$	$\text{var}[P_1] \times 10^5$	$E[P_1]$	$\text{var}[P_1] \times 10^3$
0.01	869.75	1.520	3479.0	2.432	217.43	0.950
0.02		3.056		4.889		1.910
0.03		4.607		7.371		2.879
0.04		6.172		9.876		3.858

Table 4.1 Mean value and variance of critical buckling load for the $[0/90]_{9s}$ laminate corresponding to cylindrical bending theory

Input	Simply supported		Clamped-clamped		Clamped-free	
σ^2	$E[P_1]$	$\text{var}[P_1] \times 10^4$	$E[P_1]$	$\text{var}[P_1] \times 10^5$	$E[P_1]$	$\text{var}[P_1] \times 10^3$
0.01	856.18	1.473	3424.7	2.357	214.04	0.920
0.02		2.961		4.738		1.851
0.03		4.464		7.142		2.790
0.04		5.981		9.570		3.738

Table 4.2 Mean value and variance of critical buckling load for the $[0/90]_{9s}$ laminate corresponding to one-dimensional laminated beam theory

Input	Simply supported		Clamped-clamped		Clamped-free	
σ^2	$E[P_1]$	$\text{var}[P_1] \times 10^4$	$E[P_1]$	$\text{var}[P_1] \times 10^5$	$E[P_1]$	$\text{var}[P_1] \times 10^3$
0.01	470.65	0.445	1882.6	0.712	117.66	0.278
0.02		0.894		1.431		0.559
0.03		1.349		2.158		0.843
0.04		1.807		2.892		1.129

Table 4.3 Mean value and variance of critical buckling load for the $[45/-45]_{9s}$ laminate corresponding to cylindrical bending theory

Input	Simply supported		Clamped-clamped		Clamped-free	
σ^2	$E[P_1]$	$\text{var}[P_1] \times 10^3$	$E[P_1]$	$\text{var}[P_1] \times 10^4$	$E[P_1]$	$\text{var}[P_1]$
0.01	178.88	0.643	715.52	1.029	44.72	40.20
0.02		1.292		2.068		80.80
0.03		1.948		3.118		121.80
0.04		2.611		4.178		163.20

Table 4.4 Mean value and variance of critical buckling load for the $[45/-45]_{9s}$ laminate corresponding to one-dimensional laminated beam theory

Input	Simply supported		Clamped-clamped		Clamped-free	
σ^2	$E[P_1]$	$\text{var}[P_1] \times 10^4$	$E[P_1]$	$\text{var}[P_1] \times 10^5$	$E[P_1]$	$\text{var}[P_1] \times 10^3$
0.01	715.54	1.029	2862.18	1.646	178.88	0.643
0.02		2.068		3.309		1.292
0.03		3.118		4.989		1.948
0.04		4.178		6.684		2.611

Table 4.5 Mean value and variance of critical buckling load for the $[0/-60/60]_{6s}$ laminate corresponding to cylindrical bending theory

Input	Simply supported		Clamped-clamped		Clamped-free	
σ^2	$E[P_1]$	$\text{var}[P_1] \times 10^4$	$E[P_1]$	$\text{var}[P_1] \times 10^5$	$E[P_1]$	$\text{var}[P_1] \times 10^3$
0.01	669.89	0.902	2679.5	1.443	167.47	0.563
0.02		1.813		2.900		1.133
0.03		2.733		4.372		1.708
0.04		3.661		5.859		2.288

Table 4.6 Mean value and variance of critical buckling load for the $[0/-60/60]_{6s}$ laminate corresponding to one-dimensional laminated beam theory

Input	Simply supported		Clamped-clamped		Clamped-free	
σ^2	$E[P_1]$	$\text{var}[P_1] \times 10^4$	$E[P_1]$	$\text{var}[P_1] \times 10^6$	$E[P_1]$	$\text{var}[P_1] \times 10^3$
0.01	996.83	1.997	3987.32	0.319	249.20	1.248
0.02		4.014		0.642		2.509
0.03		6.051		0.968		3.782
0.04		8.108		1.297		5.067

Table 4.7 Mean value and variance of critical buckling load for the $[0/45]_{18T}$ laminate corresponding to cylindrical bending theory

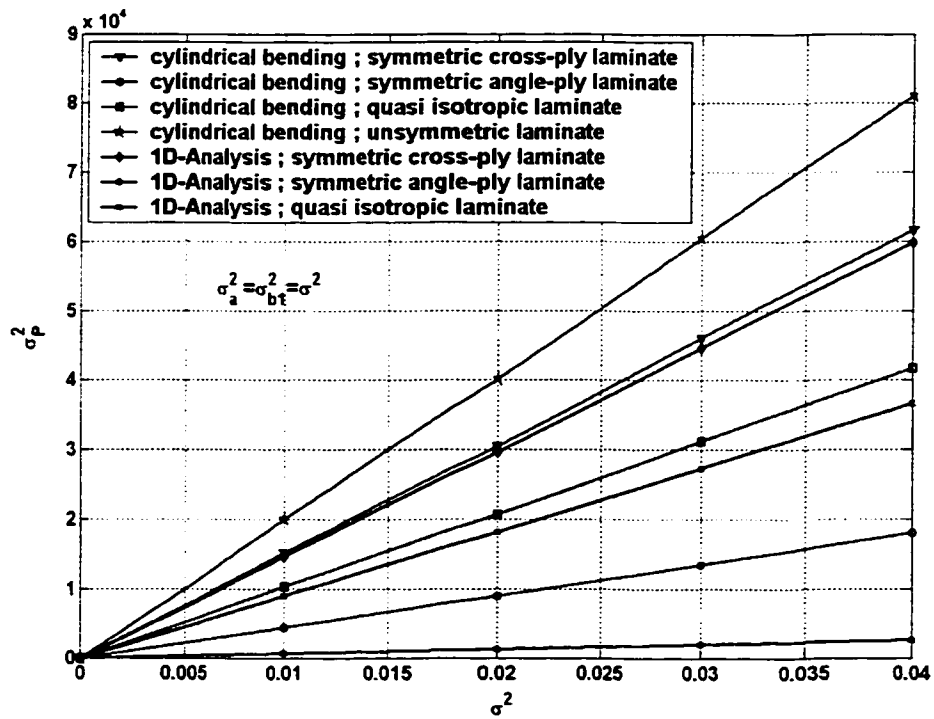


Figure 4.2 The variance of critical buckling load vs σ^2 corresponding to simply supported boundary conditions for uniform correlation

Observations:

It can be observed that the expected value of P_1 is independent of any random inputs and coincides with the solution of the corresponding deterministic buckling analysis problem.

The Figure 4.2 indicates that the variance of P_1 increases linearly with σ^2 and also it can be observed that the variance of buckling load P_1 takes on quite a very large value compared to small input of σ^2 .

Further, Figure 4.2 shows that symmetric angle-ply laminate has the lowest variance values of critical buckling loads. It can also be seen that the expected and variance values of critical buckling loads corresponding to both the theories are almost same in the case of symmetric cross-ply laminate, whereas small percentage of error occurs in quasi-isotropic laminate and further, the largest difference occurs in the case of symmetric angle-ply laminate.

It can be seen from variance Eqs. (4.48), (4.53) and (4.58), that the variance value corresponding to the clamped-free support condition is equal to $1/16^{\text{th}}$ of that of the simply supported condition, whereas the variance value corresponding to the clamped-clamped support condition is equal to 16 times of that of the simply supported condition.

From Eqn. (4.44) and Eqn. (4.48), we can say that the coefficient of variation is independent of material and geometric properties and it depends on input variance of P_1 .

4.3.1.2 Case 2: Exponential auto-correlation function

Let us consider the case where auto-correlation function has exponential distribution.

Hence we have auto-correlation functions as

$$R_a(\xi_1 - \xi_2) = \sigma_a^2 e^{-k_1|\xi_1 - \xi_2|} \quad (4.59)$$

$$R_{b_1}(\xi_1 - \xi_2) = \sigma_{b_1}^2 e^{-k_2|\xi_1 - \xi_2|} \quad (4.60)$$

where k_i 's are positive constants. The constants k_i 's govern the interval over which appreciable correlation occurs. If we introduce a correlation length ε_i for each k_i in such a way that auto-correlation function is negligible for $|\xi_1 - \xi_2| > \varepsilon_i$, then the correlation length ε_i describes the degree of the input randomness. Suppose that the auto-correlation function is reduced to 5% of its maximum value within the distances ε_i , then we have the following equations:

$$R_a(\varepsilon_1) = 0.05\sigma_a^2 \quad (4.61)$$

$$R_{b_1}(\varepsilon_2) = 0.05\sigma_{b_1}^2 \quad (4.62)$$

Now by combining Eqs. (4.59) and (4.61), we have

$$\sigma_a^2 e^{-k_1\varepsilon_1} = 0.05\sigma_a^2 \quad (4.63)$$

which gives

$$k_1 \varepsilon_1 = 2.99 \quad (4.64)$$

In a similar manner the value of $k_2 \varepsilon_2$ can also be obtained.

As explained before the expected value of buckling load is independent of any random inputs and coincides with the solution of the corresponding deterministic buckling problem. Therefore the expected values of buckling loads for three different types of supports are the same as in case 1.

Now, let us calculate the variance equation for three types of support conditions.

(a) For simply supported conditions, the displacement function, and the terms D_n and $I_n(\xi)$ are the same as explained in case 1. Now, substituting the displacement function, D_n and $I_n(\xi)$ in Eqn. (4.40), we obtain the variance of μ_n as follows:

$$\begin{aligned} \text{var}[\mu_n] = & 4n^4 \pi^4 (\sigma_a^2 + \sigma_{b_1}^2) \int_0^1 \int_0^1 e^{-k|\varepsilon_1 - \varepsilon_2|} \sin^2 n\pi\varepsilon_1 \sin^2 n\pi\varepsilon_2 d\xi_1 d\xi_2 \\ & + 4n^4 \pi^4 (\sigma_a^2 \sigma_{b_1}^2) \int_0^1 \int_0^1 e^{-2k|\varepsilon_1 - \varepsilon_2|} \sin^2 n\pi\varepsilon_1 \sin^2 n\pi\varepsilon_2 d\xi_1 d\xi_2 \end{aligned} \quad (4.65)$$

Applying the variance operation on both sides in Eqn. (4.16), we obtain the variance of P_n as follows:

$$\text{var}[P_n] = \text{var}\left[\mu_n \left[\frac{b_o D_{11_o}}{l^2} \right]\right]^2 \quad (4.66)$$

(b) For clamped-clamped support conditions, the displacement function, and the terms D_n and $I_n(\xi)$ are the same as explained in case 1. Now, substituting the displacement function, D_n and $I_n(\xi)$ in Eqn. (4.40), we obtain the variance of μ_n as follows:

$$\begin{aligned} \text{var}[\mu_n] &= 64n^4 \pi^4 (\sigma_a^2 + \sigma_{b_1}^2) \int_0^1 \int_0^1 e^{-k|\epsilon_1 - \epsilon_2|} \cos^2 2n\pi\epsilon_1 \cos^2 2n\pi\epsilon_2 d\xi_1 d\xi_2 \\ &+ 64n^4 \pi^4 (\sigma_a^2 \sigma_{b_1}^2) \int_0^1 \int_0^1 e^{-2k|\epsilon_1 - \epsilon_2|} \cos^2 2n\pi\epsilon_1 \cos^2 2n\pi\epsilon_2 d\xi_1 d\xi_2 \end{aligned} \quad (4.67)$$

The variance of buckling load, P_n , is calculated from Eqn. (4.66).

(b) For clamped-free support conditions, the displacement function, and the terms D_n and $I_n(\xi)$ are the same as explained in case 1. Now, substituting the displacement function, D_n and $I_n(\xi)$ in Eqn. (4.40), we obtain the variance of μ_n as follows:

$$\begin{aligned} \text{var}[\mu_n] &= \frac{n^4 \pi^4}{4} (\sigma_a^2 + \sigma_{b_1}^2) \int_0^1 \int_0^1 e^{-k|\epsilon_1 - \epsilon_2|} \cos^2 \frac{n\pi\epsilon_1}{2} \cos^2 \frac{n\pi\epsilon_2}{2} d\xi_1 d\xi_2 \\ &+ \frac{n^4 \pi^4}{4} (\sigma_a^2 \sigma_{b_1}^2) \int_0^1 \int_0^1 e^{-2k|\epsilon_1 - \epsilon_2|} \cos^2 \frac{n\pi\epsilon_1}{2} \cos^2 \frac{n\pi\epsilon_2}{2} d\xi_1 d\xi_2 \end{aligned} \quad (4.68)$$

The variance of buckling load, P_n , is calculated from Eqn. (4.66).

4.3.1.1.2 Numerical examples

Laminate dimensions and configurations are the same as explained in section 4.4.1.1.1.

Figure 4.3 represents the variance of critical buckling load when stiffness and geometric properties have exponential correlation for four different types of laminates.

Figures 4.4 to 4.7 show the variance of critical buckling load vs correlation length corresponding to cylindrical bending theory.

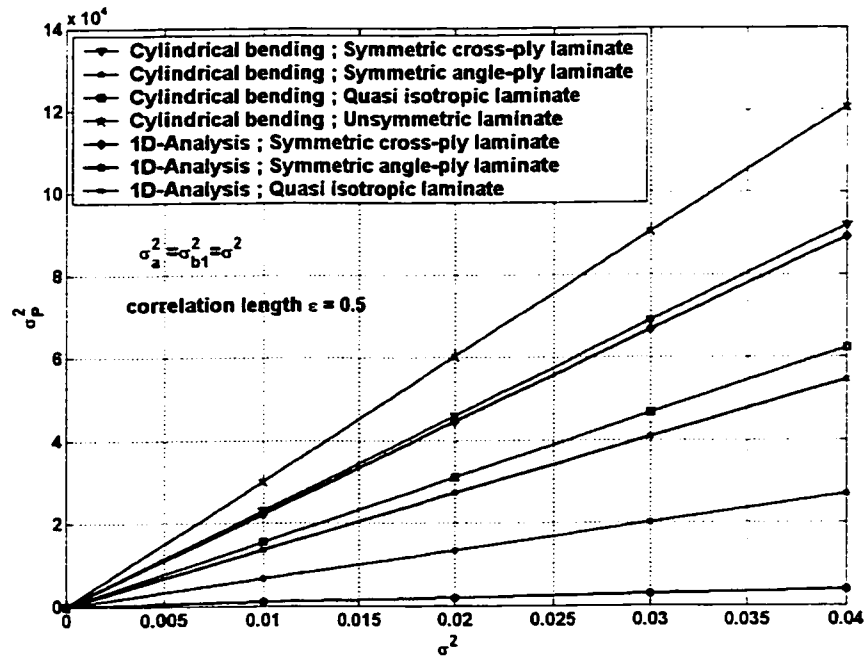


Figure 4.3 The variance of critical buckling load vs σ^2 corresponding the simply supported boundary conditions for exponential correlation

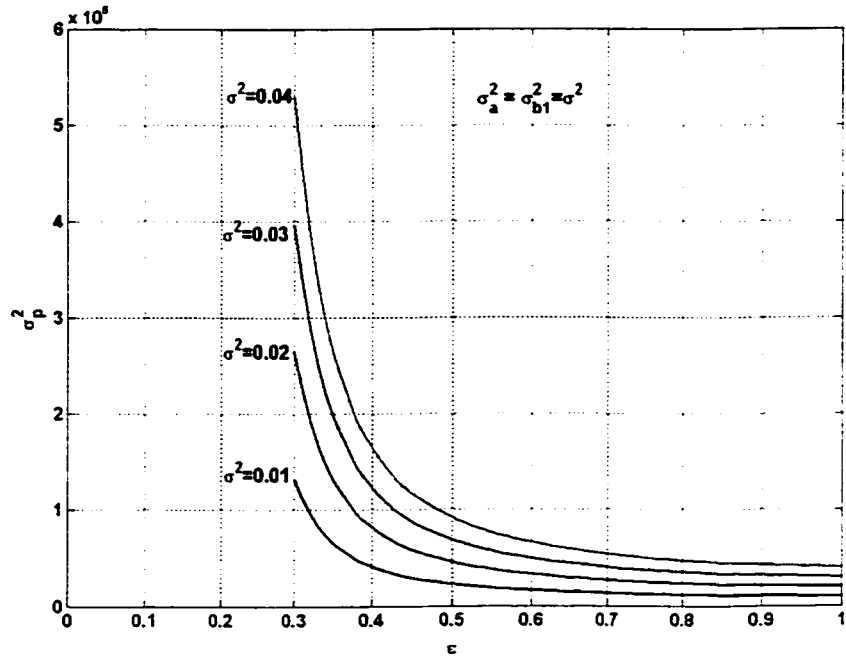


Figure 4.4 The variance of critical buckling load vs σ^2 for $[0/90]_{9s}$ laminate corresponding to cylindrical bending theory

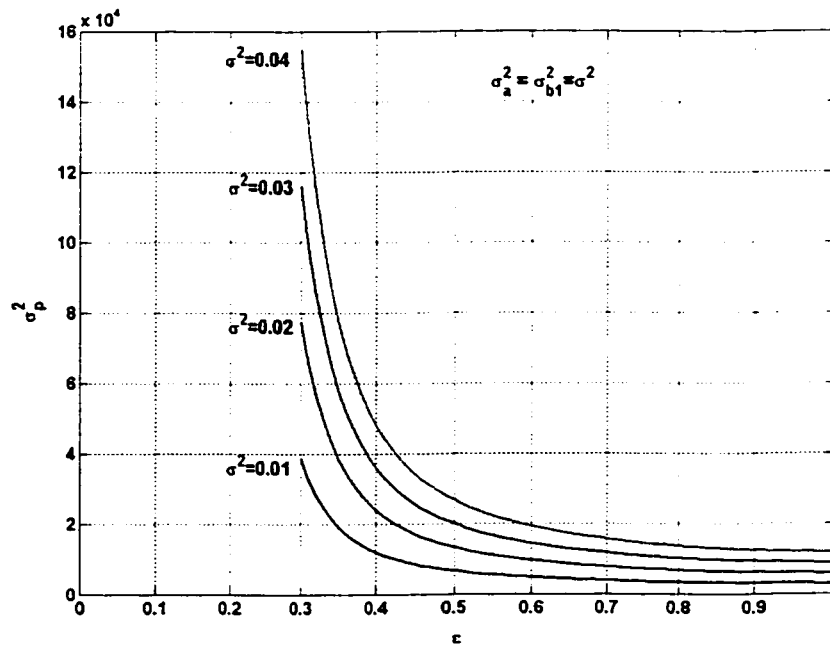


Figure 4.5 The variance of critical buckling load vs σ^2 for $[45/-45]_{9s}$ laminate corresponding to cylindrical bending theory

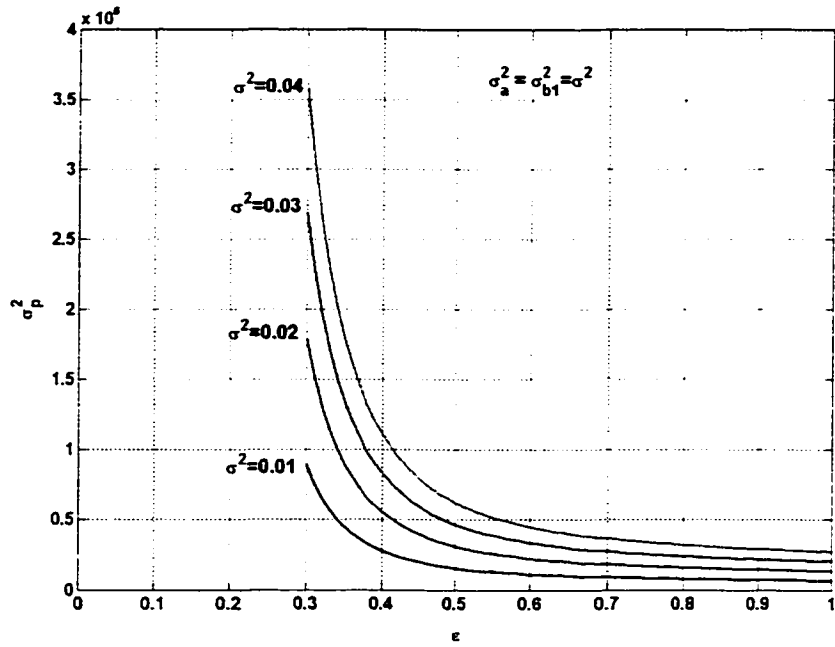


Figure 4.6 The variance of critical buckling load vs σ^2 for $[0/-60/60]_{6s}$ laminate corresponding to cylindrical bending theory

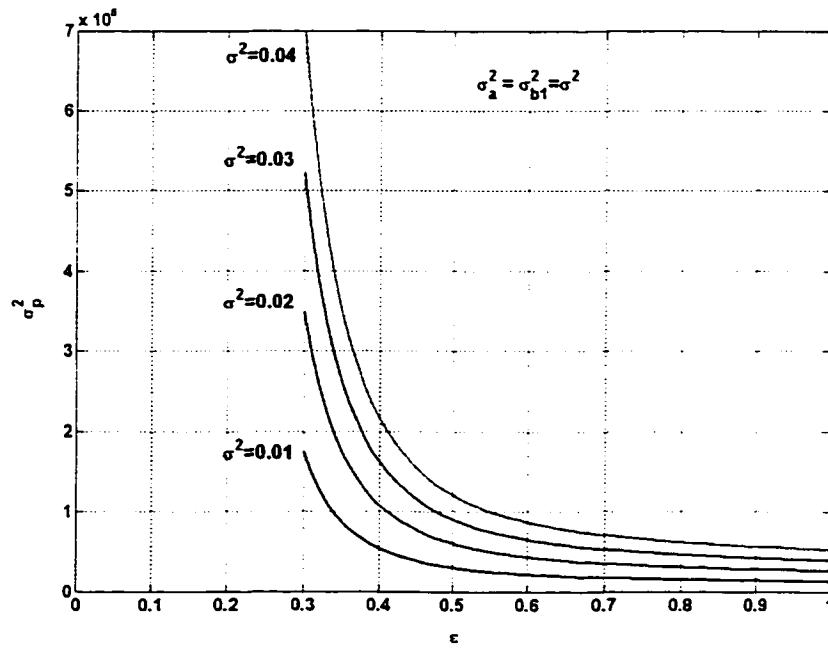


Figure 4.7 The variance of critical buckling load vs σ^2 for $[0/45]_{18T}$ laminate corresponding to cylindrical bending theory

Observations:

The Figure 4.3 shows that variance of P_1 increases linearly with σ^2 . It can be observed from this figure that symmetric angle-ply laminate has the lowest variance values of critical buckling loads. It can also be seen that the expected and variance values of critical buckling loads corresponding to both the theories are almost same in symmetric cross-ply laminate, whereas small percentage of error occurs in the case of quasi-isotropic laminate. The largest difference occurs in symmetric angle-ply laminate.

The Figures 4.4 to 4.7 indicate that the variance of P_1 increases exponentially as the correlation length, ε , decreases. The variance of P_1 is almost infinity when the correlation length is very small. This means that if the inputs at any two locations are almost uncorrelated, the variance of output becomes infinity.

4.4 Deterministic local buckling of thin-walled composite beam-columns

In the present section, theoretical view of elastic local instability of anisotropic composite beam-columns, which are, treated as assemblies of generally laminated composite plates buckling under uniaxial compressive forces is presented.

The following assumptions are introduced for the thin-walled elements:

- (1) The beam-column is initially straight.
- (2) The lateral deflection of the beam-column axis and the cross-sectional dimensions are small compared with the length of the beam-column.

- (3) Overall failure of the entire structure does not occur before local buckling of the plate elements.
- (4) The shear and rotatory inertia effects are neglected.
- (5) Stresses are sufficiently small to warrant the assumption of linear elasticity.
- (6) Equilibrium conditions are written based on the undeformed configuration of the structural element.

Consider a thin-walled composite I-section beam-column as shown in Figure 4.8. Local buckling of flange and web can be considered as an individual plate buckling.

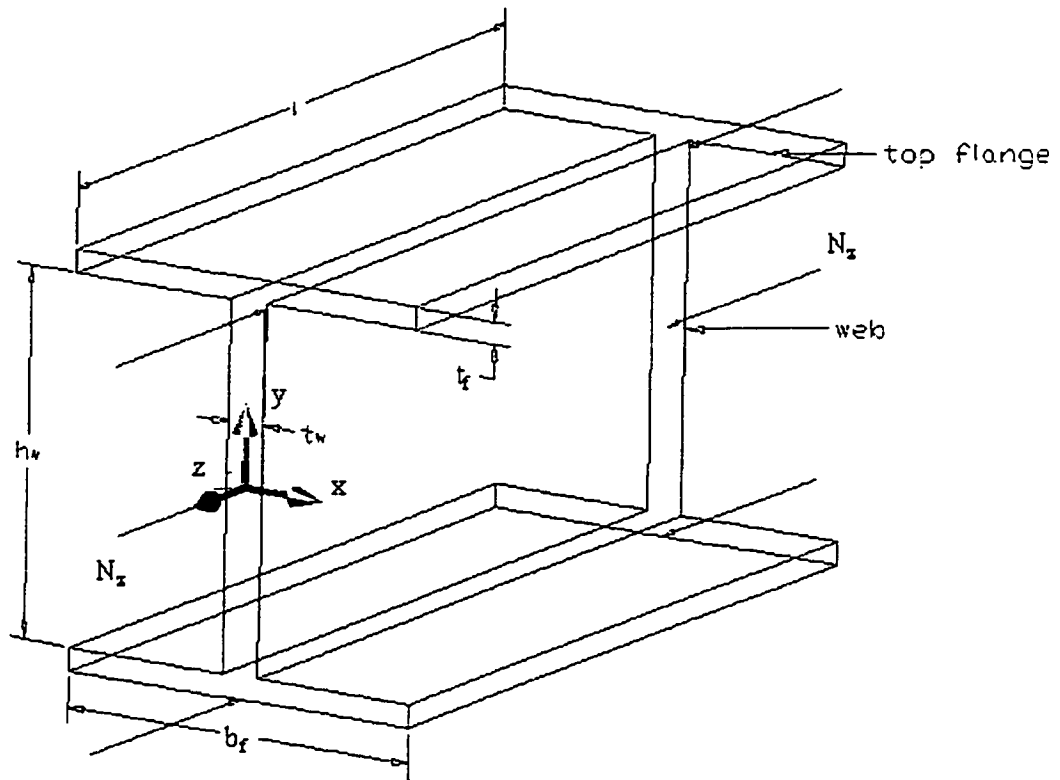


Figure 4.8 I-section beam-column and coordinate system

The variational principle for an anisotropic rectangular plate under uniform compressive loading is given as follows [1]

$$\delta \left\{ \frac{1}{2} \int_0^l \int_0^b \left\{ D_{11} W_{,zzz} + 2D_{12} W_{,zzx} + D_{22} W_{,zzx} + 4D_{16} W_{,zzx} + 4D_{26} W_{,zzx} + 4D_{66} W_{,zzx} + N_z W_{,zz} \right\} dx dz \right\} = 0 \quad (4.69)$$

where $W(x, z)$ is the flange out-of-plane displacement, $b = b_f/2$, and D_{ij} is the laminate bending stiffness term [1]. The subscripts preceded by a comma denote differentiation with respect to the corresponding coordinates. Similarly an equation is formulated for the web by replacing W with U , and x with y , where $U(y, z)$ is the web out-of-plane displacement.

By virtue of symmetry of cross section, two plates, i.e., upper half flange and web, are treated herein.

4.4.1 Flange buckling

In the following sections, different types of flange support conditions are discussed.

4.4.1.1 SCSF flange support conditions

The boundary conditions for the half flange are assumed as: one free edge, and one clamped joint with the web, and the other two edges are simply supported (SCSF), which are given as follows:

$$W = 0 \quad \text{at } z = 0, -l \text{ and } x = 0 \quad (4.70)$$

$$W_{,x} = 0 \quad \text{at } x = 0 \quad (4.71)$$

$$M_z = D_{11} W_{,zz} + D_{12} W_{,xx} + 2D_{16} W_{,zx} = 0 \quad \text{at } z = 0, -l \quad (4.72)$$

$$M_x = D_{12} W_{,zz} + D_{22} W_{,xx} + 2D_{26} W_{,zx} = 0 \quad \text{at } x = b_f/2 \quad (4.73)$$

$$Q_x = D_{16} W_{,zzz} + (D_{12} - 2D_{66}) W_{,zzx} + 3D_{26} W_{,zxx} + D_{22} W_{,xxx} = 0 \quad \text{at } x = b_f/2 \quad (4.74)$$

The deflection function which satisfies the above geometric boundary conditions is assumed of the form:

$$W(z, x) = \sum_{m=1}^M \sum_{n=1}^N A_{mn} Z_m(z) X_n(x) \quad (4.75)$$

where $Z_m(z)$ and $X_n(x)$ are characteristic shape functions along the z and x axes satisfying the boundary conditions along these axes, respectively. The shape functions are given by the following:

$$Z_m(z) = \sin\left(\frac{m\pi z}{l}\right) \quad (4.76)$$

The characteristics shape function in the x -direction satisfying the different boundary conditions can be expressed in general form as:

$$X_n(x) = A \sin\left(\frac{2\lambda_n x}{b_f}\right) + B \cos\left(\frac{2\lambda_n x}{b_f}\right) + C \sinh\left(\frac{2\lambda_n x}{b_f}\right) + E \cosh\left(\frac{2\lambda_n x}{b_f}\right) \quad (4.77)$$

where A , B , C and E are the constants obtained by substituting the appropriate boundary conditions [69].

Now, the substitution of the conditions $W = W_{,x} = 0$ at $x = 0$ into Eqn. (4.77) yields

$$A = -C \text{ and } B = -E;$$

Substituting $M_x = 0$ at $x = b_f/2$ gives

$$X_{,xx} + DN_x = 0 \quad (4.78)$$

where

$$D = D_{12} / D_{22}; \quad N = \frac{\int_0^l Z_{,zz} Z dz}{\int_0^l Z^2 dz} \quad (4.79)$$

and also substituting $Q_x = 0$ at $x = b_f/2$ gives

$$X_{,xxx} + D_1 N X_{,x} = 0 \quad (4.80)$$

where

$$D_1 = (D_{12} + 4D_{66}) / D_{22} \quad (4.81)$$

Solving Eqn. (4.78), shape function of $X(x)$, is obtained as follows:

$$X_n(x) = \sin\left(\frac{2\lambda_n x}{b_f}\right) - \sinh\left(\frac{2\lambda_n x}{b_f}\right) + \beta_1 \left(\cos\left(\frac{2\lambda_n x}{b_f}\right) - \cosh\left(\frac{2\lambda_n x}{b_f}\right) \right) \quad (4.82)$$

where

$$\beta_1 = -\left(\frac{\sin \lambda_n + \gamma \sinh \lambda_n}{\cos \lambda_n + \gamma \cosh \lambda_n}\right) ; \gamma = \left(\frac{4\lambda_n^2 - DNb_f^2}{4\lambda_n^2 + DNb_f^2}\right) \quad (4.83)$$

Solving Eqs. (4.78), (4.80) and (4.82), the frequency equation is obtained as follows:

$$\left(\frac{\cos \lambda_n + \left(\frac{4\lambda_n^2 - D_1Nb_f^2}{4\lambda_n^2 + D_1Nb_f^2}\right) \cosh \lambda_n}{\sin \lambda_n - \left(\frac{4\lambda_n^2 - D_1Nb_f^2}{4\lambda_n^2 + D_1Nb_f^2}\right) \sinh \lambda_n}\right) = -\left(\frac{\sin \lambda_n + \left(\frac{4\lambda_n^2 - DNb_f^2}{4\lambda_n^2 + DNb_f^2}\right) \sinh \lambda_n}{\cos \lambda_n - \left(\frac{4\lambda_n^2 - DNb_f^2}{4\lambda_n^2 + DNb_f^2}\right) \cosh \lambda_n}\right) \quad (4.84)$$

The above equation is dependent on material and geometric properties of the plate.

The Eqn. (4.84) is complicated to solve and therefore the following procedure is used to get the solution for λ_n . For example consider symmetric angle-ply laminate [+45/-45]_{9s}

with aspect ratio of 12. Now Eqn. (4.84) becomes,

$$\left(\frac{\cos \lambda_n + \left(\frac{4\lambda_n^2 + 0.28}{4\lambda_n^2 - 0.28}\right) \cosh \lambda_n}{\sin \lambda_n - \left(\frac{4\lambda_n^2 + 0.28}{4\lambda_n^2 - 0.28}\right) \sinh \lambda_n}\right) + \left(\frac{\sin \lambda_n + \left(\frac{4\lambda_n^2 + 0.05}{4\lambda_n^2 - 0.05}\right) \sinh \lambda_n}{\cos \lambda_n - \left(\frac{4\lambda_n^2 + 0.05}{4\lambda_n^2 - 0.05}\right) \cosh \lambda_n}\right) = 0 \quad (4.85)$$

Now, let us say that the left hand side of the above equation is $f(\lambda_n)$ and now plotting f

(λ_n) vs. λ_n gives the solution for λ_n .

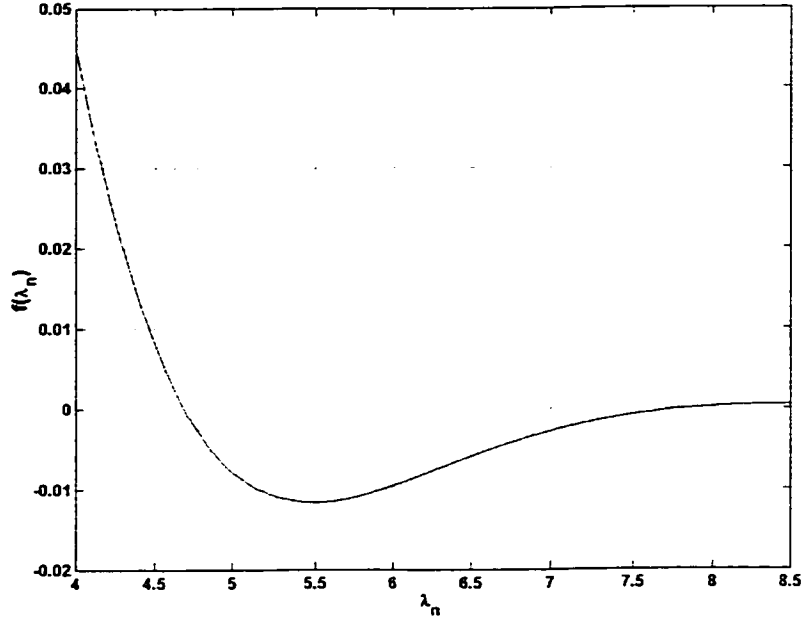


Figure 4.9 Solutions for λ_n corresponding to $[+45/-45]_{9s}$ laminate

4.4.1.2 FCFF flange support conditions

The other type of the flange boundary conditions are assumed as: one free edge along the longitudinal direction, one clamped joint with the web, and the other two edges are free (FCFF), which are given as follows:

$$W = 0 \quad \text{at } x = 0 \quad (4.86)$$

$$W_{,x} = 0 \quad \text{at } x = 0 \quad (4.87)$$

$$M_z = D_{11} W_{,zz} + D_{12} W_{,xx} + 2D_{16} W_{,zx} = 0 \quad \text{at } z = 0, -l \quad (4.88)$$

$$M_x = D_{12} W_{,zz} + D_{22} W_{,xx} + 2D_{26} W_{,zx} = 0 \quad \text{at } x = b_f/2 \quad (4.89)$$

$$Q_z = D_{11} W_{,zzz} + (D_{12} - 2D_{66})W_{,zxx} + 3D_{16} W_{,zzx} + D_{26} W_{,xxx} = 0 \quad \text{at } z = 0, -l \quad (4.90)$$

$$Q_x = D_{16} W_{,zzz} + (D_{12} - 2D_{66})W_{,zxx} + 3D_{26} W_{,zzx} + D_{22} W_{,xxx} = 0 \quad \text{at } x = b_f/2 \quad (4.91)$$

The characteristic shape functions, which satisfy the above boundary conditions, are given as follows [70]:

$$Z_m(z) = \cosh\left(\frac{\lambda_m z}{l}\right) + \cos\left(\frac{\lambda_m z}{l}\right) - \beta_2 \left(\sinh\left(\frac{\lambda_m z}{l}\right) + \sin\left(\frac{\lambda_m z}{l}\right) \right) \quad (4.92)$$

where

$$\beta_2 = \frac{\cosh \lambda_m - \cos \lambda_m}{\sinh \lambda_m - \sin \lambda_m}; \lambda_m = (2m + 1)l/2 \quad (4.93)$$

$$X_n(x) = \cosh\left(\frac{\lambda_n x}{b_f}\right) - \cos\left(\frac{\lambda_n x}{b_f}\right) - \beta_3 \left(\sinh\left(\frac{\lambda_n x}{b_f}\right) - \sin\left(\frac{\lambda_n x}{b_f}\right) \right) \quad (4.94)$$

where

$$\beta_3 = \frac{\cos \lambda_m + \cosh \lambda_m}{\sin \lambda_m + \sinh \lambda_m}; \lambda_n = (2n + 1)l/2 \quad (4.95)$$

The Ritz method is applied to the problem using the above shape functions, and geometric and natural boundary conditions. The resulting equilibrium equation is given as follows [1]:

$$\begin{aligned} & \sum_{i=1}^M \sum_{j=1}^N \left\{ D_{11} \int_0^l Z_{i,z} Z_{m,z} dz \int_0^b X_j X_n dx + D_{12} \left[\int_0^l Z_m Z_{i,z} dz \int_0^b X_j X_{n,xx} dx + \int_0^l Z_i Z_{m,z} dz \int_0^b X_n X_{j,xx} dx \right] \right. \\ & + D_{22} \int_0^l Z_i Z_m dz \int_0^b X_{j,xx} X_{n,xx} dx + 4D_{66} \int_0^l Z_{i,z} Z_{m,z} dz \int_0^b X_{j,x} X_{n,x} dx \\ & + 2D_{16} \left[\int_0^l Z_{i,z} Z_{m,z} dz \int_0^b X_j X_{n,x} dx + \int_0^l Z_{i,z} Z_{m,z} dz \int_0^b X_j X_{n,x} dx \right] \\ & + 2D_{26} \left[\int_0^l Z_i Z_{m,z} dz \int_0^b X_{j,xx} X_{n,xx} dx + \int_0^l Z_i Z_{m,z} dz \int_0^b X_{j,xx} X_{n,x} dx \right] \\ & \left. + N_x \int_0^l Z_{i,z} Z_{m,z} dz \int_0^b X_j X_n dx + \int_0^l Z_i Z_{m,z} dz \int_0^b X_n X_{j,x} dx \right\} A_{ij} = 0 \quad (4.96) \end{aligned}$$

where $m = 1, 2, \dots, M$; $n = 1, 2, \dots, N$

Setting the determinant of this system of equations to zero, a set of $M \times N$ linear homogeneous simultaneous equations is obtained. By using a standard eigen solution we extract the minimum eigenvalue and its corresponding eigenvector to give critical buckling load N_{cr} and its mode shapes respectively. A computer program is written in MATLAB® to solve the eigen value problem for the critical buckling load.

4.4.2 Web buckling

In the following sections, different types of web support conditions are discussed.

4.4.2.1 SCSC web support conditions

The boundary conditions for the web are assumed as: simply supported at two edges and clamped at the two longitudinal edges (SCSC), which are given as follows:

$$U = 0 \quad \text{at } z = 0, -l \text{ and } -h_w/2 \leq y \leq h_w/2 \quad (4.97)$$

$$U_{,z} = 0 \quad \text{at } y = -h_w/2, h_w/2; 0 \leq z \leq -l \quad (4.98)$$

$$M_z = D_{11} U_{,zz} + D_{12} U_{,xx} + 2D_{16} W_{,zx} = 0 \quad \text{at } z = 0, -l \text{ and } -h_w/2 \leq y \leq h_w/2 \quad (4.99)$$

The deflection function, which satisfies the above geometric boundary conditions, is assumed of the form:

$$U(z, y) = \sum_{m=1}^M \sum_{n=1}^N A_{mn} Z_m(z) Y_n(y) \quad (4.100)$$

where $Z_m(z)$ and $Y_n(y)$ are characteristic shape functions along the z and y axes satisfying the boundary conditions along these axes, respectively.

The characteristic shape functions, which satisfy the above boundary conditions are given as follows [70]:

$$Z_m(z) = \sin\left(\frac{m\pi z}{l}\right) \quad (4.101)$$

$$Y_n(y) = \beta_4 \left(\cos\left(\frac{\lambda_n y}{h_w}\right) - \cosh\left(\frac{\lambda_n y}{h_w}\right) \right) + \sin\left(\frac{\lambda_n y}{h_w}\right) - \sinh\left(\frac{\lambda_n y}{h_w}\right) \quad (4.102)$$

where

$$\beta_4 = \frac{\cos \lambda_n - \cosh \lambda_n}{\sin \lambda_n + \sinh \lambda_n}; \lambda_n = (2n + 1)\pi / 2 \quad (4.103)$$

4.4.2.2 FCFC web support conditions

The other type of boundary conditions for the web is assumed as: free at two edges and clamped at the two longitudinal edges (FCFC), which are given as follows:

$$U = 0 \quad \text{at } y = -h_w/2, h_w/2, 0 \leq z \leq l \quad (4.104)$$

$$U_{,z} = 0 \quad \text{at } y = -h_w/2, h_w/2; 0 \leq z \leq l \quad (4.105)$$

$$M_z = D_{11} U_{,zz} + D_{12} U_{,yy} + 2D_{16} W_{,zy} = 0 \quad \text{at } z = 0, -l \quad (4.106)$$

$$Q_z = D_{11} U_{,zzz} + (D_{12} - 2D_{66})U_{,zyy} + 3D_{16} U_{,yyz} + D_{26} U_{,yyy} = 0 \quad \text{at } z = 0, -l \quad (4.107)$$

The characteristic shape functions, which satisfy the above boundary conditions are given as follows [70]:

$$Z_m(z) = \cosh\left(\frac{\lambda_m z}{l}\right) + \cos\left(\frac{\lambda_m z}{l}\right) - \beta_5 \left(\sinh\left(\frac{\lambda_m z}{l}\right) + \sin\left(\frac{\lambda_m z}{l}\right) \right) \quad (4.108)$$

where

$$\beta_5 = \frac{\cosh \lambda_m - \cos \lambda_m}{\sinh \lambda_m - \sin \lambda_m}; \quad \lambda_m = (2m + 1) / 2 \quad (4.109)$$

$$Y_n(y) = \beta_6 \left(\cos\left(\frac{\lambda_n y}{h_w}\right) - \cosh\left(\frac{\lambda_n y}{h_w}\right) \right) + \sin\left(\frac{\lambda_n y}{h_w}\right) - \sinh\left(\frac{\lambda_n y}{h_w}\right) \quad (4.110)$$

where

$$\beta_6 = \frac{\cos \lambda_n - \cosh \lambda_n}{\sin \lambda_n + \sinh \lambda_n}; \quad \lambda_n = (2n + 1)\pi / 2 \quad (4.111)$$

Now, web critical buckling load N_{cr} and its mode shape are calculated in a similar manner as explained in flange buckling case.

4.5 Stochastic local buckling of thin-walled composite beam-columns

Most modern mechanical systems possess high degree of structural complexity. In the case of composite laminates, significant randomness is present. This is due to the stochastic spatial variations of the properties of fibers, properties of the matrix material and properties at interfaces. In addition to the above, several variations exist in the fiber

volume fraction, void contents, fiber orientation angles in various plies, and thickness of a laminate, etc. due to the significant variabilities that are introduced during the manufacturing process. As a result, tests on a single material specimen provide a specific value for each material parameter and mechanical property. However, when a number of specimens are tested, different randomly distributed values are obtained for the same material property. Therefore, the analysis of laminates has to be performed based on a probabilistic approach. For the present case Ritz method is used based on a stochastic approach such that stochastic description can be provided for the laminate bending stiffness.

Consider a laminate in (x, y) plane. The spatial variation of laminate bending stiffness D_{ij} is considered to constitute a two-dimensional homogeneous stochastic field. The fluctuating component $a(X)$ corresponding to bending stiffness D_{ij} has a zero mean.

$$D_{ij} = \bar{D}_{ij} [1 + a(X)] ; \quad E[a(X)] = 0 \quad (4.112)$$

The auto-correlation function is given by

$$R_{aa}(\xi) = E[a(X)a(X + \xi)] \quad (4.113)$$

In the above, $X = [x, y]^T$ indicates the position vector and $\xi = [\xi_x, \xi_y]^T$ represents the separation vector between two points X and $(X + \xi)$. In practical cases each stiffness value is considered to vary at each Gauss point of numerical integration. Thus, if n represents the number of regions present in the structure, and m represents the order of

Gauss quadrature, then there are N equal to $n \times m$ stiffness values associated with the structure.

Consider only the fluctuating component of the homogeneous stochastic field, which is used to model the stiffness variations around the expected value. These N values $a_i = a(X_i)$ ($i = 1, 2, 3, \dots, N$), are correlated random values with zero mean. Also X_i corresponds to the location of each Gauss point. Their correlation characteristics can be specified in terms of the covariance matrix $[C_{aa}]$ of order $N \times N$, whose ij^{th} component is given by

$$c_{ij} = \text{cov}[a_i, a_j] = E[a_i, a_j] = R_{aa}(\xi_{ij}); \quad i = 1, 2, 3, \dots, N \quad (4.114)$$

in which $\xi_{ij} = (X_j - X_i)$ = the separation distance between the Gauss points i and j .

Now a vector $\{a\} = [a_1 \ a_2 \ a_3 \ \dots \ a_N]^T$ can be generated by

$$\{a\} = [L]\{Z\} \quad (4.115)$$

in which $\{Z\} = [Z_1 \ Z_2 \ Z_3 \ \dots \ Z_N]^T$ is a vector consisting of N independent Gaussian random variables with zero mean and unit standard deviation, and $[L]$ is a lower triangular matrix obtained by the Cholesky decomposition of the covariance matrix $[C_{aa}]$. Thus,

$$[L][L]^T = [C_{aa}] \quad (4.116)$$

Once the Cholesky decomposition is accomplished, different sample vectors of $\{a\}$ are easily obtained by generating samples for the Gaussian random vectors $\{Z\}$.

The correlation properties of the stochastic field representing the fluctuating components of material properties are expressed using the Markov correlation model, also known as the First-order autoregressive model, which is given as follows [71]:

$$R_{aa}(\xi) = \sigma_o^2 \exp\left[-\left(\frac{|\xi|}{d}\right)\right] \quad (4.117)$$

where σ_o is the standard deviation of the stochastic field $a(X)$, d is the correlation length such that when it is large the correlation disappears more slowly and ξ is the separation distance between the Gauss points. Using the N values of $[D]$, the averaged value of $[D]$ is obtained using Gauss quadrature rule.

Now applying the expectation operation on Eqn. (4.96), we obtain the following:

$$\begin{aligned} & \sum_{i=1}^M \sum_{j=1}^N \left\{ E[D_{11}] \left[\int_0^l Z_{i,z} Z_{m,z} dz \int_0^b X_j X_n dx \right] \right. \\ & + E[D_{12}] \left[\int_0^l Z_m Z_{i,z} dz \int_0^b X_j X_{n,xx} dx + \int_0^l Z_i Z_{m,z} dz \int_0^b X_n X_{j,xx} dx \right] \\ & + E[D_{22}] \left[\int_0^l Z_i Z_m dz \int_0^b X_{j,xx} X_{n,xx} dx + 4E[D_{66}] \int_0^l Z_{i,z} Z_{m,z} dz \int_0^b X_{j,x} X_{n,x} dx \right. \\ & \left. + 2E[D_{16}] \left[\int_0^l Z_{i,z} Z_{m,z} dz \int_0^b X_j X_{n,x} dx + \int_0^l Z_{i,z} Z_{m,z} dz \int_0^b X_j X_{n,x} dx \right] \right. \\ & \left. + 2E[D_{26}] \left[\int_0^l Z_i Z_{m,z} dz \int_0^b X_{j,xx} X_{n,xx} dx + \int_0^l Z_i Z_{m,z} dz \int_0^b X_{j,xx} X_{n,x} dx \right] \right. \\ & \left. + E[N_x] \int_0^l Z_{i,z} Z_{m,z} dz \int_0^b X_j X_n dx + \int_0^l Z_i Z_{m,z} dz \int_0^b X_n X_{j,x} dx \right\} A_{ij} = 0 \quad (4.118) \end{aligned}$$

From the above equation, we obtain the expected value of critical buckling load N_{cr} .

Now applying the variance operation on Eqn. (4.96), we obtain the following equation after neglecting the terms that correspond to the covariances between D_{ij} terms:

$$\begin{aligned}
& \sum_{i=1}^M \sum_{j=1}^N \left\{ \text{var} \left[D_{11} \left[\int_0^l Z_{i,z} Z_{m,z} dz \int_0^b X_j X_n dx \right]^2 \right. \right. \\
& + \text{var} \left[D_{12} \left[\int_0^l Z_m Z_{i,z} dz \int_0^b X_j X_{n,xx} dx + \int_0^l Z_i Z_{m,z} dz \int_0^b X_n X_{j,xx} dx \right]^2 \right. \\
& + \text{var} \left[D_{22} \left[\int_0^l Z_i Z_m dz \int_0^b X_{j,xx} X_{n,xx} dx \right]^2 + \text{var} \left[D_{66} \left[4 \int_0^l Z_{i,z} Z_{m,z} dz \int_0^b X_{j,x} X_{n,x} dx \right]^2 \right. \right. \\
& + \text{var} \left[D_{16} \left[2 \left(\int_0^l Z_{i,z} Z_{m,z} dz \int_0^b X_j X_{n,x} dx + \int_0^l Z_{i,z} Z_{m,z} dz \int_0^b X_j X_{n,x} dx \right) \right]^2 \right. \\
& + \text{var} \left[D_{26} \left[2 \left(\int_0^l Z_i Z_{m,z} dz \int_0^b X_{j,xx} X_{n,xx} dx + \int_0^l Z_i Z_{m,z} dz \int_0^b X_{j,xx} X_{n,xx} dx \right) \right]^2 \right. \\
& \left. \left. + \text{var} \left[N_x \left(\int_0^l Z_{i,z} Z_{m,z} dz \int_0^b X_j X_n dx \right)^2 \right] \right\} A_{ij} = 0 \tag{4.119}
\end{aligned}$$

From the above equation, we obtain the variance value of critical buckling load N_{cr} .

4.5.1 Stochastic simulation of laminate bending stiffness matrix

Using the test data of the material properties [62] as shown in the Table 4.8, the stochastic process that corresponds to the laminate bending stiffness is determined from Eqn. 4.112 and further, sample realizations at each Gauss point are obtained. Using the generated sample realizations of material properties at each Gauss point the stochastic bending stiffness matrix, $[D]$, is calculated for each Gauss point. A computer program is written in MATLAB[®] to get the stochastic process that corresponds to the bending stiffness matrix, $[D]$. This program is given in the Appendix.

	E_1 (GPa)	E_2 (GPa)	ν_{21}	ν_{12}	G_{12} (GPa)	Fiber direction failure load (N)	Transverse direction failure load (N)
Mean	129.4	8.0	0.021	0.332	4.3	18617.1	1257.9
Standard deviation	2.9	0.33	0.002	0.032	0.24	2789.1	169.3
Coefficient of variation	2.22	4.12	10.43	9.55	5.52	14.98	13.46

Table 4.8 Mean values, standard deviations and coefficients of variation of various material properties of NCT 301 graphite-epoxy composite material [62]

Using the test data on elastic constants of the composite material as shown in Table 4.8, the stochastic field realizations of bending stiffness matrix are obtained at each Gauss point using the Eqn. (4.112). In the present work, a three point Gaussian numerical integration is used as it gives most accurate results. Considering 12 regions in the present structure, nine different sample realizations of each of the stochastic process are generated corresponding to nine Gauss points in each region. Therefore there will be a total of 108 coordinate points that will be generated. Here each coordinate point is considered to be a Gauss point. Considering a particular set of sample realizations generated for the entire structure, a sample realization for Gauss points in regions 2 and 10, for the $[45/-45]_{9s}$ laminate, is shown in Figure 4.9.

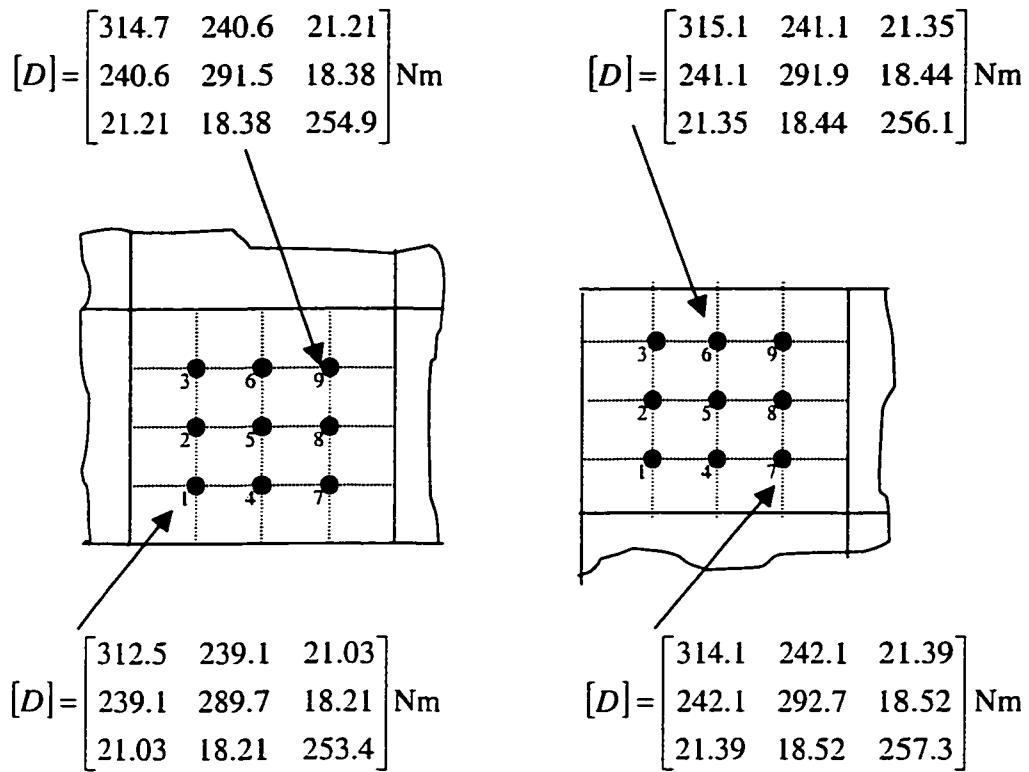


Figure 4.9 A set of sample realizations of the stochastic bending stiffness matrix at different Gauss points in regions 2 and 10

4.6 Parametric study

In the following section, parametric study is performed on composite beam-column with I shaped cross-section by varying boundary conditions, laminate configurations and aspect ratio.

A composite beam-column with I-cross-section as shown in Fig. 4.10 consisting of a total of 36 plies made of NCT-301 Graphite-Epoxy composite material, each having a ply thickness of 0.125 mm is considered. The same material properties considered in earlier chapters are also used in this chapter. The length and width of the beam-column is

changed according to the aspect ratio, R . Since the cross-section is symmetric, only half flange is considered in the analysis. Therefore aspect ratio for the flange is $2l/b_f$ and aspect ratio for the web is l/h_w . Three different types of laminates i.e. $[0/90]_{9s}$, laminate $[+45/-45]_{9s}$ laminate, and $[0/-60/60]_{6s}$ laminate are considered for the two flanges and web respectively. Buckling load is presented in non-dimensional form, K , which is given by $K = N_{cr}b^2/D_{11}$. A 9-terms solution is used to obtain critical buckling load. The boundary conditions are denoted by S for simple supports, C for clamped supports and F for free supports along the edges.

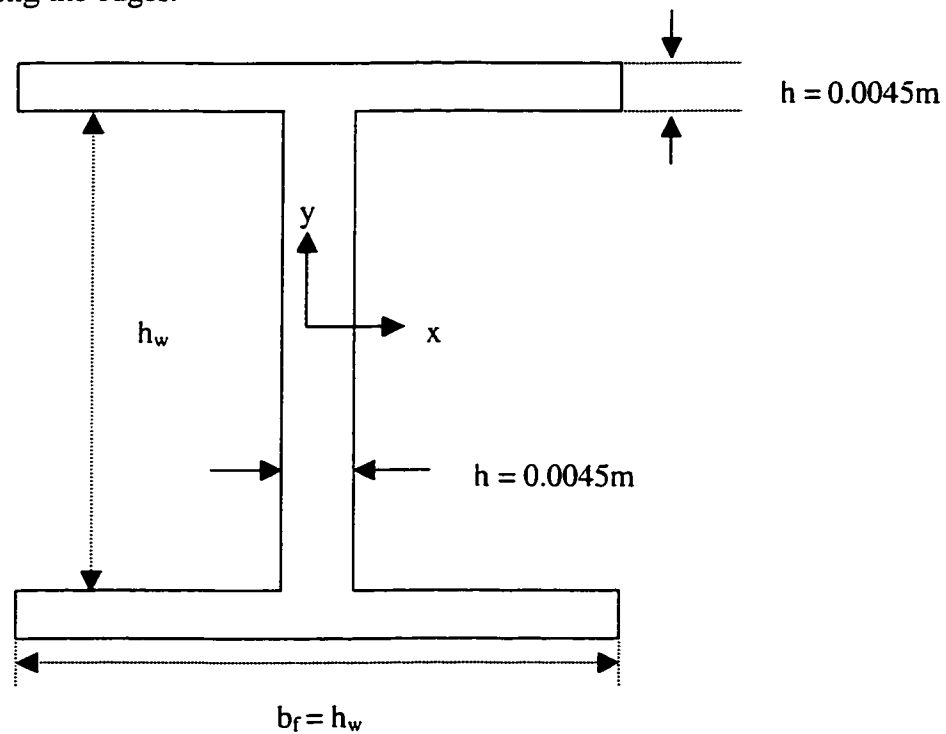


Figure 4.10 I-section beam-column with dimensions

Table 4.9 shows the deterministic, expected and variance values of critical buckling load for (a) $[0/90]_{9s}$ laminate with free boundary conditions on loading edge, (b) $[+45/-45]_{9s}$ laminate with free boundary conditions on loading edge, (c) $[0/-60/60]_{6s}$ laminate with free boundary conditions on loading edge, (d) $[0/90]_{9s}$ laminate with simply supported

boundary conditions on loading edge, (f) $[+45/-45]_{9s}$ laminate with simply supported boundary conditions on loading edge, and (e) $[0/-60/60]_{6s}$ laminate with simply supported boundary conditions on loading edge.

Figure 4.11 shows the deterministic and expected values of critical buckling load for $[0/90]_{9s}$ laminate with free boundary conditions on loading edges and completely clamped flange-web connection.

Figure 4.12 shows the deterministic and expected values of critical buckling load for $[+45/-45]_{9s}$ laminate with free boundary conditions on loading edges and completely clamped flange-web connection.

Figure 4.13 shows the deterministic and expected values of critical buckling load for $[0/-60/60]_{6s}$ laminate with free boundary conditions on loading edges and completely clamped flange-web connection.

Figure 4.14 shows the variance of buckling load for different laminate configurations with free boundary conditions on loading edge.

Figure 4.15 shows the deterministic and expected values of critical buckling load for $[0/90]_{9s}$ laminate with simply supported boundary conditions on loading edges and completely clamped flange-web connection.

Figure 4.16 shows the deterministic and expected values of critical buckling load for $[+45/-45]_{9s}$ laminate with simply supported boundary conditions on loading edges and completely clamped flange-web connection.

Figure 4.17 shows the deterministic and expected values of critical buckling load for $[0/-60/60]_{6s}$ laminate with simply supported boundary conditions on loading edges and completely clamped flange-web connection.

Figure 4.18 shows the variance of buckling load for different laminate configurations with simply supported boundary conditions on loading edge.

* $R = 2l/b_f$ (flange); $R = l/h_w$ (web);

	Flange			Web		
	FCFF	FCFF	FCFF	FCFC	FCFC	FCFC
R	Deterministic	Mean	Variance	Deterministic	Mean	Variance
0.5	48.38	49.44	2738.6	44.56	45.04	1794.6
1	25.1	26.21	1305.5	20.77	21.2	339.79
1.5	27.79	28.4	1340.3	23.37	23.9	451.34
2	30.39	31.37	1484.5	25.95	26.28	505.36
2.5	31.51	32.4	1498.1	26.97	27.1	560.23
3	34.58	35.61	1686.1	29.97	30.24	701.6
3.5	39.68	40.8	2064.1	35.02	36.2	1123.5
4	46.45	47.3	2642.8	41.77	42.1	1653.9
4.5	54.68	55.2	3828.5	49.98	50.5	2632.2
5	64.22	64.81	4744.7	59.52	59.31	3756.1

	Flange			Web		
	FCFF	FCFF	FCFF	FCFC	FCFC	FCFC
R	Deterministic	Mean	Variance	Deterministic	Mean	Variance
0.5	127.22	123.91	14654.9	82.11	81.01	3488.2
1	106.6	104.1	13258.3	59.33	58.12	2050.1
1.5	110.33	108.2	13412.2	61.61	60.4	2014.2
2	115.44	112.5	13578.5	65.22	63.1	2295.1
2.5	121.35	118.2	13742.3	68.96	65.3	2380.2
3	128.75	125.3	13945.5	74.21	72.65	2565.5
3.5	137.64	135.8	14523.1	81.16	79.1	2945.5
4	147.86	145.4	15226.4	89.7	87.5	3676.8
4.5	159.29	155.5	16423.2	99.71	97.67	4895.1
5	171.91	168.03	17709.9	111.12	108.6	6112.1

	Flange			Web		
	FCFF	FCFF	FCFF	FCFC	FCFC	FCFC
R	Deterministic	Mean	Variance	Deterministic	Mean	Variance
0.5	72.04	72.22	6324.5	55.73	55.81	2304.3
1	50.03	49.5	4901.3	31.89	31.87	848.15
1.5	52.79	52.1	4982.3	33.87	33.1	926.21
2	55.9	55.1	5127.1	36.74	36.62	1021.3
2.5	58.47	58.55	5274.2	38.5	37.5	1089.2
3	62.49	62.39	5363.5	41.74	41.53	1222.7
3.5	68.11	67.2	5805.2	46.76	45.5	1645.6
4	75.15	74.84	6330.3	53.33	52.88	2135.2
4.5	83.45	82.2	7121.3	61.28	60.8	3032.5
5	92.93	92.31	8371.5	70.48	69.71	4153.1

	Flange			Web		
	SCSF	SCSF	SCSF	SCSC	SCSC	SCSC
R	Deterministic	Mean	Variance	Deterministic	Mean	Variance
0.5	53.19	53.86	6918	53.76	54.31	1876.9
1	53.66	53.92	6914.4	53.76	54.3	1875.7
1.5	44.4	44.9	9886.1	45.12	45.45	1147.9
2	44.48	45.07	10073.5	44.76	45.19	1088.8
2.5	46.18	46.63	18368.8	47.39	47.6	1384.4
3	53.66	53.96	33802.2	56.03	56.12	2346.9
3.5	65.02	65.11	59321.9	68.75	69.1	4059.2
4	79.45	79.3	98505.7	84.75	84.36	6732.9
4.5	96.54	96.15	155506.1	103.65	104.5	10641.2
5	116.4	115.14	235037.2	125.23	124.23	16103.3

	Flange			Web		
	SCSF	SCSF	SCSF	SCSC	SCSC	SCSC
R	Deterministic	Mean	Variance	Deterministic	Mean	Variance
0.5	108.9	107.22	30907.2	108.49	106.83	4074.5
1	108.43	106.82	23951.4	108.44	106.76	4074.8
1.5	105.72	103.78	30893.8	102.91	100.94	3434.5
2	104.58	102.58	44082.6	101.59	99.73	3333.7
2.5	110.06	107.79	58536.8	106.43	104.34	3727.2
3	120.76	118.21	78604.9	117.49	115.15	4857.9
3.5	135.19	132.34	109176.3	132.91	130.27	6846.7
4	152.75	149.57	155040.8	153.9	151.92	9943.2
4.5	173.17	169.63	221275.2	175.12	171.76	14466.2
5	196.3	192.36	313453.2	200.37	197.58	20787.1

R	Flange			Web		
	SCSF	SCSF	SCSF	SCSC	SCSC	SCSC
	Deterministic	Mean	Variance	Deterministic	Mean	Variance
0.5	71.2	71	15725.1	69.48	69.45	2528.7
1	70.48	70.14	15512.9	53.76	52.1	2528.4
1.5	61.82	61.62	15719.8	60.55	59.1	1780.9
2	61.92	61.78	21014.6	60.35	60.5	1731.5
2.5	63.62	63.5	29861.7	62.69	61.1	2004.1
3	70.87	70.38	45035.1	70.91	69.1	2923.9
3.5	81.83	80.4	69693.98	83.1	82.2	4565.9
4	95.73	94.75	107388.8	98.46	96.3	7131.7
4.5	112.21	110.2	162150.1	116.62	114.2	10883.1
5	131.06	129.44	238521.7	137.37	134.57	16126.3

Table 4.9 Deterministic, mean and variance values of critical buckling loads: (a) $[0/90]_{9s}$ laminate with free boundary conditions on loading edges, (b) $[45/-45]_{9s}$ laminate with free boundary conditions on loading edges, (c) $[0/-60/60]_{6s}$ laminate with free boundary conditions on loading edges, (d) $[0/90]_{9s}$ laminate with simply supported boundary conditions on loading edges, (e) $[45/-45]_{9s}$ laminate with simply supported boundary conditions on loading edges, and (f) $[0/-60/60]_{6s}$ laminate with simply supported boundary conditions on loading edges

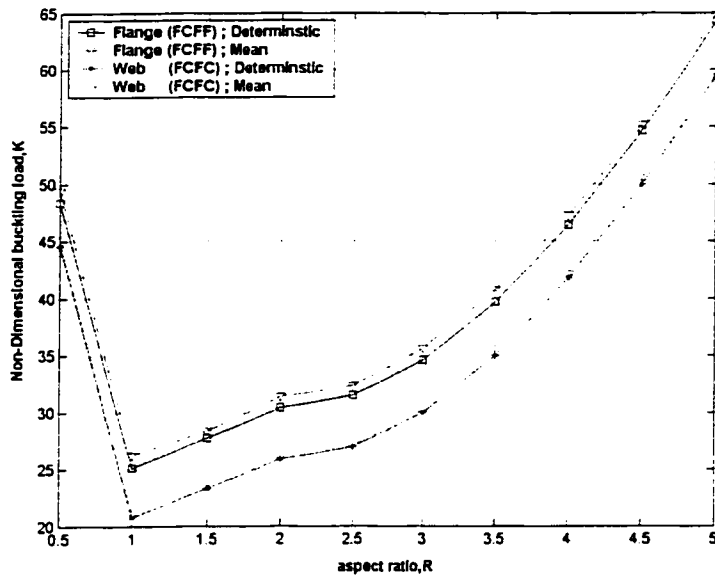


Figure 4.11 Deterministic and mean values of critical buckling load for the $[0/90]_{9s}$ laminate with free boundary conditions on loading edges

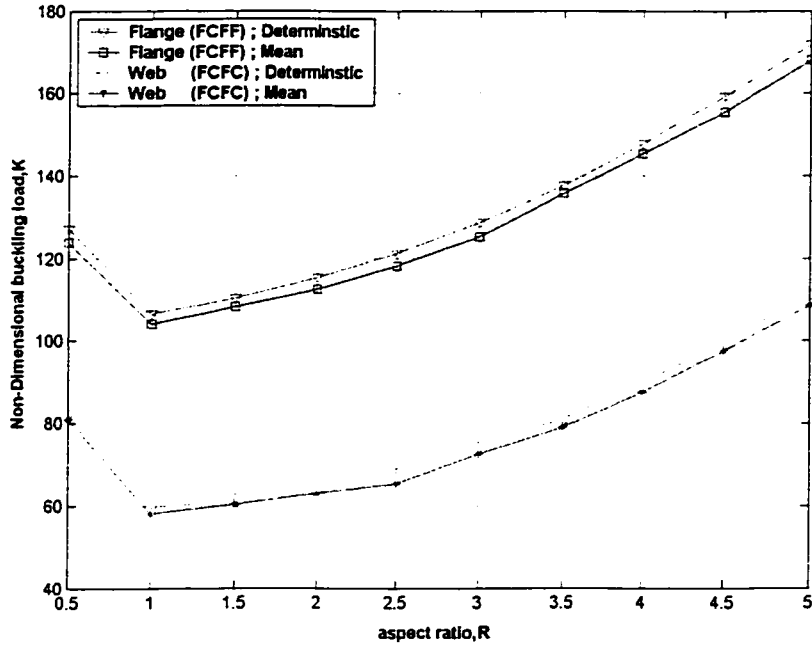


Figure 4.12 Deterministic and mean values of critical buckling load for the $[45/-45]_{9s}$ laminate with free boundary conditions on loading edges

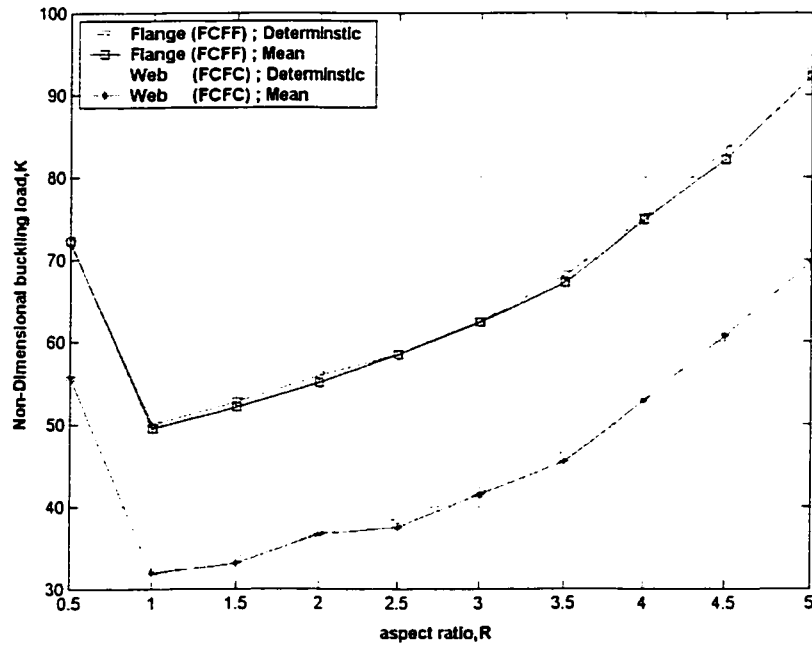


Figure 4.13 Deterministic and mean values of critical buckling load for the $[0/-60/60]_{6s}$ laminate with free boundary conditions on loading edges

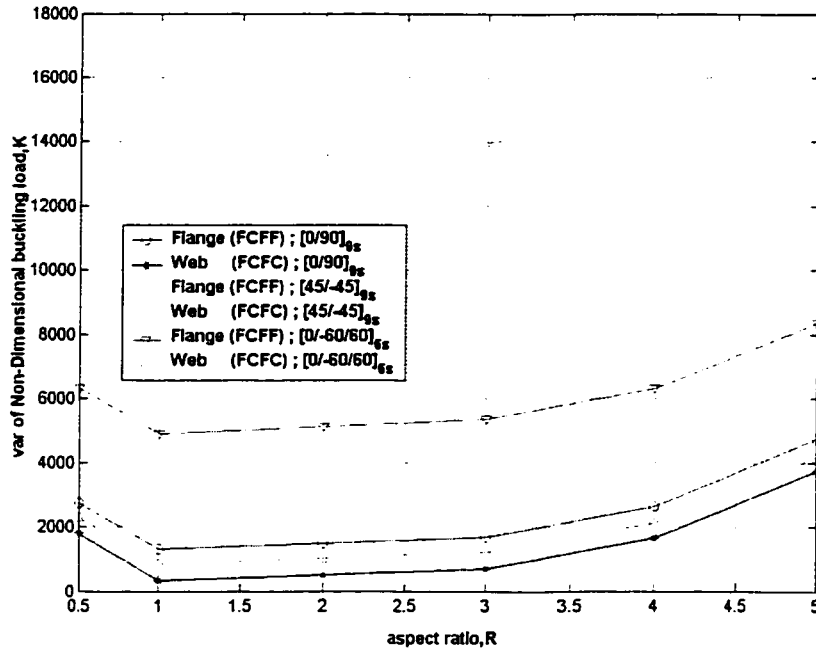


Figure 4.14 Variance values of critical buckling load for different laminate configurations with free boundary conditions on loading edges

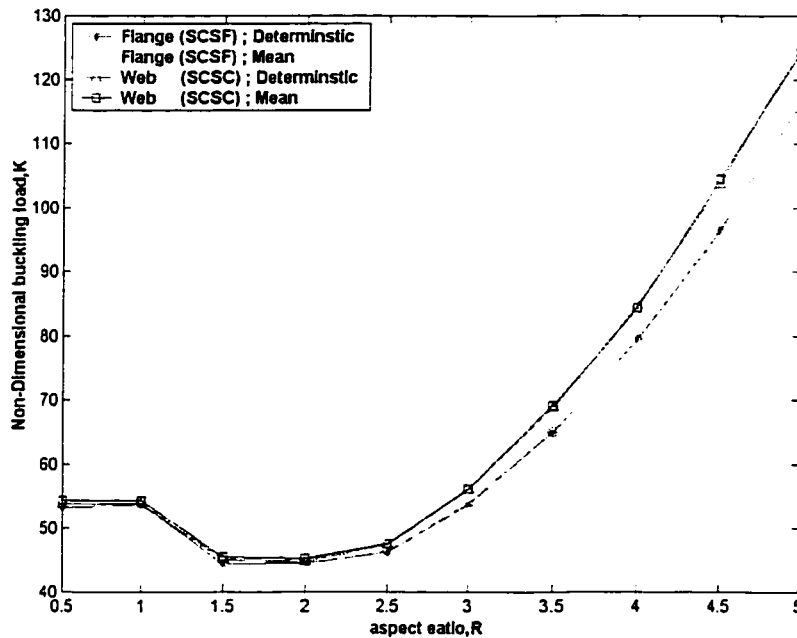


Figure 4.15 Deterministic and mean values of critical buckling load for the [0/90]_{9s} laminate with simply supported boundary conditions on loading edges

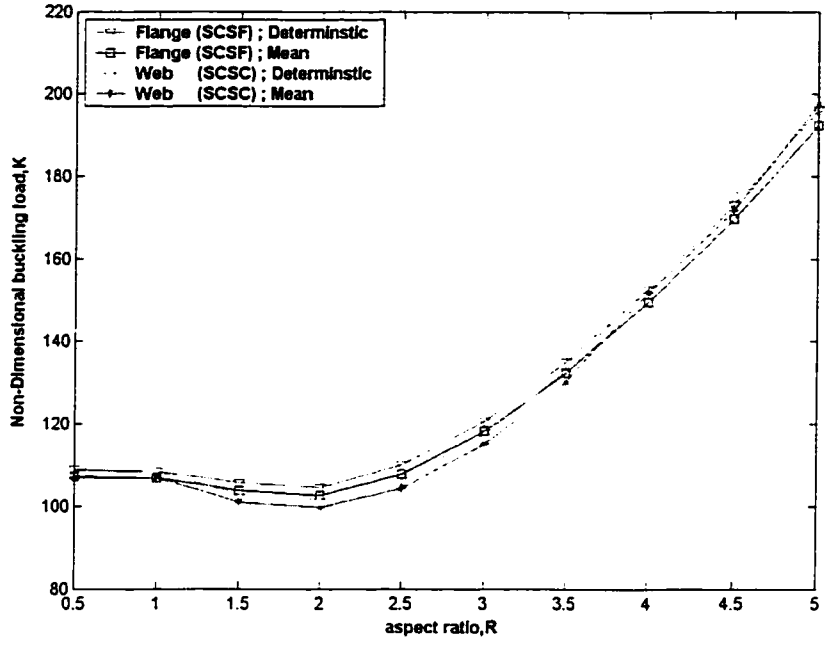


Figure 4.16 Deterministic and mean values of critical buckling load for the $[45/-45]_{9s}$ laminate with simply supported boundary conditions on loading edges

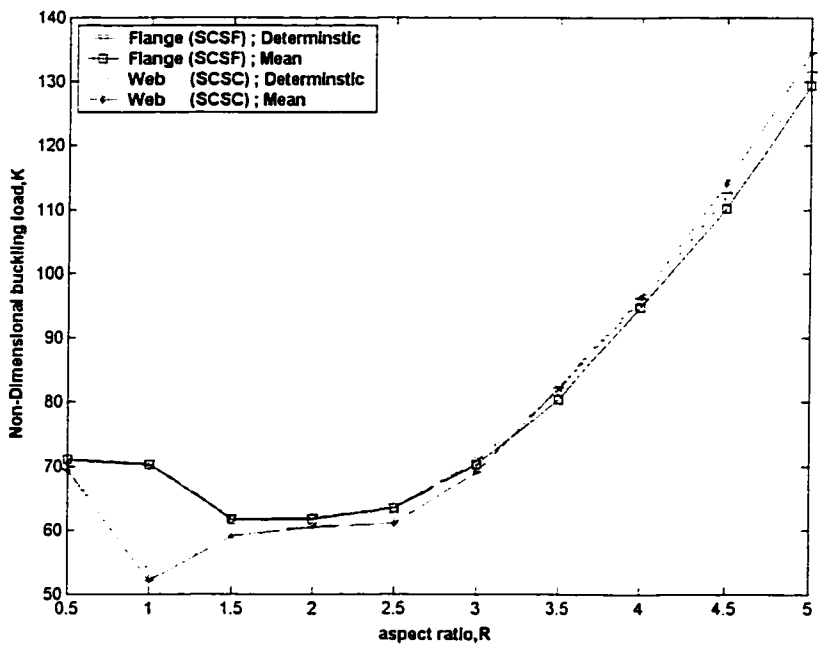


Figure 4.17 Deterministic and mean values of critical buckling load for the $[0/-60/60]_{6s}$ laminate with simply supported boundary conditions on loading edges

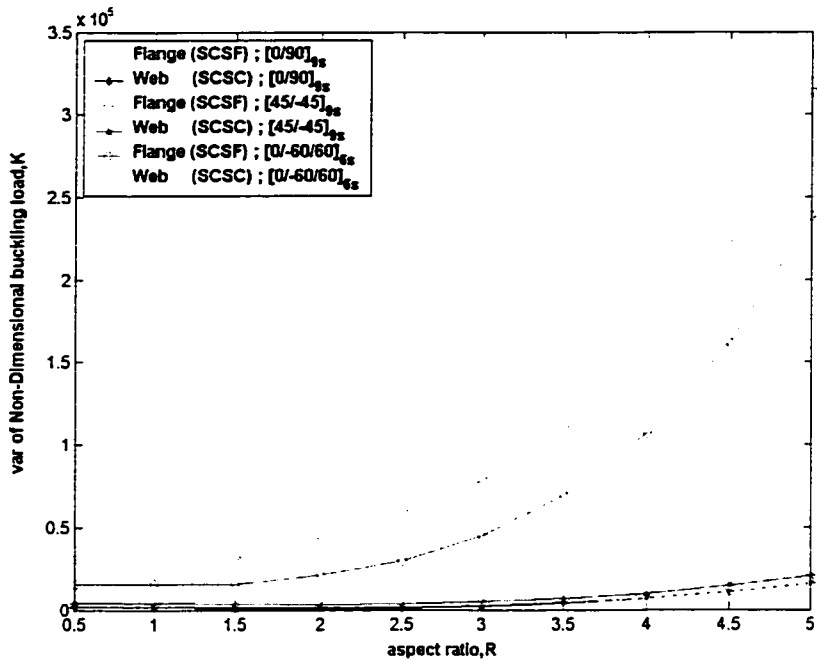


Figure 4.18 Variance values of critical buckling load for different laminate configurations with simply supported boundary conditions on loading edges

Observations:

It is observed from Figure 4.11 and Table 4.9(a) that the local buckling can occur due to web buckling. Further, it shows that the expected values of buckling loads are slightly less than the deterministic values. It is also observed that for the aspect ratio between 0.5 – 1.0 there is maximum drop in the buckling load. For aspect ratio values greater than 1.0, critical buckling load increases continuously.

It can be clearly observed from Figure 4.12 and Table 4.9(b) that local buckling can occur due to web buckling.

It is observed from Figure 4.13 and Table 4.9(c) that local buckling can occur due to web buckling. Here also we can observe that maximum drop in buckling load occurs when the aspect ratio is between 0.5 - 1.0.

It is observed from the Figures 4.11- 4.13 that the buckling load is the lowest when the aspect ratio is 1. Further, it can be seen that cross-ply laminate with free boundary conditions on loading edge possesses the largest buckling load.

It can be observed from Figure 4.14 that cross-ply laminate web (FCFC) possesses the highest variance over the other laminates. Further, it can be seen that variance value increases quite significantly as the aspect ratio increases.

It is observed from Figure 4.15 and Table 4.9(d) that the local buckling can occur due to flange buckling. Further, it shows that the buckling load is almost constant within the aspect ratio range 0.5 - 1.0.

It can be observed from Figure 4.16 that the change in the buckling load with increasing aspect ratio is quite different from the previous cases. It can be seen from Figure 4.16 and Table 4.9(e) that the local buckling may well be triggered initially in the web when the aspect ratio is between 0.5 - 3.5 and after that local buckling may occur in the flange. This is the significant observation. Further, here also it shows that the buckling load is almost constant within the range 0.5-1.0.

Observation from Figure 4.17 shows that buckling is somewhat similar to the previous case i.e. the local buckling may initially occur in the web when the aspect ratio is between 0.5 - 3 and after that local buckling may occur in the flange.

It can be observed from Figure 4.18 that the variance value increases quite significantly as the aspect ratio increases.

4.7 Conclusions and discussions

In this chapter, the formulation for the buckling analysis of composite beam-columns with stochastic properties is developed using the standard perturbation analysis. Two cases are considered i.e. (1) Random stiffness and geometric properties having uniform correlation, and (2) Random stiffness and geometric properties having exponential correlation. Expected, mean square and variance values of critical buckling loads for $[0/90]_{9s}$, $[+45/-45]_{9s}$, $[0/-60/60]_{6s}$, and $[0/45]_{18T}$ NCT-301 composite laminates are determined corresponding to cylindrical bending and one-dimensional laminated beam theories.

It is observed that un-symmetric laminate possesses the highest expected and variance values of critical buckling load whereas symmetric angle-ply laminate has the lowest expected and variance values of critical buckling load. Further, it is observed that the expected and variance values of critical buckling load corresponding to cylindrical bending and one-dimensional laminated beam theories are almost same in symmetric

cross-ply laminate whereas small percentage of difference is seen in quasi-isotropic laminate and further, the largest difference occurs in symmetric angle-ply laminate.

In the second half of the chapter, deterministic local buckling of thin-walled composite beam-columns is discussed. Further, the stochastic local buckling analysis of thin-walled composite beam-columns is developed. Program is written in MATLAB[®] to generate stochastic laminate bending stiffness matrix and to solve the eigen value problem for the critical buckling load.

From the results, it is observed that the local buckling occurs in the web in all the three different types of laminates when the loaded edges are free boundary conditions. Further, it is observed that the local buckling occurs in the flange in symmetric cross-ply laminate when the loaded edges are simply supported. Whereas in the cases of symmetric angle-ply laminate and quasi-isotropic laminate local buckling is first triggered in the web when the aspect ratio is between 0.5 -3.0 and 0.5 - 3.5 respectively, and after that local buckling occurs in the flange when the loaded edges are simply supported. Further, it can be seen that variance value increases quite significantly as the aspect ratio increases.

Chapter 5

CONCLUSIONS AND RECOMMENDATIONS

In the present thesis, the free-vibration and buckling of prismatic beam-columns made of polymer-matrix fiber-reinforced composite materials are considered first. The mean values, mean square values and variances of the natural frequencies of undamped free vibrations and that of the buckling loads of the beam-columns are determined based on the perturbation method that is employed in the context of stochastic analysis. The equations that quantify the relationships between the natural frequencies, and the laminate configurations, fiber orientations, geometric parameters and material properties of the laminate, and boundary conditions are derived. Similar relationships for the buckling loads are also determined.

The thin-walled beam-columns made of polymer-matrix fiber-reinforced composite materials are considered next. Equations for the mean values, mean square values and variance values of the natural frequencies are derived in a form that is similar to the corresponding equations derived for prismatic beam-columns. In addition to the relationships mentioned in the above for prismatic beam-columns, the relationships between the natural frequencies, and the laminate configurations and aspect ratios of the flange and web sections of the thin-walled beam-column are also quantified through relevant equations. For the thin-walled columns, the local buckling loads are also determined. In this regard, the Ritz method is applied in the context of stochastic

analysis. A program is written in MATLAB[®] to generate the stochastic laminate bending stiffness matrix and to solve the eigenvalue problem for the mean value and variance of the critical buckling load.

A detailed parametric study is conducted using the above mentioned theoretical developments to determine the influences of the material, structural, and geometric properties, and applied axial loads on the natural frequencies and buckling loads for the $[0/90]_{9s}$ laminate, $[+45/-45]_{9s}$ laminate, $[0/-60/60]_{6s}$ laminate, and $[0/45]_{18T}$ laminate.

The principal conclusions obtained in the present study are:

- The mean value of the fundamental natural frequency differs more from the deterministic fundamental natural frequency when the mean value and variance of the input random variable that corresponds to the axial load increases and also when the axial load approaches the critical buckling load.
- Un-symmetric laminate possesses the highest mean and variance values of natural frequency and critical buckling load whereas symmetric angle-ply laminate has the lowest mean and variance values of critical buckling load.
- Expected and variance values of natural frequency and critical buckling load corresponding to cylindrical bending and one-dimensional laminated beam theories are almost same for symmetric cross-ply laminate whereas small percentage of difference is seen in quasi-isotropic laminate and further, the largest difference occurs in symmetric angle-ply laminate.

- Local buckling occurs in the web section for $[0/90]_{9s}$ laminate, $[+45/-45]_{9s}$ laminate, and $[0/-60/60]_{6s}$ laminate when the loaded edges have free boundary conditions.
- Local buckling occurs in the flange section in symmetric cross-ply laminate when the loaded edges have simply supported boundary conditions.
- Local buckling first triggers in the web section when the aspect ratio is between 0.5 - 3.0 and after that local buckling occurs in the flange section when the loaded edges have simply supported boundary conditions.
- Cross-ply laminate exhibits higher mean value and variance over other laminate configurations.

The following works are suggested for future studies:

- Considering the damping effect, a generalized stochastic equation for the n^{th} natural frequency of the free-vibration of composite beam-column can be developed.
- In the thin-walled prismatic composite beam-columns, stochastic analysis can be extended to un-symmetrical sections.
- The theoretical development provided for uniform composite beam-column in this thesis can be extended to the tapered composite beam-columns.
- Stochastic local buckling analysis of thin-walled composite beam-columns presented in this thesis can be extended to different types of symmetric and un-symmetric cross-sections.

REFERENCES

- [1] Whitney, J.M. and Ashton, J.E., *Structural Analysis of Laminated Anisotropic Plates*, 1987, Technomic Publishing Company, Lancaster, Pa., U.S.A.
- [2] Bertholet, J.M., *Composite Materials - Mechanical Behavior and Structural Analysis*, 1999, Springer Verlag, New York.
- [3] Keller, J.B., "Wave Propagation in Random Media", Proceedings of the symposium of Applied Mathematics, New York, Vol. 13, 1960, pp. 227-246.
- [4] Boyce, W.E. and Goodwin, B.E., "Random Transverse Vibrations of Elastic Beams", Society for Industrial and Applied Mathematics Journal, Vol. 12, 1964, pp. 613-629.
- [5] Bharucha-Ried, A.T., *Probabilistic Methods in Applied Mathematics*, Vol. 1, 1968, Academic Press, New York.
- [6] Hoshiya, M. and Shah, C.H., "Free Vibration of Stochastic Beam-Column", Journal of the Engineering Mechanics Division, Vol. 4, 1971, pp. 1239-1255.
- [7] Lepore, J.A. and Shah, H.C., "Dynamic Stability of Axially Loaded Columns Subjected to Stochastic Excitations", AIAA Journal, Vol. 6(8), 1968, pp. 1515-1521.
- [8] Shinozuka, M. and Astill, C.J., "Random Eigen Value Problems in Structural Analysis", AIAA Journal, Vol.10 (4), 1972, pp. 456-462.
- [9] Bliven, D.O. and Soong, T.T., "On Frequencies of Elastic Beams with Random Imperfections", J.Franklin Inst., Vol. 287, 1969, pp. 297-304.

- [10] Vaicaitis, R., "Free Vibration of Beams with Random Characteristics", *Journal of Sound and Vibration*, Vol. 35, 1974, pp. 13-21.
- [11] Collins, J.D. and Thomson, W.T., "The Eigenvalue Problem for Structural Systems with Statistical Properties", *AIAA Journal*, Vol. 7, 1969, pp. 642-648.
- [12] Ramu, S.A. and Ganesan, R., "Free Vibration of a Stochastic Beam-Column using Stochastic FEM", *Int. J. for Computers and Structures*, Vol. 41(5), 1991, pp. 987-994.
- [13] Liaw, D.G. and Yang, T.Y., "Reliability of Randomly Imperfect Beam-Columns", *Journal of Engineering Mechanics*, Vol.115(10), 1989, pp. 2251-2270.
- [14] Grigoriu, M.K. and O'Rourke, T., "Stochastic Beams on Elastic Foundation", *Proceedings of the ASCE Convention*, 1985, Denver, pp. 96-106.
- [15] Ramu, S.A. and Ganesan, R., "Response and Stability of a Stochastic Beam-Column using Stochastic FEM", *Computers and Structures*, Vol. 54(2), 1995, pp. 207-221.
- [16] Jensen, H. and Iwan, W.D., "Response of Systems with Uncertain Parameters to Stochastic Excitation", *Journal of Engineering Mechanics*, Vol. 118(5), 1992, pp. 1012-1025.
- [17] Liu, W.K., Belytschko, T., and Mani, A., "Applications of Probabilistic Finite Element Methods in Elastic/Plastic Dynamics", *Journal of Engineering for Industry*, Vol. 109, 1987, pp. 2-8.
- [18] Ghanem, R. and Spanos, P.D., "Polynomial Chaos in Stochastic Finite Elements", *Journal of Applied Mechanics*, Vol. 57, 1990, pp. 197-202.

- [19] Ganesan, R., Sankar, T.S., and Ramu, S.A., "Non-Conservatively Loaded Stochastic Columns", *Int. J. of Solids and Structures*, Vol. 30(17), 1993, pp. 2407-2424.
- [20] Ramu, S.A. and Ganesan, R., "Parametric Instability of Stochastic Columns", *International Journal of Solids and Structures*, Vol. 30(10), 1993, pp. 1339-1354.
- [21] Ramu, S.A. and Ganesan, R., "Stability of Stochastic Leipholz Column with Stochastic Loading", *Ingenieur-Archiv*, Vol. 62(6), 1992, pp. 363-375.
- [22] Ramu, S.A. and Ganesan, R., "Stability Analysis of a Stochastic Column Subjected to Stochastically Distributed Loadings using the Finite Element Method", *Finite Elements in Analysis and Design*, Vol.11(2), 1992, pp. 105-115.
- [23] Ahamadi, G. and Sattaripour, S.A., "Dynamic Stability of a Column Subjected to an Axial Random Load", *Industrial Mathematics*, Vol. 26(2), pp. 67-77.
- [24] Sankar, T.S., Ramu, S.A., and Ganesan, R., "Stochastic Finite Element Analysis for High Speed Rotors", *Journal of Vibration and Acoustics*, Vol. 115, 1993, pp. 59-64.
- [25] Nakagiri, S., Takabatake, H., and Tani, S., "Uncertain Eigenvalue Analysis of Composite Laminated Plates by the Stochastic Finite Element Method", *Journal of Engineering for Industry*, Vol. 109, 1987, pp. 9-12.
- [26] Borri A., *Stochastic Behaviour of Special Materials: The Composite Material in Dynamic Motion: Chaotic and Stochastic Behaviour*, Ed.: F. Casciati, 1993, Springer Verlag, New York.

- [27] Ganesan, R., "Vibration Analysis for Stability of Singular Non-self-adjoint Beam-Columns using stochastic FEM", *Computers and Structures*, Vol. 68(5), 1998, pp. 543-554.
- [28] Oh, D.H. and Librescu, L., "Free-vibration and Reliability of Composite Cantilevers Featuring Uncertain Properties", *Reliability Engineering & System Safety*, Vol. 56(3), 1997, pp. 265-572.
- [29] Venini, P. and Mariani, C., "Free Vibrations of Uncertain Composite Plates via Stochastic Rayleigh-Ritz Approach", *Computers and Structures*, Vol. 64(1-4), 1997, pp. 407-423.
- [30] Liaw, D.G. and Henry T.Y., "Reliability and Nonlinear Supersonic Flutter of Uncertain Laminated Plates", *AIAA Journal*, Vol. 31(12), 1993, pp. 2304-2311.
- [31] Chung, I. and Weitsman, Y., "On the Buckling Compressive Failure of Fibrous Composites", *International Journal of Solids and Structures*, Vol. 32(16), 1995, pp. 2329-2344.
- [32] Hilton, H.H., Yi, S., and Danyulk, M.J., "Probabilistic Analysis of Delamination Onset in Linear Anisotropic Elastic and Viscoelastic Composite Columns", *Reliability Engineering & System Safety*, Vol. 56(3), 1997, pp. 237-248.
- [33] Lin, S.C., Kam, T.Y., and Chu, K.H., "Evaluation of Buckling and First-ply Failure Probabilities of Composite Laminates", *International Journal of Solids and Structures*, Vol. 35(13), 1998, pp. 1395-1410.
- [34] Lin, S.C., "Buckling Failure Analysis of Random Composite Laminates Subjected to Random Loads", *International Journal of Solids and Structures*, Vol. 37(51), 2000, pp. 7563-7576.

- [35] Barbero, E. and Tomblin, J., "Euler Buckling of Thin-Walled Composite Columns", *Thin-Walled Structures*, Vol. 17(4), 1993, pp. 237-258.
- [36] Kolakowski, Z., Krolak, M., and Kowal-Michalska, K., "Modal Interactive Buckling of Thin-Walled Composite Beam-Columns Regarding Distortional Deformations", *International Journal of Engineering Science*, Vol. 37(12), 1999, pp. 1577-1596.
- [37] Shield, C. and Morey, T., "Buckling of Laminated Composite Beams", *Proceedings of ASCE*, Vol. 2, 1996, Fort Lauderdale, FL, pp. 1010-1013.
- [38] Rehfield, L W. and Muller, U., "Design of Thin-Walled Laminated Composite Beams to Resist Buckling", *Proceedings of the AIAA/ASME/ASCE/ASC*, 1999, St. Louis, MO, pp. 1479-1488.
- [39] Pandey, M.D., Kabir, M.Z., and Sherbourne, A N., "Flexural-torsional Stability of Thin-Walled Composite I-section Beams", *Composites Engineering*, Vol. 5(3), 1995, pp. 321-342.
- [40] Almanzar, L. and Godoy, L., "Design Sensitivity of Buckled Thin-walled Composite Structural Elements", *Applied Mechanics Reviews*, *Proceedings of the 1997 5th Pan-American Congress of Applied Mechanics*, Vol. 50(11), 1997, San Juan, PR, USA, pp. S3-S10.
- [41] Barbero, E.J. and Raftoyiannis Ioannis G., "Euler Buckling of Pultruded Composite Columns", *Composite Structures*, Vol. 24(2), 1993, pp. 139-147.
- [42] Barbero, E.J. and Raftoyiannis Ioannis G., "Buckling Analysis of Pultruded Composite Columns", *ASME, Aerospace Division, Winter Annual Meeting of the ASME*, Vol. 20, 1990, Dallas, TX, pp. 47-52.

- [43] Krolak, M. and Zaras, J., "Investigation into Thin-walled Structures at the Technical University of Lodz", *Thin-Walled Structures*, Vol. 28(3-4), 1997, pp. 225-231.
- [44] Hancock, G.J. and Rasmussen, K.J.R., "Recent research on Thin-walled Beam-Columns", *Thin-Walled Structures*, Vol. 32(1-3), 1998, pp. 3-18.
- [45] Silvestre, N. and Camotim, D., "Second-order Generalized Beam Theory for Arbitrary Orthotropic Materials", *Thin-Walled Structures*, Vol. 40(9), 2002, pp. 791-820.
- [46] Barbero, E.J., "Optimization of Pultruded Composite Beams and Columns", 36th Int. SAMPE Symposium, Vol. 36(2), 1991, San Diego, CA, pp. 1343-1354.
- [47] Godoy, L.A., Barbero, E.J., and Raftoyiannis Ioannis G., "Interactive Buckling Analysis of Fiber-Reinforced Thin-Walled Columns", *Journal of Composite Materials*, Vol. 29(5), 1995, pp. 591-613.
- [48] Godoy, L.A. and Almanzar, L.L., "Improving Design in Composite Thin-walled Columns", *Proceedings of the 11th Conference on Engineering Mechanics*, Vol. 2, 1996, Fort Lauderdale, FL, pp. 1155-1158.
- [49] Barbero, E.J., Dede, E.K., and Jones, S., "Experimental Verification of Buckling-Mode Interaction in Intermediate-length Composite Columns", *International Journal of Solids and Structures*, Vol. 37(29), 2000, pp. 3919-3934.
- [50] Tomblin, J. and Barbero, E., "Local Buckling Experiments on FRP Columns", *Thin-Walled Structures*, Vol. 18(2), 1994, pp. 97-116.

- [51] Barbero, E. and Tomblin, J., "Phenomenological Design Equation for FRP Columns with Interaction Between Local and Global Buckling", *Thin-Walled Structures*, Vol. 18(2), 1994, pp. 117-131.
- [52] Barbero, E.J. and Raftoyiannis Ioannis G., "Local Buckling of FRP Beams and Columns", *Journal of Materials in Civil Engineering*, Vol. 5(3), 1993, pp. 339-335.
- [53] Kabir, M.Z. and Sherbourne, A.N., "Local Buckling of Thin-walled Fibre Composite Beams under Transverse Loading", *Canadian Journal of Civil Engineering*, Vol. 26(1), 1999, pp. 107-118.
- [54] Reddy, A.D. and Rehfield, L.W., "Local Buckling and Crippling of Thin-walled Composite Structures under Axial Compression", *Journal of Aircraft*, Vol. 26(2), 1989, pp. 97-102.
- [55] Molnar, C., "Correlation Between Static and Dynamic Collapse of Compressed Thin-Walled Tubes", *Rozprawy Inzynierskie*, Vol. 29(1), 1981, pp. 69-81.
- [56] Tylinkowski, A., "Stochastic Stability of a Thin-Walled Beam Subjected to a Time and Space-Dependent Loading", *Zeitschrift fuer Angewandte Mathematik und Mechanik*, Vol. 66(4), 1986, pp. 97-98.
- [57] Arbocz, J. and Hol, J.M.A.M., "Collapse of Axially Compressed Cylindrical Shells with Random Imperfections", *Thin-Walled Structures*, Vol. 23(1-4), 1995, pp. 131-158.
- [58] Chryssanthopoulos, M.K. and Poggi, C., "Stochastic Imperfection Modelling in Shell Buckling Study", *Thin-Walled Structures*, Vol. 23(1-4), 1995, pp.179-200.

- [59] Yushanov, S.P. and Bogdanovich, A.E., "Analytical Probabilistic Modeling of Initial Failure and Reliability of Laminated Composite Structures", *International Journal of Solids and Structures*, Vol. 35(7-8), 1998, pp. 665-685.
- [60] Arbocz, J., Starnes, J.M., and Nemeth, M.P., "Towards a Probabilistic Criterion for Preliminary Shell Design", *Proceedings of the AIAA/ASME/ASCE/AHS, Structural Dynamics and Materials*, Vol. 4, 1998, Long Beach, CA, pp. 2941-2955.
- [61] Hyer, M.W., *Stress Analysis of Fiber-Reinforced Composite Materials*, 1998, McGraw-Hill, New York.
- [62] Haque, Md. Zakiul, "A Combined Experimental and Stochastic Finite Element Analysis Methodology for the Probabilistic Fracture Behavior of Composite Laminates", M. A. Sc. Thesis, 1999, Concordia University.
- [63] Haugen, E.B., *Probabilistic Approaches to Design*, 1968, J.Wiley, New York.
- [64] Bendat, J.S. and Piersol, A.G., *Measurement and Analysis of Random Data*, 1966, J.Wiley, New York.
- [65] Dato, M.H., *Mechanics of Fibrous Composites*, 1991, Elsevier Applied Science, New York.
- [66] Nettles, A.T., "Basic Mechanics of Laminated Composite Plates" NASA Reference Publication 1351, Marshall Space Flight Center, Alabama, 1994.
- [67] Boreisi, A.P., Schmidt, R.J., and Sidebottom, O.M., *Advanced Mechanics of Materials*, 1993, J.Wiley, New York.
- [68] Weaver, W. Jr., Timoshenko, S.P., and Young, D.H., *Vibration Problems in Engineering*, 1990, J.Wiley, New York.

- [69] Mukhopadhyay, M.. “A Semi-Analytic Solution for Free-vibration of Rectangular Plates”, *Journal of Sound and Vibration*, Vol. 60(1), 1978, pp. 71-85.
- [70] Paz, Mario., *Structural Dynamics: Theory and Computation*, 1997, Chapman & Hall New York.
- [71] Vanmarcke, E., Shinozuka, M., Nakagiri, S., Schueller, G.I, and Grigoriu, M., “Random Fields and Stochastic Finite Elements”, *Structural Safety*, Vol. 3, 1986, pp. 143-166.

Appendix

Programs used in the local buckling analysis

```
%% Program for the local buckling of expected value of flange fcff boundary conditions

close all;
clear all;
clc;

M = input('enter the value for M: ');
N = input('enter the value for N: ');
a = input('enter the value for Length of a plate a: ');
b = input('enter the value for width of a plate b: ');

syms x y m n

%% Replace the functions here according to the boundary conditions

for r = 1:M

    lam    = (2*r+1)*pi/2;
    Gama   = (cosh(lam)-cos(lam))/(sinh(lam)-sin(lam));
    X(r)   = cosh(lam*x/a)+cos(lam*x/a)-Gama*(sinh(lam*x/a)+sin(lam*x/a))

end

for r = 1:N

    lam    = (2*r+1)*pi/2;
    Beta   = (cos(lam)+cosh(lam))/(sin(lam)+sinh(lam));
    Y(r)   = cosh(lam*y/b)-cos(lam*y/b)-Beta*(sinh(lam*y/b)-sin(lam*y/b))

end

D11=315.44;D12=242.26;D16=17.1;
D21=242.26;D22=310.30;D26=23.01;
D61=17.1;D62=23.01;D66=253.80;

p=0;

for m=1:M

    for n=1:N

        mn=(m-1)*M+n;

        for u=1:M

            for v=1:N

                p=p+1
```

```

uv=(u-1)*M+v;

A1=D11*((int((diff(X(u),'x',2)*diff(X(m),'x',2)),x,0,a))*(int((Y(v)*Y(n)),y,0,b)));

A2=D12*[int(X(m)*diff(X(u),'x',2),x,0,a)*int(Y(v)*diff(Y(n),'y',2),y,0,b)+int(X(u)*diff(X(m),'x',2),x,0,a)*
int(Y(n)*diff(Y(v),'y',2),y,0,b)];

A3=D22*int(X(u)*X(m),x,0,a)*int(diff(Y(v),'y',2)*diff(Y(n),'y',2),y,0,b);
A4=4*D66*int(diff(X(u),'x',1)*diff(X(m),'x',1),x,0,a)*int(diff(Y(v),'y',1)*diff(Y(n),'y',1),y,0,b);

A5=2*D16*[int(diff(X(u),'x',2)*diff(X(m),'x',1),x,0,a)*int(Y(v)*diff(Y(n),'y',1),y,0,b)+int(diff(X(u),'x',1)*
diff(X(m),'x',2),x,0,a)*int(Y(n)*diff(Y(v),'y',1),y,0,b)];

A6=2*D26*[int(X(m)*diff(X(u),'x',1),x,0,a)*int(diff(Y(v),'y',1)*diff(Y(n),'y',2),y,0,b)+int(X(u)*diff(X(m),'
x',1),x,0,a)*int(diff(Y(v),'y',2)*diff(Y(n),'y',1),y,0,b)];

A7=int(diff(X(u),'x',1)*diff(X(m),'x',1),x,0,a)*int(Y(v)*Y(n),y,0,b);

A8=int(X(u)*diff(X(m),'x',1),x,0,a)*int(Y(n)*diff(Y(v),'y',1),y,0,b);

Q=A1+A2+A3+A4+A5+A6+A8;

EG(mn,uv)=Q;
B(mn,uv)=A7;

end

end

T1=numeric(EG);
T2=numeric(B);

end

end

Nx=eig(T1,T2) %% Buckling load

K=(Nx*b^2)/D11 %% Non-Dimensional Buckling load



---



%% Main program has been given using which we calculate the D matrix. Subroutine, which calculates the
D matrix, is also given. All other subroutines pertaining to finite element analysis is not relevant to present
D matrix calculation.

clear all;
%close all;
%clc;

tic;
format long;

```

```

dummy=0;      % To pass a dummy variable to GETDAT & GETARR

nelem=0;
    %%%%%%%%%%%
%%%%%%%%%%%
ndofn=0;      %
nnode=0;      %      Initialize all the relevant variables which are %
ngaus=0;      %
nnode=0;      %
nmat=0;      %      passed to the data functions so that all the relevant %
numnp=0;      %      data is passed back through the same variables. %
nstr=0;      %
nstr1=0;
    %%%%%%%%%%%
%%%%%%%%%%%

props = 0;
lnods = 0;
coord = 0;

nlami = 1;
D11 = zeros(108,1);
D12 = zeros(108,1);
D16 = zeros(108,1);
D21 = zeros(108,1);
D22 = zeros(108,1);
D26 = zeros(108,1);
D31 = zeros(108,1);
D32 = zeros(108,1);
D36 = zeros(108,1);
j=0;

%%%%%%%%%%%
%%%%%%%%%%%      GETDAT - Get are relevant scalar variables %%%%%%%%%%%
%%%%%%%%%%%

kgaus = 0; % Keep track over the gauss points in each entire structure.

% HERE STARTS THE PROGRAM FOR TENSILE ANALYSIS

for ilami = 1 : nlami

fprintf('\n RESULTS CORRESPONDS TO TENSILE ANALYSIS \n');

fprintf('\n Spatial values of the Material are stored in "propg.m" FILE \n ');

%%%%%%%%%%%
%%%%%%%%%%%

for ilami = 1 : nlami

%%%%%%%%%%%
%%%%%%%%%%%      GETDAT - Get are relevant scalar variables %%%%%%%%%%%
%%%%%%%%%%%

kgaus = 0; % Keep track over the gauss points in each entire structure.

```



```

for ielem = 1 : nelem          % Loop over NELEM

%%% Get the coordinates of each node in the element
%%% Get the coordinates of each node in the element

for inode = 1 : nnode
  Inode = round(abs(lnods(ielem,inode)));
  for idime = 1 : ndofn
    elcod(idime,inode) = coord(Inode,idime);
  end
end

shape = zeros(8,1);
deriv = zeros(2,8);
xjacm = zeros(2,2);
cartd = zeros(2,8);
estif = zeros(nevab,nevab);

%%% Start GAUSSIAN INTEGRATION
%%% Start GAUSSIAN INTEGRATION

kgasp = 0;  % Keep track over the gauss points in each element.

[posgpp,weigp] = GAUSSQ(ngaus);

for igaus = 1 : ngaus        % Loop over each Gauss point along "ZETA" axis
  % i.e., horizontally, starting from left.
  for jgaus = 1 : ngaus    % Loop over each Gauss point along "ETA" axis
    % i.e., vertically, starting from bottom.

    kgasp = kgasp + 1;
    kgaus = kgaus + 1;

    lprop = matno(kgaus);
    ThetaPly = tetag(kgaus,:);
    thick = sum(plytk(kgaus,:));

%%% Evaluate the Shape functions, derivatives, dvolu.. etc.
%%% Evaluate the Shape functions, derivatives, dvolu.. etc.

    exisp = posgpp(igaus);
    etasp = posgpp(jgaus);

    [dmatx,matxD] = MODPS(notype,nstre,nmats,lprop,propp,ThetaPly,kgaus);

    matxD
    j=j+1;
    D11(j) = matxD(1,1);
    D12(j) = matxD(1,2);
    D16(j) = matxD(1,3);
    D21(j) = matxD(2,1);
    D22(j) = matxD(2,2);

```



```

D26(j) = matxD(2,3);
D31(j) = matxD(3,1);
D32(j) = matxD(3,2);
D36(j) = matxD(3,3);

% fprintf('elasticity matrix');
% disp(ielem);
% disp(dmatx);

[shape,deriv] = SFR2(exisp,etasp);

[xjacm,djacb,gpcod,cartrd]=JACOBS2(ielem,kgasp,ndofn,nnode,shape,deriv,elcod);

dvolu = djacb*weigp(igaus)*weigp(jgaus); % volume calculation : t*j*ds*dt

if thick>0.0
    dvolu = dvolu*thick;
end

%%%% Evaluate the 'B' matrix and 'DB' matrices
[bmatx] = BMATPS(nnode,cartrd);

[dbmat] = DBE(dmatx,bmatx);

%%%% Calculate the element stiffness matrices
estif = estif + transpose(bmatx)*dbmat*dvolu;

%%%% Endof GAUSSIAN INTEGRATION

end

end

%%%% Assemble the element stiffness matrices

[globK] = ASMBLK(ielem,nevab,lm,estif,globK);

end

%%%% END OF ASSEMBLY FOR "estif" OF "ielem"

for iRuns = 1 : 3

```

```

% Solve for Nodal Loads and Assemble into Global Force Vector
% Solve for Nodal Loads and Assemble into Global Force Vector
% Solve for Nodal Loads and Assemble into Global Force Vector
% Solve for Nodal Loads and Assemble into Global Force Vector

```

```

[eload]
LOADPS(nelem,numnp,nnode,nevab,ndofn,ngaus,postp,weigr,coord,lnods,matno,props,iRuns);

```

```

[asmbLF] = FORCE(nelem,nevab,lm,eload);

```

```

% Solve for Displacements
% Solve for Displacements
% Solve for Displacements
% Solve for Displacements

```

```

[displ,eldis] = BCSOLVE(ndofn,coord,asmbLF,globK,lm,nelem,nevab,numnp,nnode,iRuns);

```

```

% Solve for GAUSS POINT STRESSES
% Solve for GAUSS POINT STRESSES
% Solve for GAUSS POINT STRESSES
% Solve for GAUSS POINT STRESSES

```

```

strsp=zeros(nstre,ngaus*ngaus,nelem);
sgtot=zeros(nstrl,ngaus*ngaus,nelem);

```

```

[sgtot,strsp]=STREPS(nelem,matno,props,propp,tetag,ntype,nmats,nnode,ndofn,coord,ngaus,nstre,nevab,nstrl,eldis,lnods,iRuns);

```

```

end % End of "for iRuns = 1 : 2"

```

```

end

```

```

RunTime = toc

```

```

end

```

```

function [propp,tetag,plytk] = RNDPROPS(nelem,ndofn,nnode,ngaus,ntotg,coord,lnods,ThetaPly,props)

```

```

format long;

```

```

% Sample data for Covariance matrix.
% Sample data for Covariance matrix.
% Sample data for Covariance matrix.
% Sample data for Covariance matrix.

```

```

sdE1 = 0.022188;
dE1 = 500;

```

```

sdE2 = 0.041248;
dE2 = 500;

```

```

sdV21 = 0.1043;
dV21 = 500;

```

```

sdG12 = 0.05523;
dG12 = 500;

sdangl = 0.05;
dangl = 500;

sdtply = 0.1;
dtply = 500;

%%%%%%%%%%%%%%%%%%%%%%%%%%%%%%%%%%%%%%%%%%%%%%%%%%%%%%%%%%%%%%%%%%%%%%%%

xgcod = zeros(ntotg,1);          % X co-ordiante of each gauss point.
ygcod = zeros(ntotg,1);          % Y co-ordiante of each gauss point.
gdist = zeros(ntotg,ntotg);

%%%%%%%%%%%%%%%%%%%%%%%%%%%%%%%%%%%%%%%%%%%%%%%%%%%%%%%%%%%%%%%%%%%%%%%%

kgaus = 0;

for ielem = 1 : nelelem

    for inode = 1 : nnode
        lnode = lnods(ielem,inode);
        for idime = 1 : ndofn
            elcod(idime,inode) = coord(lnode,idime);
        end
    end

    [posgp,weigp] = GAUSSQ(ngaus);

    kgasp = 0;

    for igauss = 1 : ngauss
        for jgauss = 1 : ngauss

            kgaus = kgaus + 1;
            kgasp = kgasp + 1;

            exisp = posgp(igauss);
            etasp = posgp(jgauss);

            [shape,deriv] = SFR2(exisp,etasp);

            for idime = 1 : ndofn
                gpcod(idime,kgasp) = 0.0;
                for inode = 1 : nnode
                    gpcod(idime,kgasp) = gpcod(idime,kgasp) + elcod(idime,inode)*shape(inode);
                end
            end

            xgcod(kgaus) = gpcod(1,kgasp);
            ygcod(kgaus) = gpcod(2,kgasp);

        end
    end
end

```

end

%%%%%%%%%%

```
for itotg = 1 : ntotg
  for jtotg = 1 : ntotg
    gdist(itotg,jtotg) = (1.0e3)*sqrt( (xgcod(itotg)-xgcod(jtotg))^2 + (ygcod(itotg)-ygcod(jtotg))^2 );
    cvmE1(itotg,jtotg) = (sdE1^2)*exp( -(abs( gdist(itotg,jtotg) )/dE1) );
    cvmE2(itotg,jtotg) = (sdE2^2)*exp( -(abs( gdist(itotg,jtotg) )/dE2) );
    cvmV21(itotg,jtotg)=(sdV21^2)*exp( -(abs( gdist(itotg,jtotg) )/dV21) );
    cvmG12(itotg,jtotg)=(sdG12^2)*exp( -(abs( gdist(itotg,jtotg) )/dG12) );
    cvmangl(itotg,jtotg)=(sdangl^2)*exp( -(abs( gdist(itotg,jtotg) )/dangl) );
    cvmtply(itotg,jtotg)=(sdtply^2)*exp( -(abs( gdist(itotg,jtotg) )/dtply) );
  end
end
```

```
[uprE1,ecE1] = chol(cvmE1);
[uprE2,ecE2] = chol(cvmE2);
[uprV21,ecV21] = chol(cvmV21);
[uprG12,ecG12] = chol(cvmG12);
[uprangl,ecangl] = chol(cvmangl);
[uprtply,ectply] = chol(cvmtply);
```

```
lwrE1 = transpose(uprE1);
lwrE2 = transpose(uprE2);
lwrV21 = transpose(uprV21);
lwrG12 = transpose(uprG12);
lwrangl = transpose(uprangl);
lwrtply = transpose(uprtply);
```

```
randn('state',sum(100*clock));
```

```
temp1 = randn(ntotg,1);
temp2 = randn(ntotg,1);
temp3 = randn(ntotg,1);
temp4 = randn(ntotg,1);
temp5 = randn(ntotg,1);
temp6 = randn(ntotg,1);
```

```
avect = lwrE1*temp1;
bvect = lwrE2*temp2;
cvect = lwrV21*temp3;
dvect = lwrG12*temp4;
evect = lwrangl*temp5;
fvect = lwrtply*temp6;
```

```
for itotg = 1 : ntotg
  propg(itotg,1) = props(1)*( 1.0 + avect(itotg) );
  propg(itotg,2) = props(2)*( 1.0 + bvect(itotg) );
  propg(itotg,4) = props(4)*( 1.0 + cvect(itotg) );
  propg(itotg,3) = propg(itotg,4)*propg(itotg,1)/propg(itotg,2);
  propg(itotg,5) = props(5)*( 1.0 + dvect(itotg) );
  propg(itotg,6) = props(6);
```

```

    propg(itotg,7) = props(7);
end

gvect = randn(props(7));

for itotg = 1 : ntotg
    for iply = 1 : props(7)
        tetag(itotg,iply) = ThetaPly(iply)*( 1.0 + sdangl*gvect(iply));
        plytk(itotg,iply) = props(6)*( 1.0 + sdtply*gvect(iply));
        tetag(itotg,iply) = ThetaPly(iply)*( 1.0 + sdangl*gvect(iply));
    end
end

```

```

function [props,tetag,plytk,matno,propg,lnods,coord,ThetaPly] =
GETARR(nelem,ngaus,ndofn,nnode,ntotg,aW_Ratio,WL_Ratio,ctnode)

```

```

format long;

```

```

%%%%%%%%%%%%%%%%%%%%%%%%%%%%%%%%%%%%%%%%%%%%%%%%%%%%%%%%%%%%%%%%%%%%%%%%%%
%%%%%%%%%%%%%%%%%%%%%%%%%%%%%%%%%%%%%%%%%%%%%%%%%%%%%%%%%%%%%%%%%%%%%%%%
%%%%%%%%%%%%%%%%%%%%%%%%%%%%%%%%%%%%%%%%%%%%%%%%%%%%%%%%%%%%%%%%%%%%%%%%
%%%%%%%%%%%%%%%%%%%%%%%%%%%%%%%%%%%%%%%%%%%%%%%%%%%%%%%%%%%%%%%%%%%%%%%%
%%%%%%%%%%%%%%%%%%%%%%%%%%%%%%%%%%%%%%%%%%%%%%%%%%%%%%%%%%%%%%%%%%%%%%%%
%%%%%%%%%%%%%%%%%%%%%%%%%%%%%%%%%%%%%%%%%%%%%%%%%%%%%%%%%%%%%%%%%%%%%%%%
%%%%%%%%%%%%%%%%%%%%%%%%%%%%%%%%%%%%%%%%%%%%%%%%%%%%%%%%%%%%%%%%%%%%%%%%

```

PROGRAM CHECK

Give arbitrary values to the function arguments

Array having the Properties of every Element

```

% In the order E1 E2 v12 v21 G12 t(ply) Num.ofPlies
% These are the Mean(average) Values of E1, E2, v12, v21, G12 and t(ply).
% laminate is considered thin if the thickness is less than 3 mm
% Grapite-Epoxy Composite AS4/3502 page 117 : table 5.1 : seng c tan : stress concentration in laminated
composites

```

```

props = [ 129.43e9 7.99e9 0.3322 0.0205 4.28e9 1.25e-4 36];

    ThetaPly = [ 0 -60 60 0 -60 60 0 -60 60 0 -60 60 0 -60 60 60 -60 0 60 -60 0 60 -
60 0 60 -60 0];

    ThetaPly = ThetaPly*pi/180;

```

```

% NCT-301 Grapite-Epoxy Composite "[0/90]6s"

```

```

for itotg = 1 : ntotg
    matno(itotg) = itotg;
end

```

```

%%%%%%%%%%%%%%%%%%%%%%%%%%%%%%%%%%%%%%%%%%%%%%%%%%%%%%%%%%%%%%%%%%%%%%%%

```

Relate the Local Node numbers to Global Node Numbers

```

lnods = [ 1 3 17 15 2 11 16 10
          3 5 19 17 4 12 18 11
          5 7 21 19 6 13 20 12

```

```

7 9 23 21 8 14 22 13
21 23 37 35 22 28 36 27
19 21 35 33 20 27 34 26
17 19 33 31 18 26 32 25
15 17 31 29 16 25 30 24
29 31 45 43 30 39 44 38
31 33 47 45 32 40 46 39
33 35 49 47 34 41 48 40
35 37 51 49 36 42 50 41];

```

```

%% Co-ordinates of Each node in the Global co-ordinate System

```

```

width=0.0379; % width of the plate
dia=0.0051 ; % dia of the hole
radius=dia/2 ; % radius of the hole
length= 0.0379*2; % length of the laminate

```

```

[coord] = MESHrefine(length,width,dia,radius,Inods);

```

```

%%

```

```

%[coord] = AUTOMESH(ctnode,coord,aW_Ratio,WL_Ratio);

```

```

%%

```

```

[propg,tetg,plytk] = RNDPROPS(nelem,ndofn,nnode.ngaus,ntotg,coord,Inods,ThetaPly,props);

```

```

%%

```

```

function [dmatx,matxD] = MODPS(nstype,nstre,nmats,lprop,propg,ThetaPly,kgaus)

```

```

format long;

```

```

%%
%
% Calculate the matrices :- [A] , [B] , [D]
%
%
%%

```

```

qm126 = zeros(nstre,nstre);
qmxys = zeros(nstre,nstre);
matxA = zeros(nstre,nstre);
matxB = zeros(nstre,nstre);
matxD = zeros(nstre,nstre);

```

```

props = propg(kgaus,:);

```

```

yung1 = props(1);
yung2 = props(2);
nue12 = props(3);
nue21 = props(4);
shr12 = props(5);

```

```
plytk = props(6);
nplys = props(7);
```

```
%%%%%%%%% On-Axis Stiffness Matrix %%%%%%%%%
```

```
qml26(1,1) = yung1/(1.0 - nue12*nue21);
qml26(2,2) = yung2/(1.0 - nue12*nue21);
qml26(1,2) = nue12*yung2/(1.0 - nue12*nue21);
qml26(2,1) = qml26(1,2);
qml26(1,3) = 0.0;
qml26(2,3) = 0.0;
qml26(3,1) = 0.0;
qml26(3,2) = 0.0;
qml26(3,3) = shr12;
```

```
for iplys = 1 : nplys
```

```
theta = ThetaPly(iplys);
```

```
m = cos(theta);
n = sin(theta);
```

```
qmxys(1,1) = m^4*qml26(1,1) + n^4*qml26(2,2) + 2*m^2*n^2*qml26(1,2) + 4*m^2*n^2*qml26(3,3);
qmxys(2,2) = n^4*qml26(1,1) + m^4*qml26(2,2) + 2*m^2*n^2*qml26(1,2) + 4*m^2*n^2*qml26(3,3);
qmxys(1,2) = m^2*n^2*(qml26(1,1)+qml26(2,2)) + (m^4 + n^4)*qml26(1,2) -
4*m^2*n^2*qml26(3,3);
qmxys(2,1) = qmxys(1,2);
qmxys(1,3) = m^3*n*qml26(1,1) - m*n^3*qml26(2,2) + (m*n^3 - m^3*n)*(qml26(1,2) +
2*qml26(3,3));
qmxys(3,1) = qmxys(1,3);
qmxys(2,3) = m^3*n*qml26(1,1) - m^3*n*qml26(2,2) + (m^3*n - m*n^3)*(qml26(1,2) +
2*qml26(3,3));
qmxys(3,2) = qmxys(2,3);
qmxys(3,3) = m^2*n^2*(qml26(1,1) + qml26(2,2)) - 2*m^2*n^2*qml26(1,2) + (m^2 -
n^2)^2*qml26(3,3);
```

```
botom = -(nplys/2)*plytk;
```

```
hite1 = botom + iplys*plytk;
hite2 = botom + (iplys-1)*plytk;
```

```
matxA = matxA + qmxys*( hite1 - hite2 );
matxB = matxB + (1/2)*qmxys*(hite1^2 - hite2^2);
matxD = matxD + (1/3)*qmxys*(hite1^3 - hite2^3);
```

```
end
```

```
dmatx = matxA/(nplys*plytk);
```

```
-----
```